

ornl

RECEIVED
SEP 17 1997
OSTI

ORNL/TM-13191

OAK RIDGE
NATIONAL
LABORATORY

LOCKHEED MARTIN 

Laboratory Tests in Support of the MSRE Reactive Gas Removal System

J. C. Rudolph
G. D. Del Cul
J. Caja
L. M. Toth
D. F. Williams
K. S. Thomas
D. E. Clark

MASTER 

DISTRIBUTION OF THIS DOCUMENT IS UNLIMITED

MANAGED AND OPERATED BY
LOCKHEED MARTIN ENERGY RESEARCH CORPORATION
FOR THE UNITED STATES
DEPARTMENT OF ENERGY

ORNL-27 (3-96)

This report has been reproduced directly from the best available copy.

Available to DOE and DOE contractors from the Office of Scientific and Technical Information, P. O. Box 62, Oak Ridge, TN 37831; prices available from (423) 576-8401, FTS 626-8401.

Available to the public from the National Technical Information Service, U.S. Department of Commerce, 5285 Port Royal Road, Springfield, VA 22161.

This report was prepared as an account of work sponsored by an agency of the United States Government. Neither the United States Government nor any agency thereof, nor any of their employees, makes any warranty, express or implied, or assumes any legal liability or responsibility for the accuracy, completeness, or usefulness of any information, apparatus, product, or process disclosed, or represents that its use would not infringe privately owned rights. Reference herein to any specific commercial product, process, or service by trade name, trademark, manufacturer, or otherwise, does not necessarily constitute or imply its endorsement, recommendation, or favoring by the United States Government or any agency thereof. The views and opinions of authors expressed herein do not necessarily state or reflect those of the United States Government of any agency thereof.

DISCLAIMER

Portions of this document may be illegible electronic image products. Images are produced from the best available original document.

Chemical Technology Division

LABORATORY TESTS IN SUPPORT OF THE MSRE
REACTIVE GAS REMOVAL SYSTEM

J. C. Rudolph
G. D. Del Cul
J. Caja
L. M. Toth
D. F. Williams
K. S. Thomas
D. E. Clark

July 1997

Prepared by the
OAK RIDGE NATIONAL LABORATORY
Oak Ridge, Tennessee 37831-6285
managed by
LOCKHEED MARTIN ENERGY RESEARCH CORP.
for the
U.S. DEPARTMENT OF ENERGY
under contract DE-AC05-96OR22464

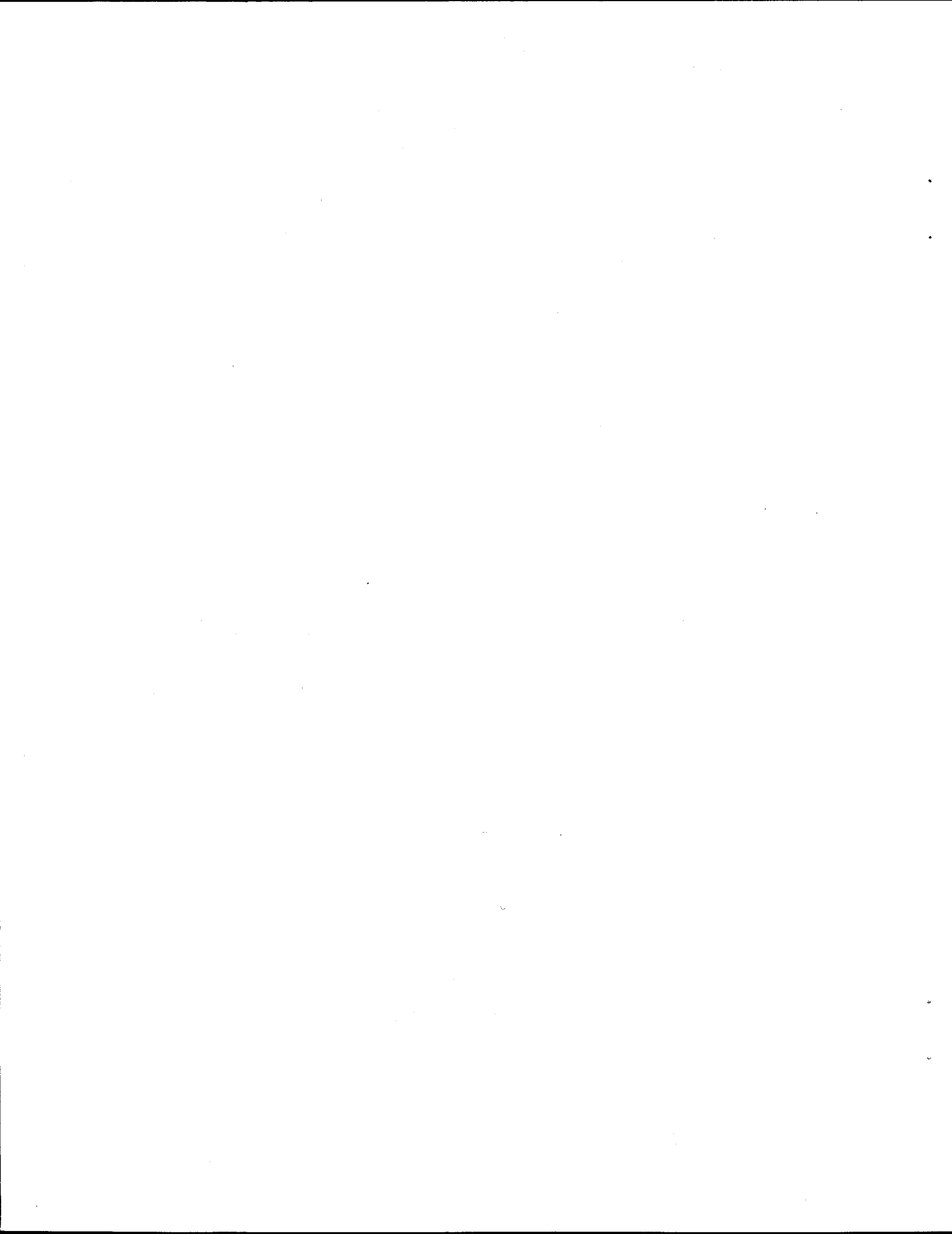
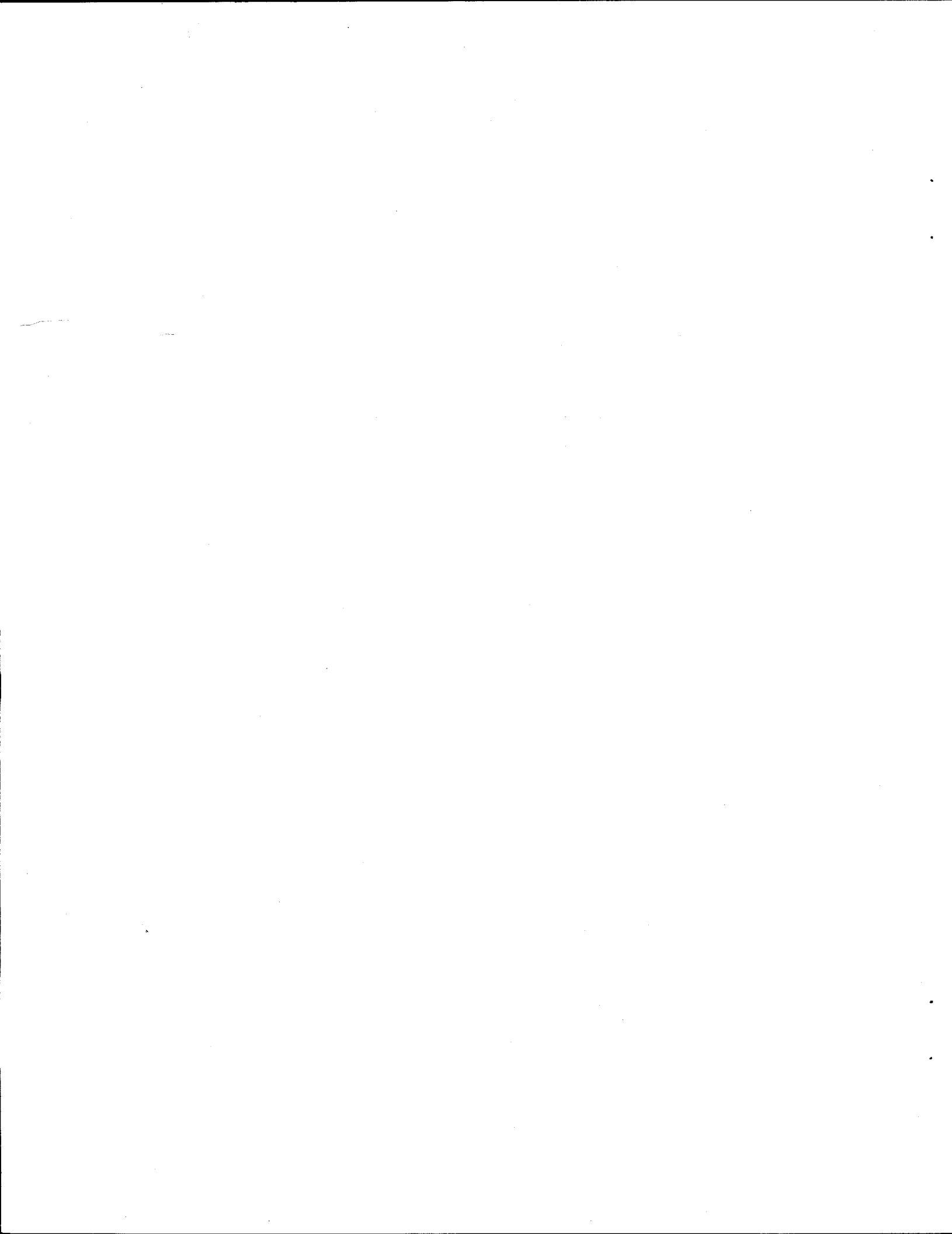


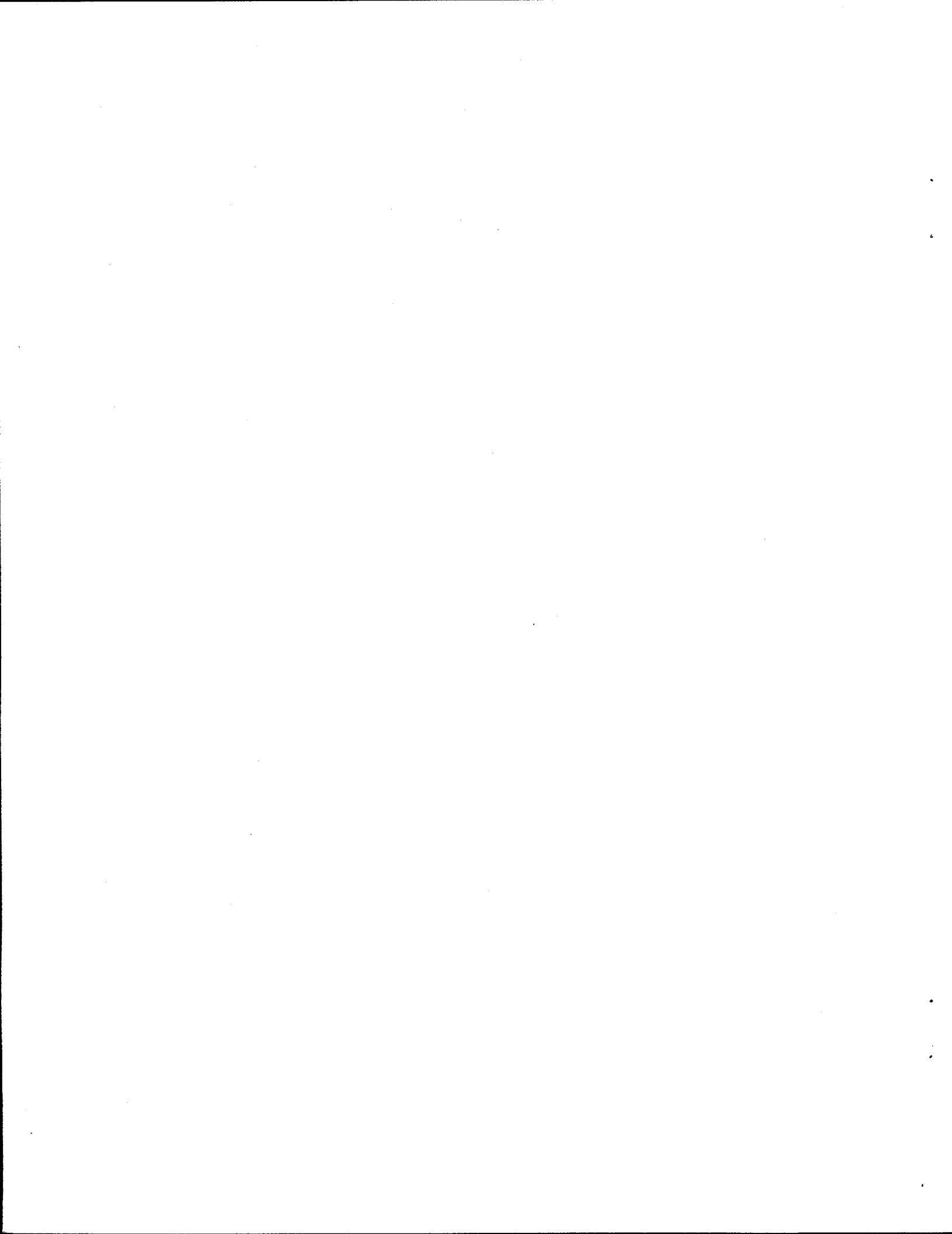
TABLE OF CONTENTS

LIST OF TABLES	v
LIST OF FIGURES	vii
ACRONYMS	xi
ACKNOWLEDGMENTS	xiii
ABSTRACT	xv
1. INTRODUCTION	1
2. OBJECTIVES	3
3. DESCRIPTION OF TEST APPARATUS	3
4. DESCRIPTION AND PROPERTIES OF GAS TRAPPING MATERIAL	10
5. FLUORINE TRAPPING RESULTS (FTT)	12
6. UF ₆ TRAPPING RESULTS (UTT)	18
7. SIMPLE INTEGRATED TEST (SIT)	21
8. GLOVE BOX TESTS	24
8.1 POSITIVE PRESSURE FLOW TESTS (GBTP)	24
8.2 VACUUM TESTS (GBTV)	28
9. ANALYSIS AND CONCLUSIONS	33
10. REFERENCES	36
Appendix A. ADDITIONAL FIGURES	A-1
Appendix B. DETERMINATION OF FLUORINE LOADING PER GRAM INCREASE OF TRAP WEIGHT	B-1
Appendix C. CALCULATION OF FLUORINE FLOW RATE BASED ON EXIT FLOWMETER READING AND HOLDING TANK PRESSURE RISE	C-1



LIST OF TABLES

1. Gas analysis of two samples taken from the MSRE off-gas system	2
2. Equipment used in fluorine trapping tests (FTT)	4
3. Physical properties of NaF pellets for MSRE	10
4. Summary of alumina properties	10
5. Summary of molecular sieve (13X) properties	11
6. Preparative drying results for alumina	11
7. Major parameters for fluorine trapping tests (FTT)	12
8. Peak temperatures measured in 3-in. alumina bed	16
9. Measured fluorine loading of alumina traps	16
10. Characteristics of liquid collected from the alumina trap exhaust	18
11. Metals analysis of FTT-4 condensate	19
12. Test conditions for UF ₆ loading onto 1-in. NaF trap	20
13. Test conditions for the simple integrated test (SIT)	22
14. Parameters and results from direct loading of UF ₆ onto alumina	24
15. Axial positioning of thermocouples and NDA detectors on gas traps	25
16. Parameters for GBTP	26
17. Maximum NaF and alumina temperatures and UF ₆ and F ₂ loading for GBTP	28
18. Metals analysis of downstream piping wash (GBTP)	29
19. Parameters for GBTV	30
20. Maximum temperatures and UF ₆ and F ₂ loading in GBTV	31
21. Pressure measurements from GBTV	31

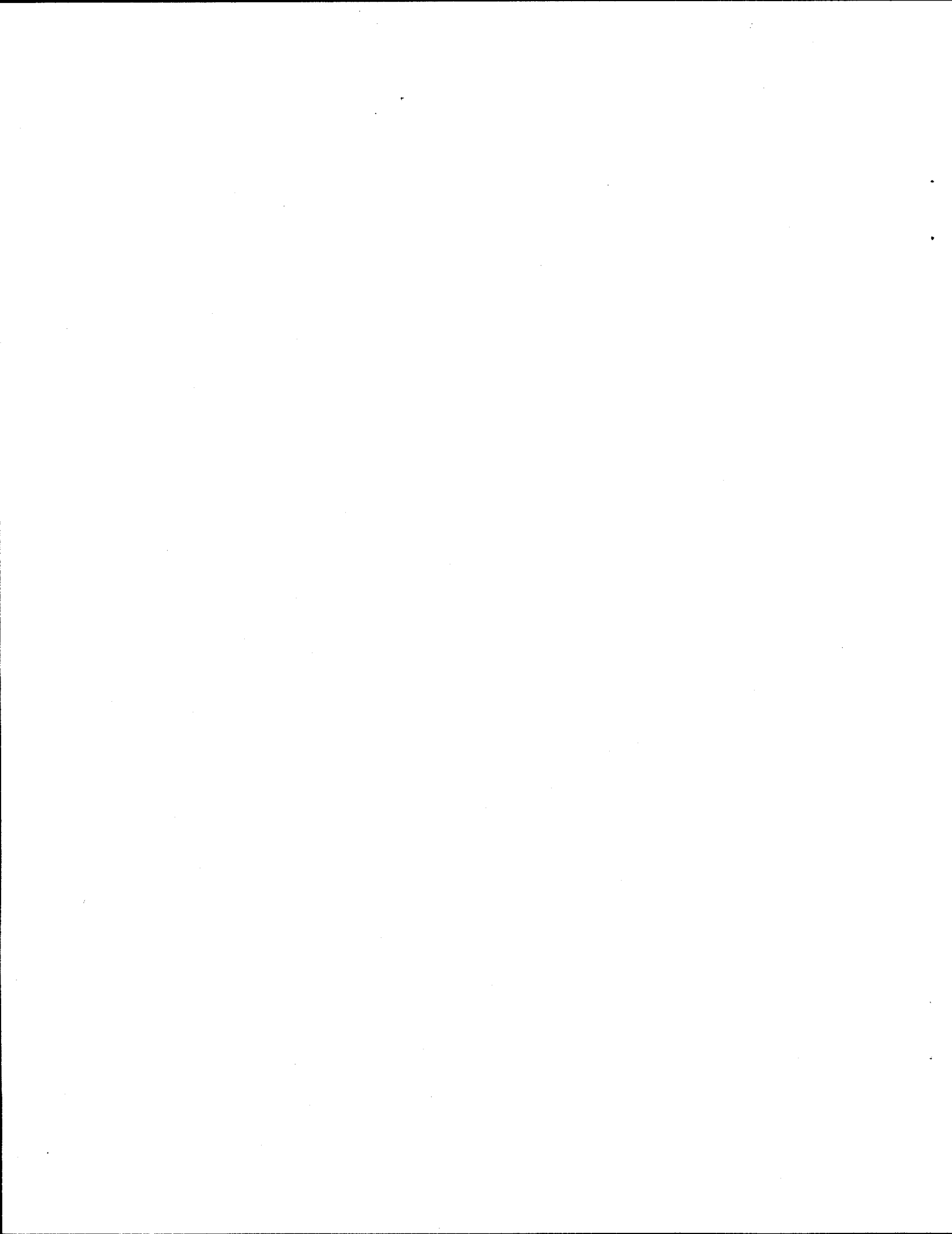


LIST OF FIGURES

1.	Diagram of fluoride trapping test (FTT)	5
2.	Diagram of UF ₆ trapping test (UTT)	6
3.	Diagram of simple integrated trapping test (SIT)	7
4.	Diagram of hood portion of glove box tests under pressure (GBTP)	8
5.	Diagram of hood portion of glove box tests under vacuum (GBTV)	9
6.	Skin temperatures for FTT-2, 150 sccm fluorine, 1-in.-ID trap	14
7.	Fluorine breakthrough during FTT-2, 150 sccm fluorine, 1-in.-ID trap	15
8.	Fluorine breakthrough during FTT-3F, 600 sccm fluorine, 3-in.-ID trap	15
9.	Summary of peak temperatures measured in FTT with 3-in.-ID column	17
10.	Skin temperatures and UF ₆ flow rate vs time, 1-in. NaF trap, February 9, 1996	20
11.	Sodium fluoride temperatures and UF ₆ flow rate, SIT	23
12.	Alumina internal temperatures and F ₂ flow rate, SIT	23
13.	Sodium fluoride temperatures and UF ₆ breakthrough curve, GBTP, March 28, 1996	27
14.	Gamma transmission for NDA detectors over entire GBTP	27
15.	Sodium fluoride temperatures and UF ₆ flow rate, GBTV-3, April 11, 1996	32
16.	Alumina temperatures and F ₂ flow rate, GBTV-3, April 11, 1996	32
A-1.	TGA of uniform alumina prior to drying	A-3
A-2.	Skin temperatures for FTT-1A, 100-200 sccm fluorine, 1-in.-ID trap	A-4
A-3.	Skin temperatures for FTT-1B, 100-200 sccm fluorine, 1-in.-ID trap	A-4
A-4.	Skin temperatures for FTT-3A, 300 sccm fluorine	A-5
A-5.	Internal temperatures for FTT-3A, 300 sccm fluorine	A-5
A-6.	Skin temperatures for FTT-3B, 250 sccm fluorine	A-6

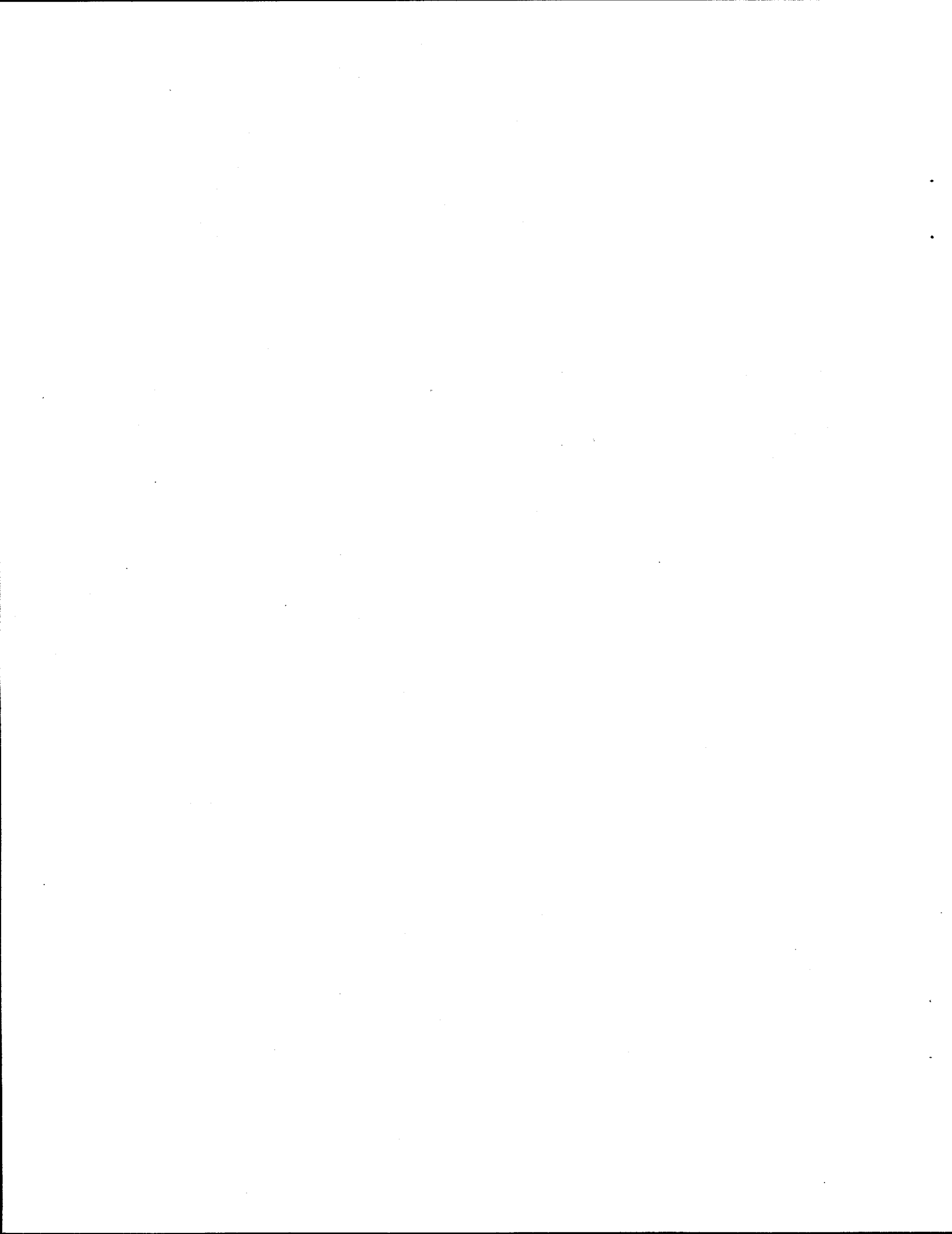
A-7. Internal temperatures for FTT-3B, 250 sccm fluorine	A-6
A-8. Skin temperatures for FTT-3C, 300 sccm fluorine	A-7
A-9. Internal temperatures for FTT-3C, 300 sccm fluorine	A-7
A-10. Skin temperatures for FTT-3D, 500 sccm fluorine	A-8
A-11. Internal temperatures for FTT-3D, 500 sccm fluorine	A-8
A-12. Skin temperatures for FTT-3E, 600 sccm fluorine	A-9
A-13. Internal temperatures for FTT-3E, 600 sccm fluorine	A-9
A-14. Skin temperatures for FTT-3F, 600 sccm fluorine	A-10
A-15. Internal temperatures for FTT-3F, 600 sccm fluorine	A-10
A-16. Valve temperatures for FTT-3A, 300 sccm fluorine	A-11
A-17. Valve temperatures for FTT-3B, 250 sccm fluorine	A-11
A-18. Valve temperatures for FTT-3C, 300 sccm fluorine	A-12
A-19. Valve temperatures for FTT-3D, 500 sccm fluorine	A-12
A-20. Valve temperatures for FTT-3E, 600 sccm fluorine	A-13
A-21. Valve temperatures for FTT-3F, 600 sccm fluorine	A-13
A-22. Skin temperatures for FTT-4A, 600 sccm fluorine	A-14
A-23. Internal temperatures for FTT-4A, 600 sccm fluorine	A-14
A-24. Skin temperatures for FTT-4B, 800 sccm fluorine	A-15
A-25. Internal temperatures for FTT-4B, 800 sccm fluorine	A-15
A-26. Valve temperatures for FTT-4A, 600 sccm fluorine	A-16
A-27. Valve temperatures for FTT-4B, 800 sccm fluorine	A-16
A-28. Skin temperatures for FTT-5A, 800 sccm fluorine	A-17
A-29. Internal temperatures for FTT-5A, 800 sccm fluorine	A-17
A-30. Skin temperatures for FTT-5B, 1000 sccm fluorine	A-18

A-31. Internal temperatures for FTT-5B, 1000 sccm fluorine	A-18
A-32. Valve temperatures for FTT-5A, 800 sccm fluorine	A-19
A-33. Valve temperatures for FTT-5A, 1000 sccm fluorine	A-19
A-34. Peak height (1157cm^{-1}) vs UF_6 partial pressure in the 10-cm IR cell	A-20
A-35. Peak height (625cm^{-1}) vs UF_6 partial pressure in the 20-cm IR cell	A-20
A-36. Sodium fluoride temperatures and UF_6 flow rate, GBTP, March 25, 1996	A-21
A-37. Alumina temperatures and F_2 flow rate, GBTP, March 25, 1996	A-21
A-38. Sodium fluoride temperatures and UF_6 flow rate, GBTP, March 26, 1996	A-22
A-39. Alumina temperatures and F_2 flow rate, GBTP, March 26, 1996	A-22
A-40. Sodium fluoride temperatures and UF_6 flow rate, GBTP, March 27, 1996	A-23
A-41. Alumina temperatures and F_2 flow rate, GBTP, March 27, 1996	A-23
A-42. Sodium fluoride temperatures and UF_6 flow rate, GBTP, March 28, 1996	A-24
A-43. Alumina temperatures, no F_2 flow, GBTP, March 28, 1996	A-24
A-44. Sodium fluoride temperatures and UF_6 flow rate, GBTV-1, April 9, 1996	A-25
A-45. Alumina temperatures and F_2 flow rate, GBTV-1, April 9, 1996	A-25
A-46. Sodium fluoride temperatures and UF_6 flow rate, GBTV-2, April 10, 1996	A-26
A-47. Alumina temperatures and F_2 flow rate, GBTV-2, April 10, 1996	A-26
A-48. Sodium fluoride temperatures and UF_6 flow rate, GBTV-4, April 12, 1996	A-27
A-49. Alumina temperatures and F_2 flow rate, GBTV-4, April 12, 1996	A-27
A-50. Exit flow measurements, GBTV-2, April 10, 1996	A-28
A-51. Tank pressure rise, GBTV-2, April 10, 1996	A-29
A-52. Gamma transmission received by second NDA detector throughout GBTV	A-30



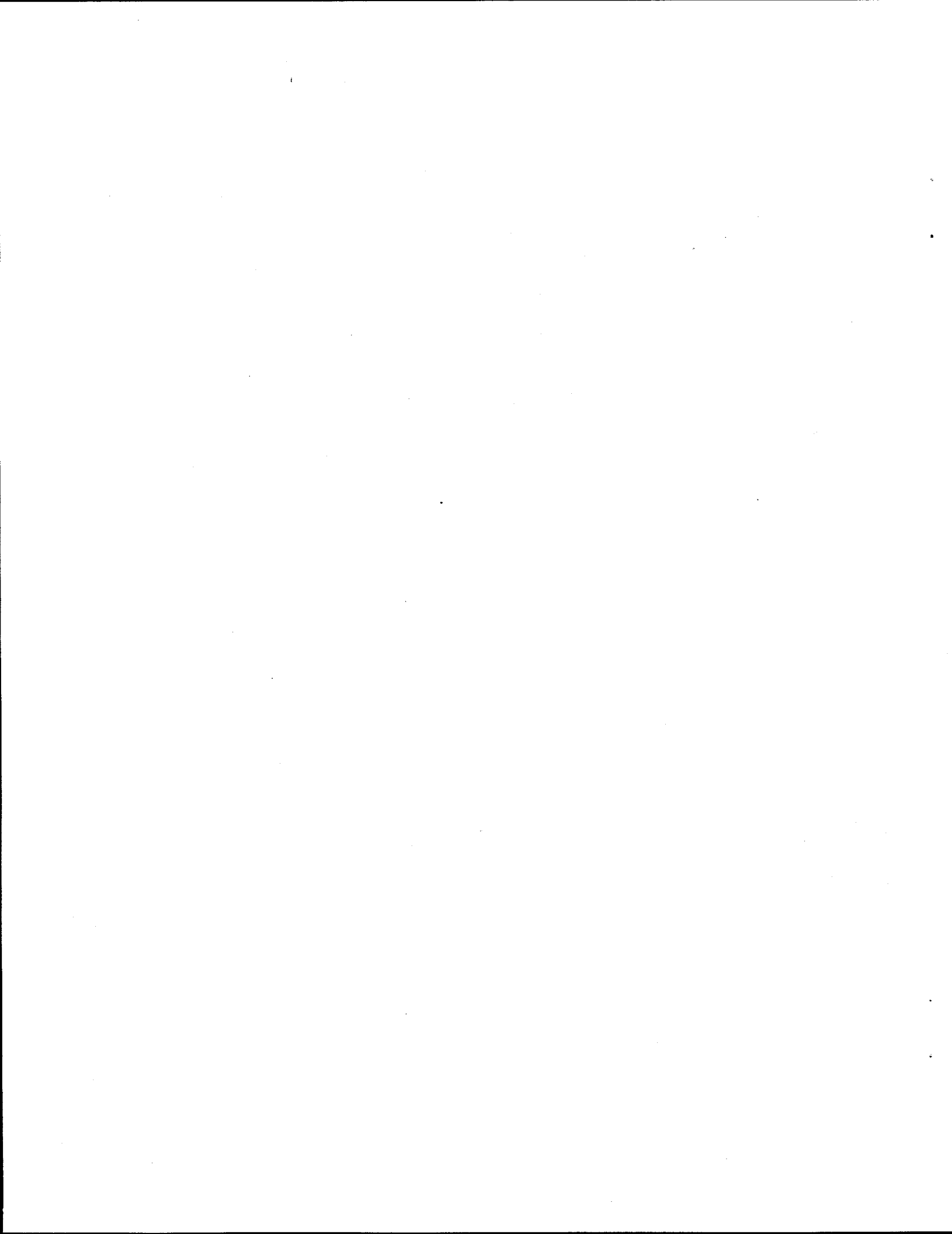
ACRONYMS

AFMR	actual flowmeter reading
CPS	counts per second
FTIR	Fourier transform interferometer
FTT	fluorine trapping tests
GBTP	glove box tests under pressure
GBTV	glove box tests under vacuum
ID	internal diameter
IR	infrared
MSRE	Molten Salt Reactor Experiment
NDA	nondestructive analysis
RGRS	reactive gas removal system
sccm	standard cubic centimeters per minute
SIT	simple integrated test
SL	standard liter (at 0°C and 1 atm of pressure)
SLM	standard liters per minute
TGA	thermogravimetric analysis
UTT	UF ₆ trapping tests



ACKNOWLEDGMENTS

The laboratory testing of the Molten Salt Reactor Experiment reactive gas removal system was a team effort, and we thank all those involved in the project for their constant support. Special thanks go to Ron Battle and Mike Buchanan of the Instrumentation and Controls Division at Oak Ridge National Laboratory for resolving problems with instrumentation and computer monitoring and to Norm Smyrl and Quirinus Grindstaff of the Analytical Services Organization at the Oak Ridge Y-12 Plant for their assistance with the Fourier transform interferometers.



ABSTRACT

The Molten Salt Reactor Experiment (MSRE) at Oak Ridge National Laboratory has been shut down since December 1969, at which time the molten salt mixture of $\text{LiF-BeF}_2\text{-ZrF}_4\text{-}^{233}\text{UF}_4$ (64.5-30.3-5.0-0.13 mol %) was transferred to fuel salt drain tanks for storage. In the late 1980s, increased radiation in one of the gas lines from the drain tank was attributed to $^{233}\text{UF}_6$. In 1994 two gas samples were withdrawn (from a gas line in the Vent House connecting to the drain tanks) and analyzed. Surprisingly, 350 mm Hg of F_2 , 70 mm Hg of UF_6 , and smaller amounts of other gases were found in both of the samples.

To remove this gas from above the drain tanks and all of the associated piping, the reactive gas removal system (RGRS) was designed. This report details the laboratory testing of the RGRS, using natural uranium, prior to its implementation at the MSRE facility. The testing was performed to ensure that the equipment functioned properly and was sufficient to perform the task while minimizing exposure to personnel. In addition, the laboratory work provided the research and development effort necessary to maximize the performance of the system. Throughout this work, technicians and staff who were to be involved in RGRS operation at the MSRE site worked directly with the research staff in completing the laboratory testing phase. Consequently, at the end of the laboratory work, the personnel who were to be involved in the actual operations had acquired all of the training and experience necessary to continue with the process of reactive gas removal.

1. INTRODUCTION

The Molten Salt Reactor Experiment (MSRE) was operated at the Oak Ridge National Laboratory from 1965 to 1969 to test the concept of a high-temperature homogeneous fluid-fueled reactor.¹ It was fueled with a molten salt mixture of LiF-BeF₂-ZrF₄-UF₄ (64.5-30.3-5.0-0.13 mol %), melting at approximately 450°C, which served as both the fuel and the primary coolant. This fluid was circulated by a large impeller pump between the reactor core and the primary heat exchanger. A secondary coolant of LiF-BeF₂ (66-34 mol %), circulated by a similar impeller pump, transferred or "shuttled" heat from this heat exchanger to an air-cooled radiator. Approximately 4350 kg (~2 m³) of fuel salt constituted the fuel charge circulating in the fuel salt circuit. Originally, the MSRE was fueled with ²³⁵UF₄; however, after successful operation with this isotope, the ²³⁵U was removed by fluorination of the tetrafluoride to the volatile hexafluoride, UF₆. Afterward, the salt was reconstituted with ²³³UF₄ (containing 220 ppm ²³²U) to demonstrate that the system could function equally well on the product of a ²³²Th thermal breeding cycle. After the successful completion of this campaign, reactor operation was terminated on December 12, 1969, when the fuel salt from the reactor circuit was drained and solidified in two drain tanks at a lower level of the MSRE facility.

The fuel salt has remained there for the past 27 years. At the time of the MSRE operation, radiolytic effects on the fuel salt were recognized as a probable occurrence if the salt were stored below 100°C, with the net effect that fluorine gas (F₂) could be liberated from the frozen salt mixture and cause corrosion and/or overpressurization of the drain tank containment system. To prevent the accumulation of this halogen gas, the frozen salt (which was normally at approximately 40°C due to the self-heating generated by fission product decay) was heated to 250°C on an annual basis to recombine the fluorine generated with the "reduced" sites left in the salt. The fluorine pressure in the drain tanks prior to and after annealing was not monitored; therefore, the effectiveness of this annual procedure has never been established.

In the late 1980s, an increase in radioactivity in one of the gas line protrusions into the North Electrical Services Area, a room adjacent to the drain tank cell, was identified as coming from UF₆. Because the annual annealing operation would drive this condensable gas from the drain tanks to cooler surfaces such as the gas line protrusion into the North Electrical Services Area, the annual annealing operation was postponed until a better understanding of the fuel salt behavior was obtained.

In early 1994, two 1000-mL gas samples were withdrawn (from a gas line in the Vent House connecting to the drain tanks) and analyzed. Surprisingly, 350 mm Hg of F₂, 70 mm Hg of UF₆, and smaller amounts of other gases were found in both of the samples (see Table 1), confirming that the

annual annealing operations had not been successful in recombining the fluorine with the fuel salt and, more importantly, that the temperature gradient created during the annealing operation had definitely contributed to the displacement of UF₆ from the fuel salt.

Table 1. Gas analysis of two samples taken from the MSRE off-gas system^a

Species	First sample	Second sample
UF ₆	70 mm Hg (0.8 g/L)	68 mm Hg (0.8 g/L)
HF	1200 ppm	1000 ppm
MoF ₆	10 mm Hg	<i>b</i>
CF ₄	5 mm Hg	<i>b</i>
F ₂	<i>c</i>	350 mm Hg
He, Ar, N ₂ , O ₂ ^d	305 mm Hg	305 mm Hg

^aIdentification by mass spectroscopy.

^bPresent as in first sample.

^cNot determined analytically but assumed to be the same as the second sample.

^dQuantity determined by difference from total sample pressure.

On further investigation, it was found that the gas line from the drain tank also ran to large charcoal beds (U tubes of 6-in. diam and 24-ft length), which could not be isolated due to a shutoff valve that had failed in the open position. Gamma scan and thermal analyses indicated that 2.6 kg of the uranium from the drain tanks had been deposited at the charcoal bed inlet. This material, along with carbon-fluorine reaction products, presents chemical as well as radiological hazards.²

On November 20, 1995, this shutoff valve was closed to prevent the further adsorption of uranium and fluorine onto the charcoal bed. One of the significant remediation activities planned for the MSRE is the removal of the UF₆, F₂, and the other gases shown in Table 1. For this purpose, the reactive gas removal system (RGRS) project was initiated. The RGRS was designed to remove the reactive gases from the system using three-stage chemical trapping on solid reagents during evacuation of the off-gas volume. The main components of the system are two chemical traps, one filled with sodium fluoride (NaF) and the other filled with activated alumina (Al₂O₃). The UF₆ present in the MSRE off-gas system will be chemisorbed onto the NaF, forming Na₂UF₆, while the fluorine will react with alumina to form aluminum fluoride and oxygen. A third trap containing molecular sieve was added to the system to remove water vapor containing traces of hydrogen fluoride (HF) exiting the alumina trap during fluorine loading. A more detailed description of the RGRS can be found in *Technical Bases of Selection of*

*Trapping Technology for the MSRE Interim Vent Project.*³ This report discusses the laboratory test program that was performed to examine the system's capabilities and limitations and to identify any improvements that could be implemented.

2. OBJECTIVES

Because of the highly radioactive nature of the $^{233}\text{U}/^{232}\text{U}$ daughters and the extreme reactivity and corrosivity of the gases involved, it was necessary to ascertain the compatibility of all of the material and equipment used while minimizing personnel exposure. There were two major objectives of the RGRS testing. The first was to ensure that all process equipment functioned properly and was debugged as much as possible. The process equipment included the actual MSRE reactive gas traps, filled with NaF, alumina, and molecular sieve from the same stock to be used in the process itself. The piping, valves, instrumentation [including pressure transducers, flow controllers, Fourier transform interferometer (FTIR) cells, and thermocouple assemblies], and data monitoring equipment were also to be checked. Based on the results of these tests, recommendations were to be made on modifications and additions that would benefit the overall process. The second objective of the testing was to determine the optimum and safe operating conditions for the overall process. This included maximum gas flow rates, UF_6 concentration, maximum trap temperatures, and loading percentage of gas traps. The laboratory testing operations have been developed through several stages, which are detailed in this report: (1) fluorine trapping tests (FTT); (2) uranium trapping tests (UTT); (3) simple integrated tests (SIT), which combine the previous two traps in the testing procedure; (4) glove box tests at positive pressure (GBTP); and (5) glove box test under vacuum conditions (GBTV). The test runs are identified with these designations so that the reader can more easily follow the numerous figures and other results.

3. DESCRIPTION OF TEST APPARATUS

Figure 1 is a schematic representation of the system used to perform the fluorine trapping tests. The standard equipment used for the fluorine tests is listed in Table 2. To make rapid progress, the initial test setup was small and very simple, achieving full scale only near the end of testing. The use of a simple flanged 1-in.-ID pipe alumina bed was particularly useful in the early tests because complete trials could be completed in only a day or two, and the results provided guidance about limits on the operating parameters (e.g., maximum permissible fluorine flow).

As depicted in Fig. 1, five thermocouples (TE 1–5) recorded outer-wall (i.e., "skin") temperatures, while the other five thermocouples (TE 6–10) registered the internal temperatures and were located in an axial thermowell located about halfway between the centerline and the wall (i.e., the "core" temperature).

Table 2. Equipment used in fluorine trapping tests (FTT)

Equipment item	Description
Alumina trap (1 in.)	1 in.- ID × 12-in. - long nickel-plated flanged pipe
Alumina trap (3 in.)	MSRE trap, drawing ^a
He flowmeter/controller	FC-260, Tylan Corp.
F ₂ flowmeter/controller	FC-260, Tylan Corp.
Data logging and control	SCXI-1000 – Labview – National Instruments Interface
Thermocouples	Type K, 1/8 in. and 1/16 in.
Pressure transducers	Baratron Model 146, MKS, Inc.

^a“MSRE HF/F₂ Trap Assembly,” LMES Central Engineering Services Drawing No. X3E020794A013.

Thermocouples 11 and 12 logged temperatures from the lines leading to the inlet and outlet valve to the alumina bed, respectively. Pressures at the trap inlet and outlet were also measured during the 3-in.-column runs, but a significant pressure drop was never detected.

Figure 2 is a schematic representation of the UF₆ trapping test. The NaF trap was the same 1-in.-diam trap used in the initial fluorine tests. A UF₆ saturator, consisting of a nickel vessel with a dip tube, was used to add UF₆ to the gas stream. The saturator was kept at the desired temperature with a water bath. This temperature was used to control the UF₆ concentration at a given helium flow rate. Thermocouples TE 1–5 measured the skin temperatures at five axial locations along the NaF trap. Also shown is a 10-cm-long gas cell with zinc selenide (ZnSe) windows connected to an infrared (IR) spectrometer (FTIR Bomem MB-104) that was used to continuously determine UF₆ inlet concentration, except when nearing breakthrough, at which time where it was used to continuously monitor to obtain the breakthrough curve.

Figure 3 shows a schematic of the simple test that integrated the trapping of fluorine and UF₆ from a pressurized source. The actual MSRE traps were used in this test. TE 1–5 and TE 6–10 measured the internal temperatures of the NaF and alumina traps, respectively. TE 11–15 measured “skin” temperatures of the alumina trap, while TE 16–17 monitored the temperatures of the valves connected to the alumina trap.

Figure 4 shows a diagram of the process equipment used to generate and control the flow of gases into the glove box containing the traps. Inlet and outlet flowmeters (Tylan Corporation, FC-2901V) were added to the system to measure overall flow rates. Also an actual MSRE trap filled with molecular sieve was added downstream of the alumina trap to retain water and residual hydrofluoric acid released because of the high temperatures in the alumina trap. Refer to the MSRE drawing⁴ for glove box details.

Figure 5 illustrates the system that simulated the proposed removal of gases from the MSRE off-gas system by evacuation.

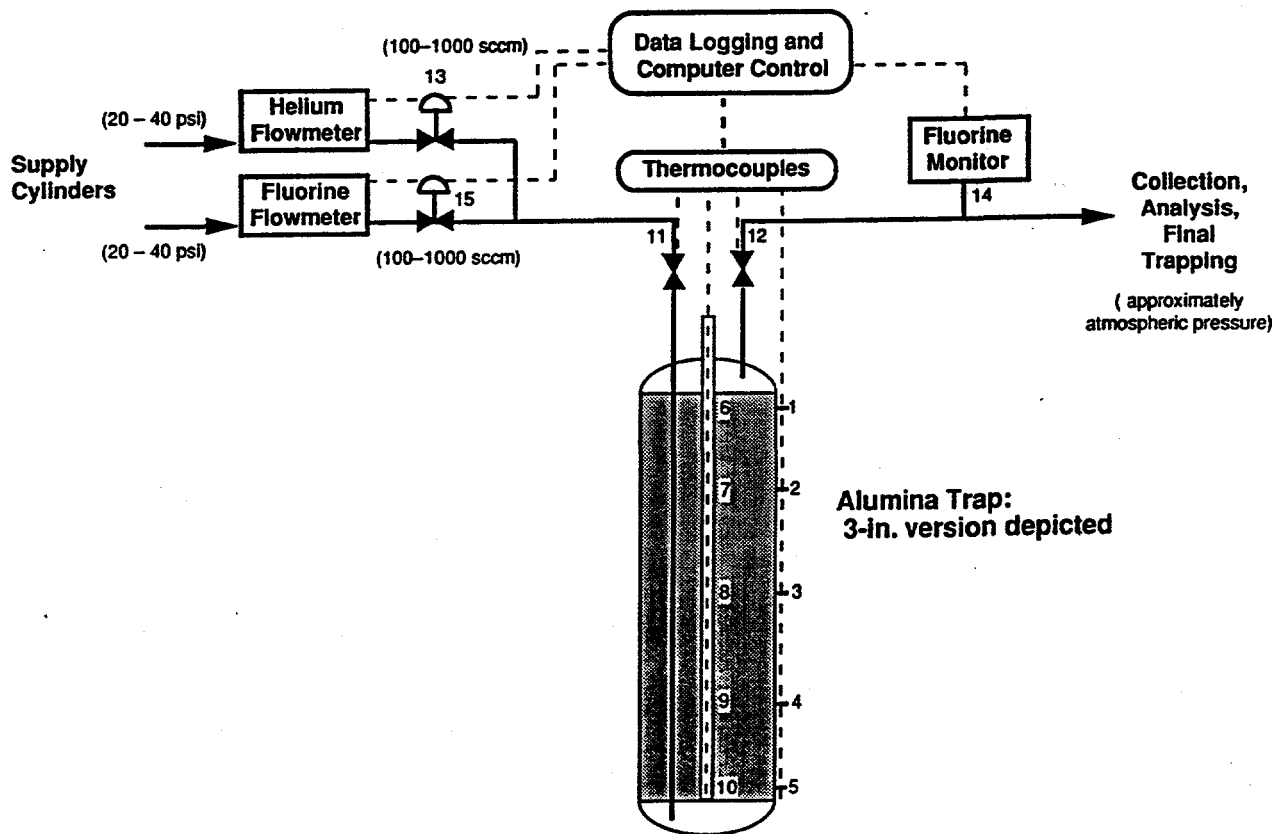


Fig. 1. Diagram of fluorine trapping test (FTT).

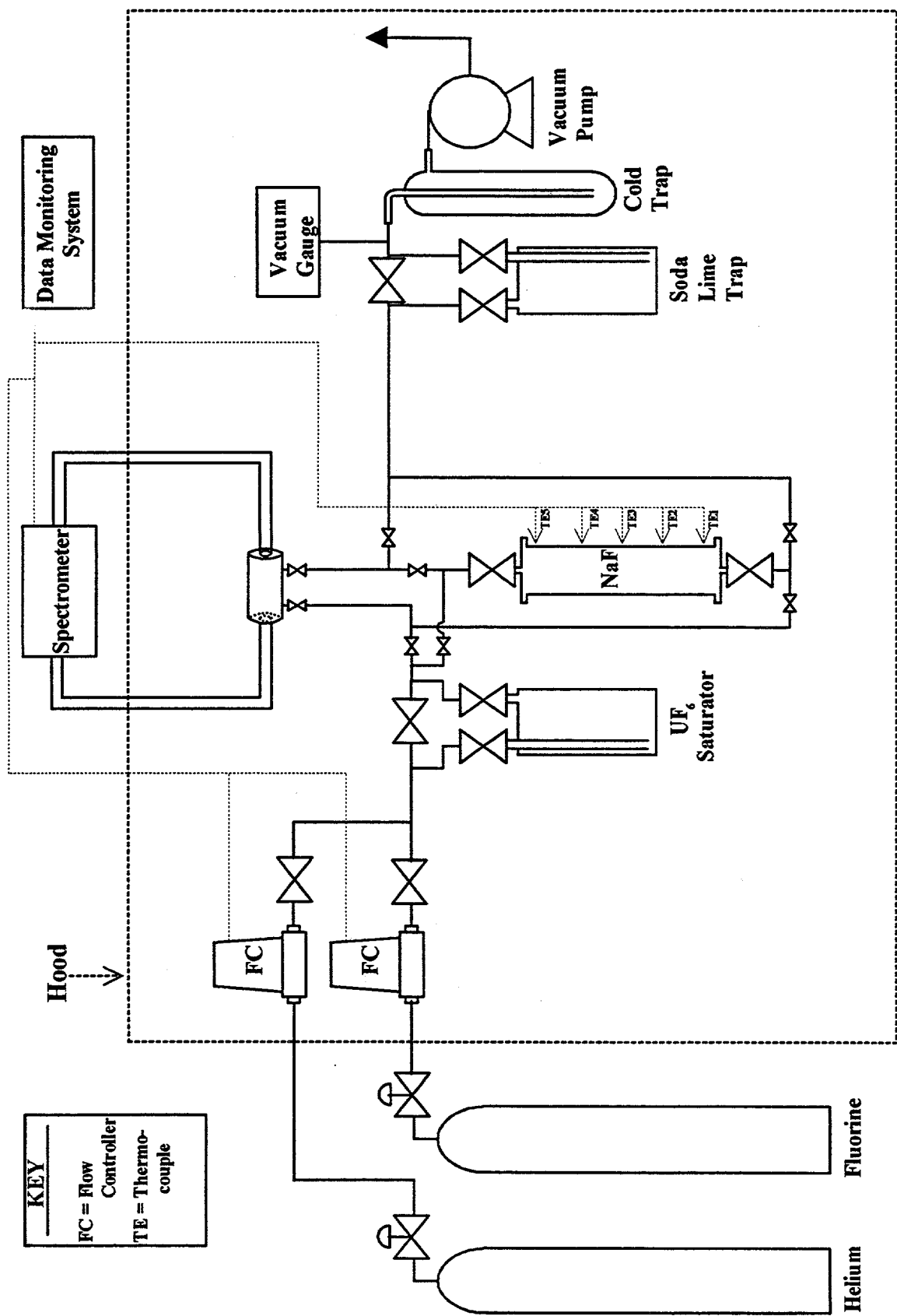


Fig. 2. Diagram of UF₆ trapping test (UTT).

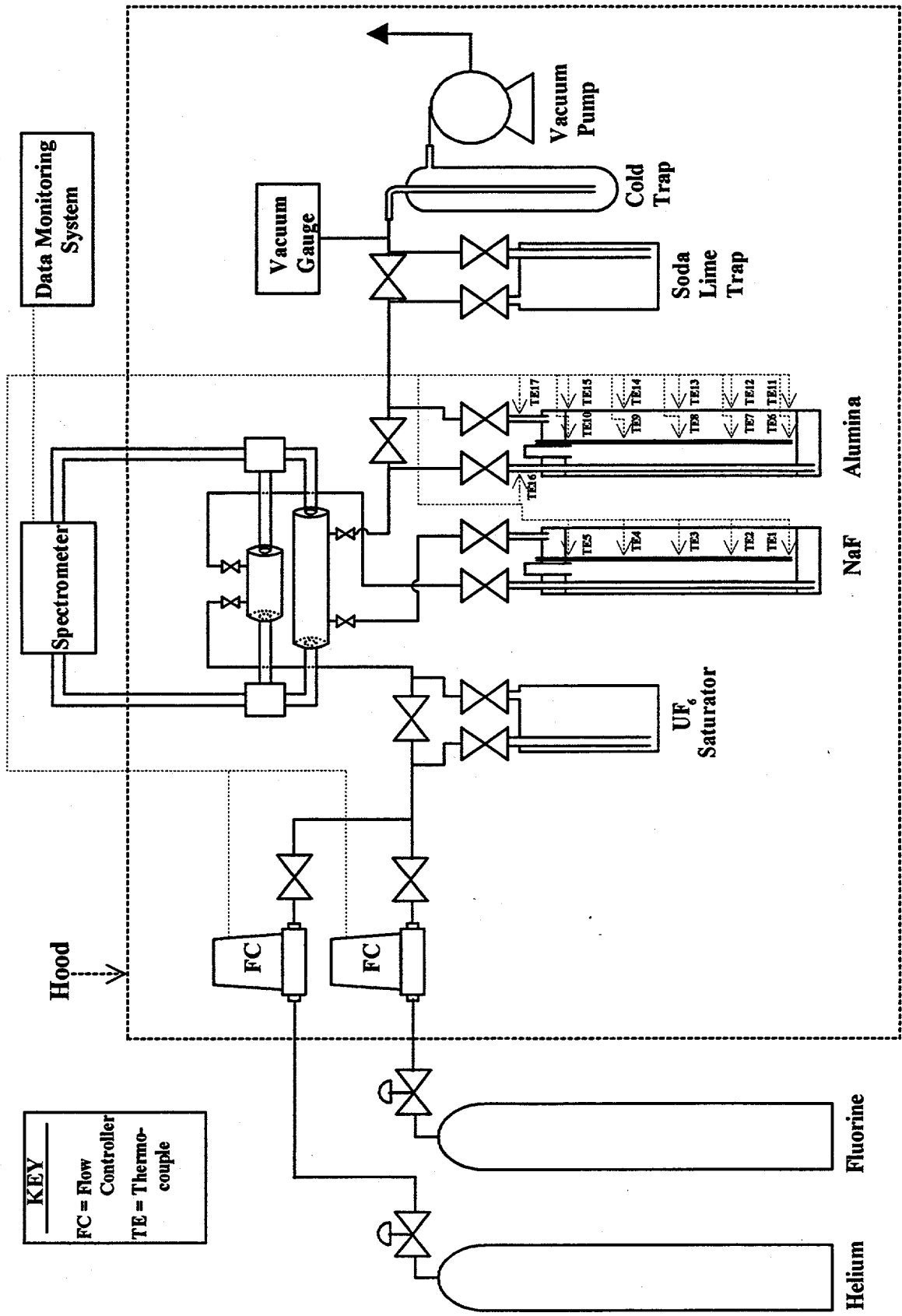


Fig. 3. Diagram of simple integrated trapping test (SIT).

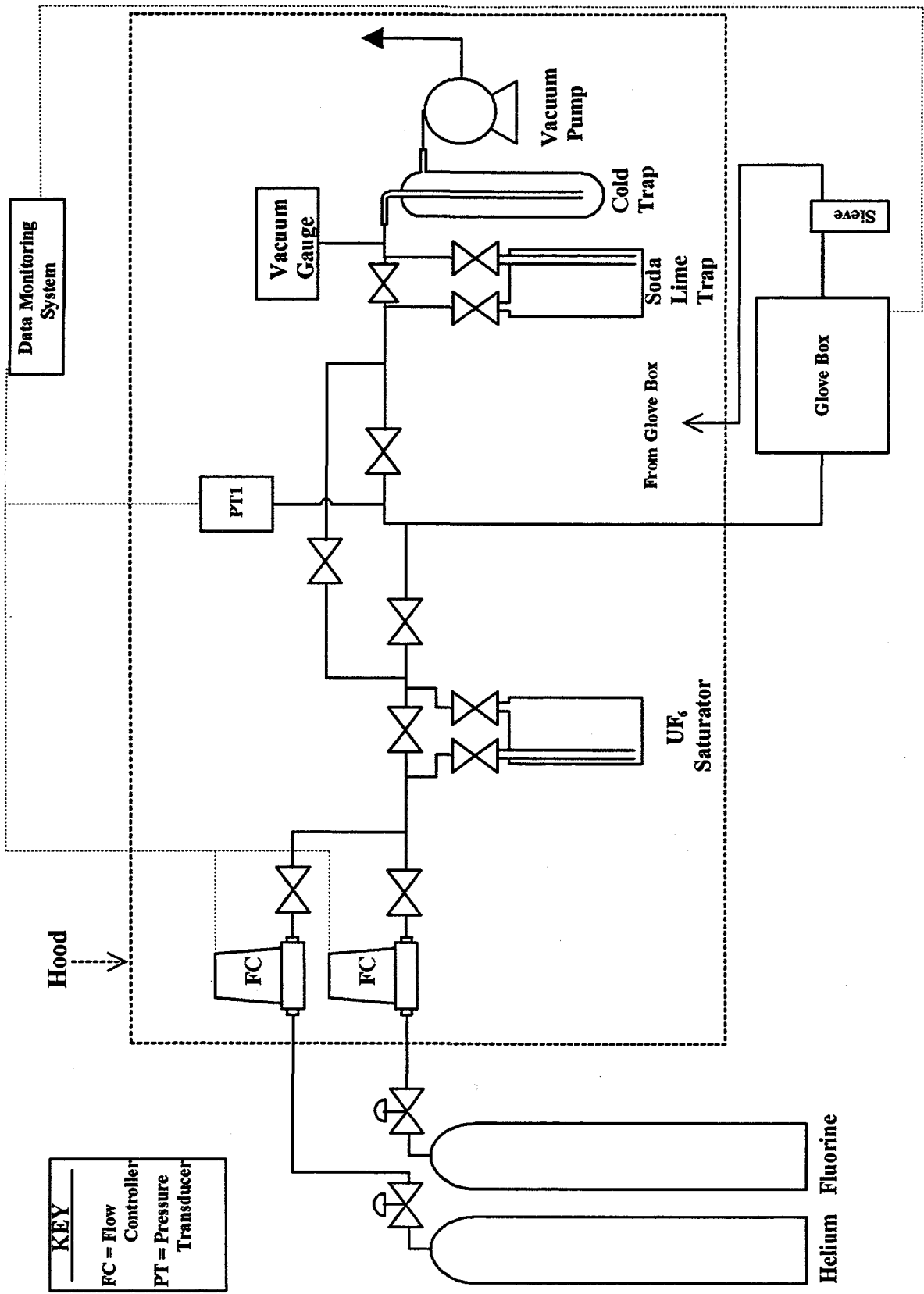


Fig. 4. Diagram of hood portion of glove box tests under pressure (GBTTP).

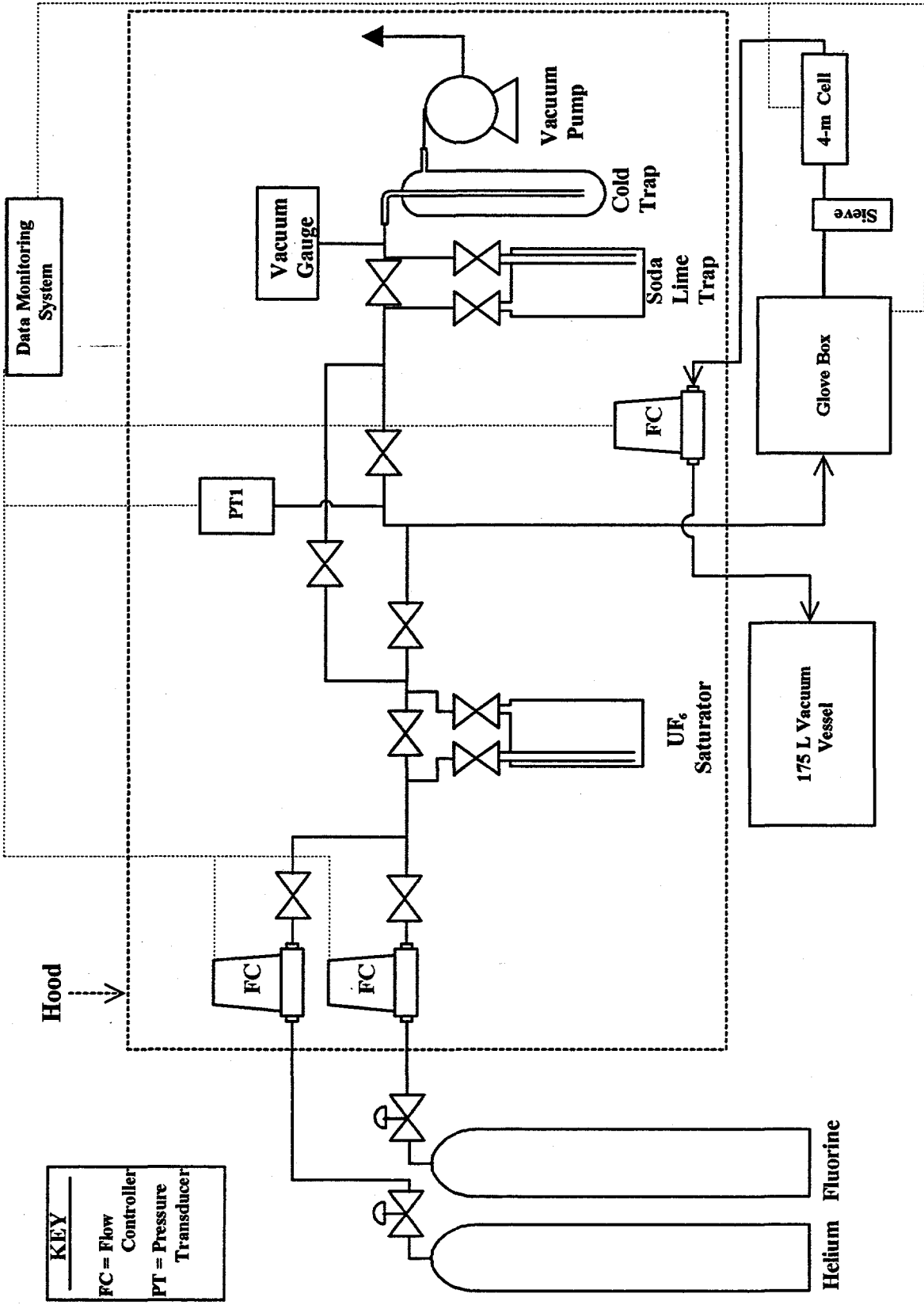


Fig. 5. Diagram of hood portion of glove box tests under vacuum (GBTV).

4. DESCRIPTION AND PROPERTIES OF GAS TRAPPING MATERIAL

Three different gas trapping materials were implemented in the RGRS process: NaF (to trap UF₆); alumina (to trap fluorine); and a molecular sieve, which is a high-surface-area sodium aluminosilicate (to trap water and HF being produced in the alumina trap). As mentioned in the introduction, the molecular sieve was introduced into the process after it was observed that aqueous HF was emitted at the outlet of the alumina trap. The properties of all the materials tested are given in Tables 3–5.

Table 3. Physical properties of NaF pellets for MSRE

Physical property	Units	Portsmouth NaF ^a	K-25 NaF (1987) ^b
Pellet diameter	cm	0.42	0.31
BET surface area	m ² /gm	0.1	1.4
Helium density (dry)	gm/cm ³	2.77	2.79
Pellet density (dry)	gm/cm ³	1.96	1.49
Bulk density (dry)	gm/cm ³	1.02	0.85
Water loss on mild drying	wt %	0.2%	---

^aMeasurements made by L. E. Powell, Membrane Technology Department, Oak Ridge K-25 Site, Jan. 17, 1996.

^bK-25 NaF tests: R. G. Russell, KY/L-1457 (1987).

Table 4. Summary of alumina properties^a

Physical property	Granular alumina ^b	Uniform alumina ^c
BET surface area (m ² /g)	208	346
He density, dry ^d (g/cm ³)	3.19	3.31
Pellet density, dry (g/cm ³)	—	1.21
Bulk density, dry (g/cm ³)	0.81	0.67
Weight loss on mild drying (%)	15.5	1.2

^aMeasurements made by L. E. Powell, Membrane Technology Department, Oak Ridge K-25 Site, Dec. 8, 1995.

^b"Granular" surplus K-25 activated alumina, ~4 × 8 mesh, believed to be F-1 grade.

^c"Uniform" spherical A-201, 5 × 8 mesh, La Roche Chemicals.

^dDried under mild conditions.

Table 5. Summary of molecular sieve (13X) properties^a

Physical property	
Diameter (cm)	0.318
Bulk density (g/cm ³)	0.61
Equilibrium H ₂ O capacity (wt %)	28.5
Heat of adsorption (kcal/g H ₂ O)	1.00

^a*Handbook of Separation Techniques for Chemical Engineers*, ed. P. A. Schweitzer, McGraw Hill Book Company, pp. 3-22, New York, 1979.

The NaF used in the test runs was received as sodium bifluoride (NaHF₂). The material was heated to 400°C for periods in excess of 24 h with a helium purge to remove HF. The material was then fluorinated at 0.3 atm for 30 min (also at 400°C) to remove any residual oxides from the system.

The alumina was also pretreated by heating for periods greater than 3 h under a helium purge to reduce the water content. For the initial test, the alumina was dried at 300°C. For the remaining FTT, it was treated at 400°C; for the integrated tests, it was treated at 600°C (Table 6). The reason for the increased treatment temperature was to minimize the moisture (and therefore the HF) liberated during fluorine loading.

Table 6. Preparative drying results for alumina^a

Material	Drying temperature (°C)	Drying period (h)	% Weight loss
Granular alumina	30	2	12
		4	20.9
		7	21.6
		24	21.6
Uniform alumina	300	4-6	3.4-4.1
	400	4-6	4.5-5.1
	500	3-6	5.5-6.5
	600	3-4	6.0-7.0

^aAll drying conducted with a helium purge.

Thermogravimetric results on a small sample of uniform alumina are shown in Fig. A.1 (see Appendix A). The molecular sieve material (a porous sodium aluminosilicate cage) was treated by heating at 200°C for 24 h with a helium purge.

5. FLUORINE TRAPPING RESULTS (FTT)

The major test parameters were (1) trap diameter, (2) fluorine flow rate, and (3) the wall condition, that is, "naked" or "shrouded" operation (with or without carrier in place). The values of these primary parameters for the fluorine trapping trials are summarized in Table 7.

Table 7. Major parameters for fluorine trapping tests (FTT)

FTT no.	Trial date	Column ID (in.)	Nominal fluorine flow (SLM)	Wall condition	Type of alumina
1A	11/15/95	1	0.10–0.20	Naked	Granular
1B	11/16/95	1	0.10–0.20	Naked	Granular
2	11/22/95	1	0.15	Naked	Uniform
3A	11/29/95	3	0.30	Naked	Uniform
3B	11/30/95	3	0.25	Naked	Uniform
3C	12/1/95	3	0.30	Naked	Uniform
3D	12/4/95	3	0.50	Naked	Uniform
3E	12/5/95	3	0.60	Naked	Uniform
3F	12/6/95	3	0.60	Naked	Uniform
4A	12/18/95	3	0.60	Shrouded	Uniform
4B	12/21/95	3	0.80	Shrouded	Uniform
5A	1/8/96	3	0.80	Shrouded	Uniform
5B	1/9/96	3	1.00	Shrouded	Uniform

The term "nominal" fluorine flow represents an average flow after it stabilized. The flow was started at a low value at the beginning of a run and increased in steps to avoid uncontrolled excursions. This had only a minor effect upon the peak temperatures and the breakthrough behavior. In all cases the helium flow was roughly equal to the fluorine flow.

The first two runs, made using a 1-in.-ID column, present the clearest picture of an uninterrupted trap loading. For these runs (1A and B, 2), only the skin temperature was measured. During the first trial the fluorine flow was changed a number of times in the 0.10–0.20 standard liter per minute (SLM) range, in order to find the maximum flow consistent with a 300°C skin temperature (Figs. A.2 and A.3, see Appendix A). It appears that this flow is somewhere between 0.15 and 0.20 SLM of fluorine for a 1-in-ID trap with granular alumina. The second test involved a complete loading trial (Fig. 6) and was conducted using the actual uniform spherical alumina particles to be used at MSRE. The fluorine flow was held steady at 0.15 SLM during the entire run, and a distinct fluorine breakthrough was evident at the end of the run. Fluorine breakthrough occurred just after the temperature maximum at the bed exit was reached (Fig. 7). It was obvious from these runs that the initial design flow rate of 20 L/min was too high by at least one, and possibly two, orders of magnitude.

The first series of trials with the 3-in.-ID trap (test no. 3) was conducted "naked" (i.e., without the trap carrier in place.) It required 6 days of flow to completely load the trap at fluorine flow rates that ranged from 0.30 to 0.60 SLM. During each successive trial the nominal fluorine flow was increased to determine its influence on the measured bed temperatures. The results from these trials are somewhat marred due to a data-logging error caused by a bug in the software that produces steps in the measured temperatures (Figs. A.4 to A.15 in Appendix A). However, it was confirmed that the logged temperatures were substantially correct during the trial by comparison with an independent readout device. Again the fluorine breakthrough occurred near the maximum in temperature at the bed exit (Fig. 8). For these runs the valve temperatures ranged from 20 to 105°C, as seen in Figs. A.16 to A.21 (Appendix A).

The second set of trials with the 3-in. bed (test no. 4) was conducted with the trap loaded in its carrier (i.e., "shrouded") and at the highest fluorine flow rates that were expected to be tolerable (0.60–0.80 SLM). The bed and valve temperatures for these runs ranged from 20 to 180°C and are shown in Figs. A.22–A.27 (Appendix A).

The final operation with the 3-in.-ID trap was conducted at a fluorine flow rate of 0.80–1.00 SLM with the carrier in place. The main purpose was to identify the maximum temperature the trap could reach under these flow conditions. It was not necessary to run to breakthrough to achieve this objective. The bed and valve temperatures for this test are displayed in Figs. A.28–A.33 in Appendix A.

A fairly consistent trend can be seen when the maximum observed temperatures are plotted as a function of the fluorine flow rate. Figure 9 and Table 8 suggest that the peak temperatures (skin,

internal, and valve) are proportional to the fluorine flow rate. Measured internal temperatures were 100–200°C hotter than the skin temperatures. The actual temperature in the alumina particles is significantly hotter than the measured internal temperatures. The presence of the external carrier around the trap accounts for about a 100°C rise in both the skin and internal temperatures at the 0.60-SLM fluorine flow rate.

Table 9 contains the overall trap loadings achieved after operation up to breakthrough. The

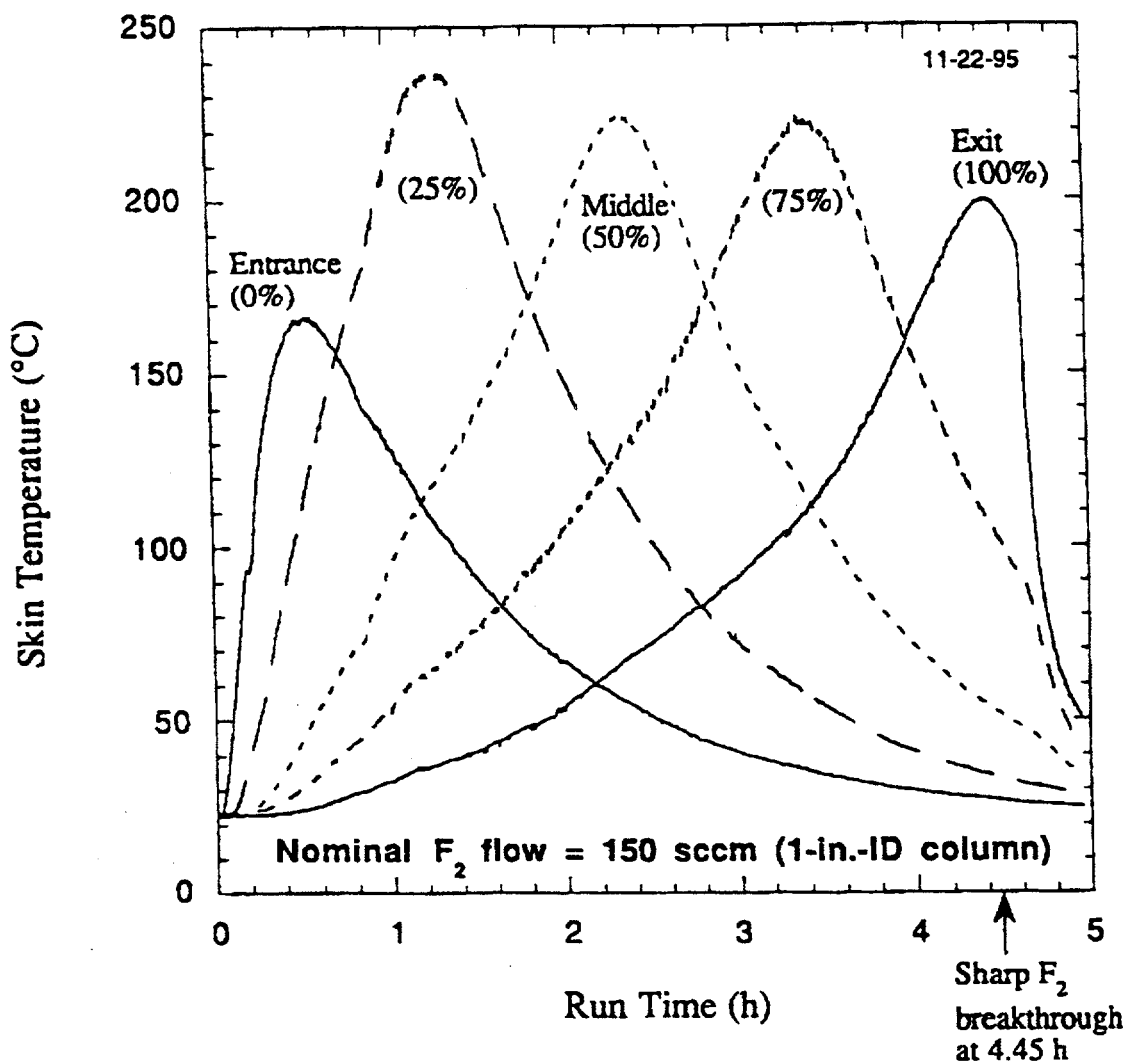


Fig. 6. Skin temperatures for FTT-2, 150 sccm fluorine, 1-in.-ID trap.

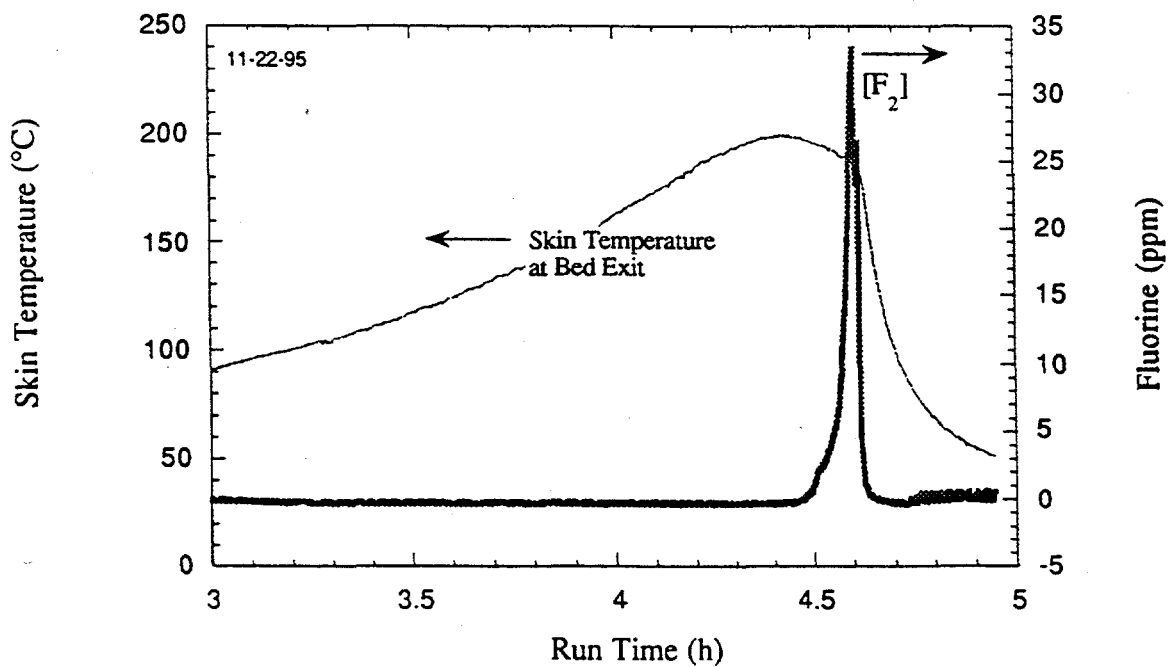


Fig. 7. Fluorine breakthrough during FTT-2, 150 sccm fluorine, 1-in.-ID trap.

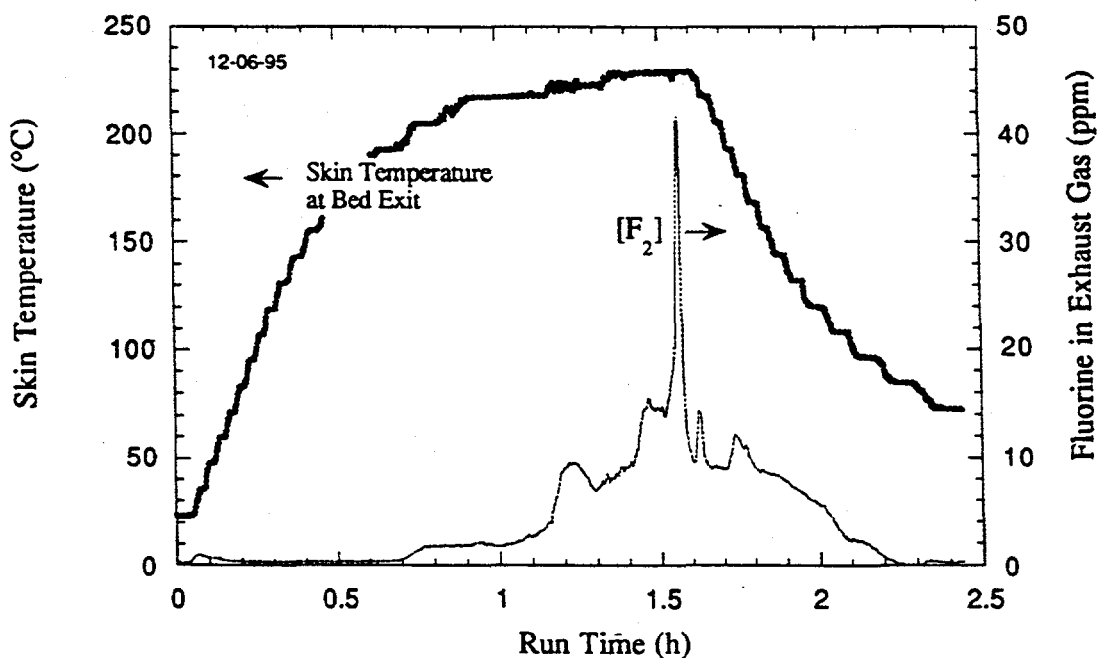


Fig. 8. Fluorine breakthrough during FTT-3F, 600 sccm fluorine, 3-in.-ID trap.

Table 8. Peak temperatures measured in 3-in. alumina bed

Fluorine flow (SLM)	Wall condition	Skin temperature (°C)	Interior temperature (°C)	Outlet valve temperature (°C)
0.30	"Naked"	149	270	28
0.50		216	382	48
0.60		254	452	104
0.60	"Shrouded"	375	540	60
0.80		450	640	180
1.00		460	695	—

Table 9. Measured fluorine loading of alumina traps

FTT no.	Measured peak temperature (°C)		% Weight gain	Loading (liters F ₂ per gram alumina)	Theoretical loading (%)
	Skin	Interior			
1	330	—	41	0.415	63.4
2	240	—	36	0.366	55.6
3	250	420	44.9	0.457	69.3
4	450	580	45	0.458	69.5

loadings correlate as expected with the temperature of the bed. The weight change per standard liter (SL) of fluorine, based on a stoichiometric reaction with alumina, is 1.014 SL per gram of weight change (see Appendix B). This provides a quick estimate of the fluorine trapped.

Some final comments are required regarding the fluorine breakthrough during the high-temperature operation of the 3-in. traps during tests 4 and 5. For these runs the fluorine breakthrough was somewhat obscured by the presence of HF in a moist atmosphere. The F₂ breakthrough in Fig. 8 is correct, but small amounts of HF left the trap long before the true breakthrough. The water vapor resulted from the dehydration of alumina due to the extreme heating in the reaction front beyond the temperatures originally used to dry the alumina (in this case, ~ 400°C). This moist, corrosive, and acidic exhaust collected as a liquid in the cool exit lines and in a downstream cold trap. Thus a clear

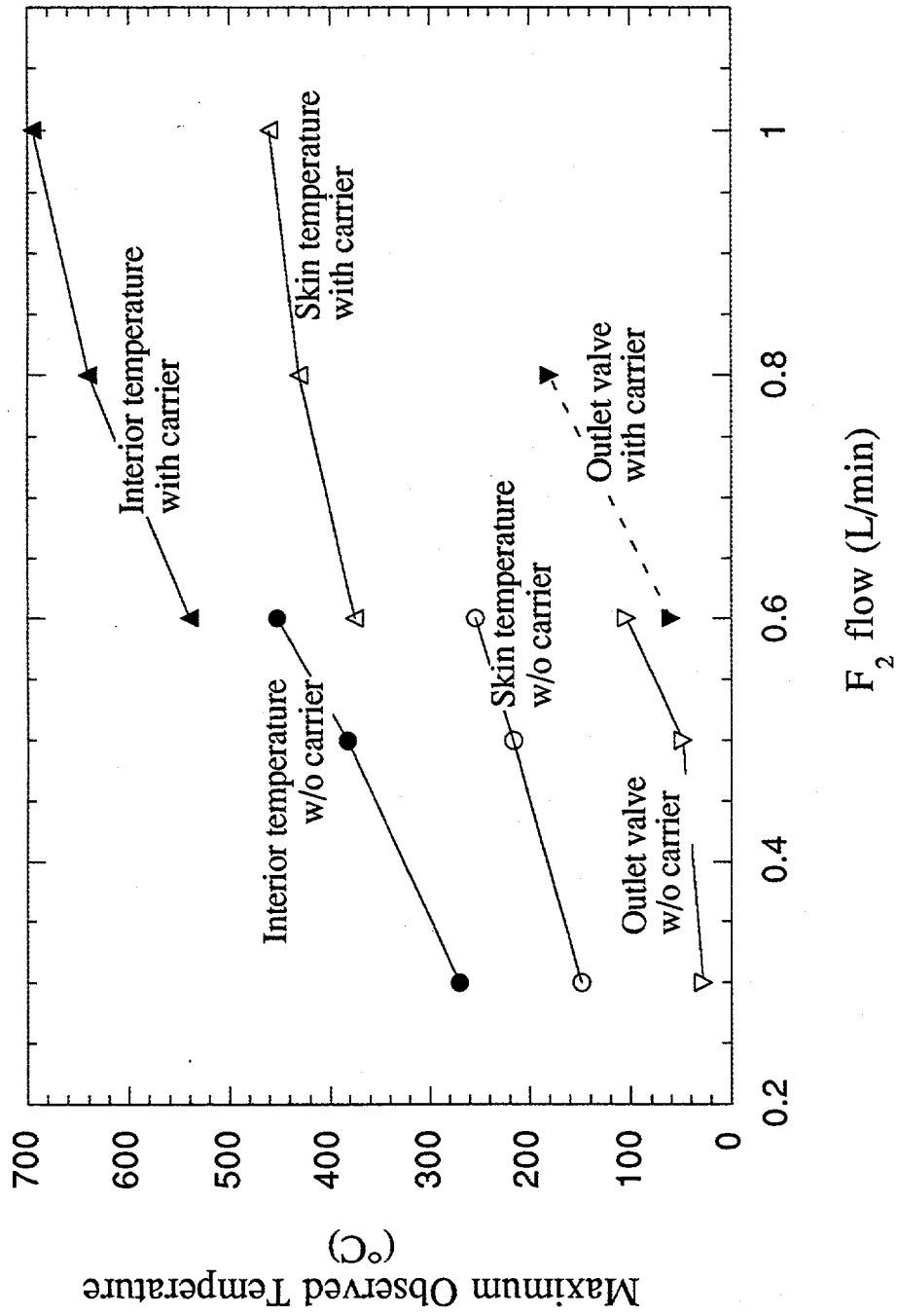


Fig. 9. Summary of peak temperatures measured in FFT with 3-in.-ID column.

(measured) history of the evolution of HF from the trap exhaust is not available. A summary of the fluid collected during runs 4 and 5 is presented in Table 10.

Table 10. Characteristics of liquid collected from the alumina trap exhaust

FTT no.	Volume (mL)	[F ⁻] (M)
4	8.4	0.36
5	16.5	0.03

The liquid collected from run 4 is only a portion of the condensable vapor that was generated near the completion of the run, but the liquid from run 5 represents all of the vapor in the exhaust gas. Note that the fluid is mainly water, and that for run 5, when only 50% of the trap was reacted, the fluoride concentration was much lower. The metal ions present, shown in Table 11 for run 4, originated from corrosion of the metal parts present in the exhaust piping. An examination of the bronze elements of the exit valve revealed severe corrosion, which correlated with the difficulty of maintaining a good valve seal during and after operation.

6. UF₆ TRAPPING RESULTS (UTT)

The UF₆ trapping test was a simple test that had several purposes. The most important was to examine the loading characteristics of UF₆ onto the NaF. It was necessary to make sure that the NaF pellets could effectively trap UF₆ at the same flow rates used in the F₂ trapping tests. The UF₆ inlet and outlet concentrations were determined by FTIR spectroscopy. The spectrometer was calibrated with known partial pressures of UF₆ to obtain a calibration curve (Fig. A.34, see Appendix A). This calibration curve agrees very well with literature data.⁵ Another calibration with low concentrations of UF₆ (as would be expected at breakthrough) was also performed (Fig. A.35). The IR absorbances for these gases were only ~ 50% of those predicted by the literature.⁵ It is believed this was because the system was not completely passivated and some of the UF₆ deposited on the walls. The lower absorbances were apparent in the second calibration, and not in the first, because of the very low pressures used in the second. However, the calibration is conservative since, for given absorbance, the partial pressure translated is higher than that given in the literature.⁵ Therefore, the total amount of material which breaks through is overestimated. The test was also used to evaluate the behavior of the UF₆ saturator as a means of transferring UF₆ to the gas stream and the FTIR as an on-line analysis

technique. The test conditions are shown in Table 12. The results showed that the UF₆ saturator worked well, but the water bath temperature had to be continuously adjusted to obtain a relatively constant inlet concentration of UF₆ (Fig. 10). The maximum temperature observed on the NaF trap was 54°C (Fig. 10).

Table 11. Metals analysis of FTT-4 condensate^a

Metal	Result (mg/L)
Ag	<0.25
Al	10.0
As	<2.5
B	<4.0
Ba	<0.05
Be	<0.05
Ca	0.74
Cd	<0.25
Co	7.1
Cr	330.0
Cu	4.5
Fe	1000.0
Li	98.0
Mg	<1.0
Mn	36.0
Mo	<2.0
Na	29.0
Ni	1200.0
P	<15.0
Pb	<2.5
Sb	<2.5
Se	<5.0
Si	46.0
Sn	<2.5
Sr	<0.05
Ti	<2.0
V	<0.1
Zn	2.7
Zr	<2.

^aAnalysis Procedure No. EPA 200.7.

Table 12. Test conditions for UF₆ loading onto 1-in. NaF trap

Amount of NaF used	96.1 g
Helium flow rates	0.1 SL/min for <8 min 0.5 SL/min for 8 – 22 min 1.2 SL/min for 22 – 63 min
UF ₆ partial pressure	45 – 80 torr
Total pressure	Atmospheric
UF ₆ loaded	74.8 g (by weight), 75.1 g (by flow data)
NaF utilization	0.78 g UF ₆ /g NaF (68% of theoretical)
Equilibrium loading	1.15 g UF ₆ /g NaF

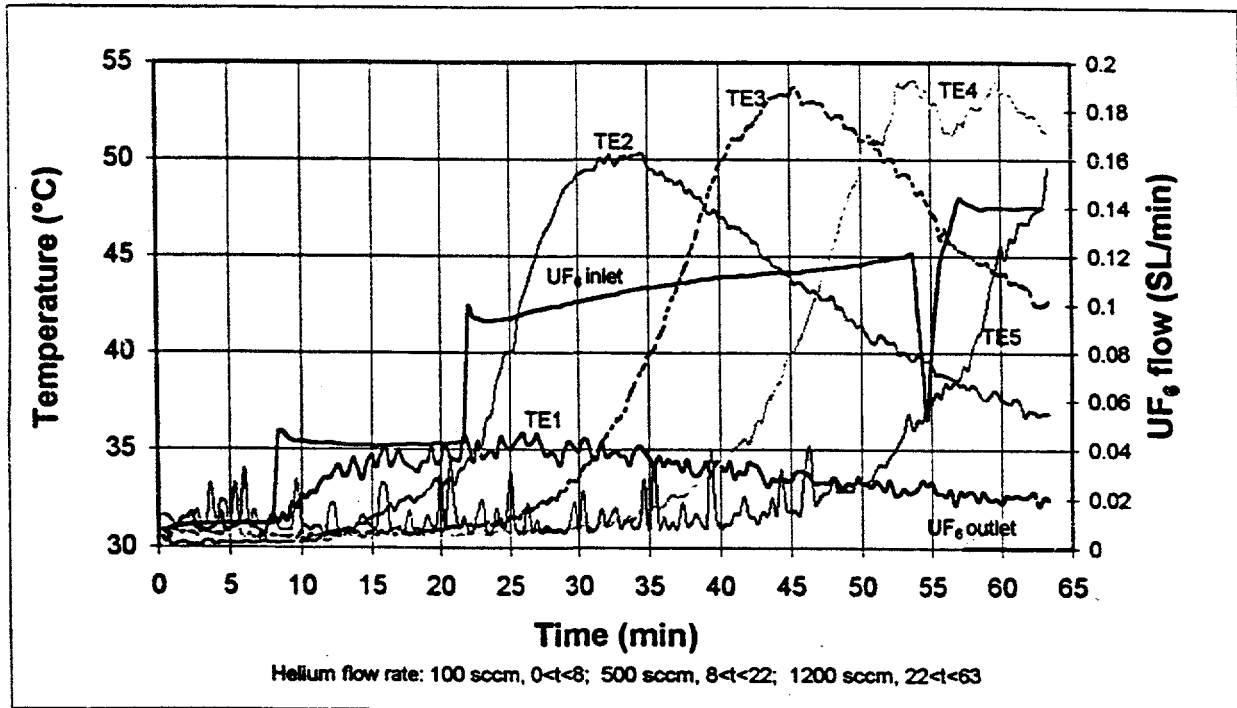
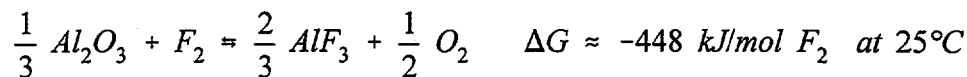


Fig. 10. Skin temperatures and UF₆ flow rate vs time, 1-in. NaF trap, February 9, 1996.

As depicted, breakthrough of the trap was observed prior to reaching a peak temperature at the top of the trap. This demonstrates that the reaction front in the NaF trap is broader than that of the alumina trap. This is consistent with the smaller free energy change (ΔG) associated with the NaF/UF₆ reaction (or chemisorption):³



The smaller free energy change, along with lower concentrations of UF_6 and slower kinetics, is responsible for the broader, less intense thermal reaction front seen in the NaF bed.

The measured loading of UF_6 onto the NaF was 74.8 g, which corresponds 0.78 g UF_6 /g NaF. The loading of UF_6 was also determined by integrating the UF_6 flow rate (UF_6 concentration/total flow) over the length of the run. The loading obtained by integration was 75.1 g of UF_6 . This excellent mass balance provides good confidence in the FTIR as a quantitative tool for determining UF_6 loading. This loading also was consistent with the 1.15 g UF_6 /g NaF loading achieved in a 24-h equilibrium test performed earlier.

A desorption test was performed on this material, but was only partially successful. This was because the vessel used for desorption, thought to be nickel, was actually stainless steel. The steel suffered severe corrosion, forming CrF_3 . The presence of CrF_3 made a weight loss desorption analysis impossible.

7. SIMPLE INTEGRATED TEST (SIT)

This test was designed to test key process components without excess system hardware. It was run under conditions very similar to those in the fluorine tests previously described. Table 13 shows the run parameters and results. The gas flow rates were adjusted, as when the alumina internal thermocouple reading the highest temperature (i.e., the location of the front) reached a peak. Figures 11 and 12 show temperatures on the NaF and alumina trap, respectively. The maximum temperatures on the NaF and alumina were 55 and 530°C, respectively. The alumina trap was not surrounded by a carrier during this run, which explains the lower temperatures observed. The overall loading of UF_6 was 1273 g. (67.5 wt %). This result is reasonably close to that obtained in the 1-in. trap test. The slightly lower loading

percentage could be partially due to the earlier shutdown after breakthrough. The alumina loading was 410 SL of F₂, or 0.298 L/g of alumina. This represents ~ 65% of the expected capacity based on the fluorine test 3 (Table 9).

Table 13. Test conditions for the simple integrated test (SIT)

NaF loaded	1886 g
Alumina loaded	1377 g
F ₂ flow rate	0.56 SL/min for < 1.5 h 0.74 SL/min for 1.5 – 6.1 h 0.93 SL/min for 6.1 – 9.0 h (end)
He flow rate	Equal to F ₂ flow
UF ₆ partial pressure	56 – 79 torr
UF ₆ loaded	1273 g or 0.675 g UF ₆ /g NaF
F ₂ reacted	410 SL or 0.298 L/g alumina
Maximum NaF temperature	55°C
Maximum alumina temperature	533°C

After achieving breakthrough, the NaF trap was replaced by the alumina trap to test the direct loading of UF₆ onto alumina. The conditions and results of this test are shown in Table 14: 154 g of UF₆ was adsorbed by the alumina trap, but there was partial breakthrough before this quantity of UF₆ was loaded. The UF₆ breakthrough was not immediately obvious because the UF₆ reacted with water generated by dehydration of alumina. This formed UO₂F₂·xH₂O in the trap, some of which was carried into the downstream piping. Therefore, although uranium had penetrated the alumina trap, it was not detected in the FTIR cell because no UF₆ was present. The test was ended when a plug of UO₂F₂ formed in the inlet valve to the FTIR.

Upon completion of the test, it was noticed that light transmission through the 20-cm cell (downstream cell) had decreased by two orders of magnitude. It was determined that this was caused by the reaction of aqueous HF, released from the alumina trap, with the ZnSe cell windows. This attack clouded the windows and greatly reduced their transparency. The windows were replaced prior to additional testing.

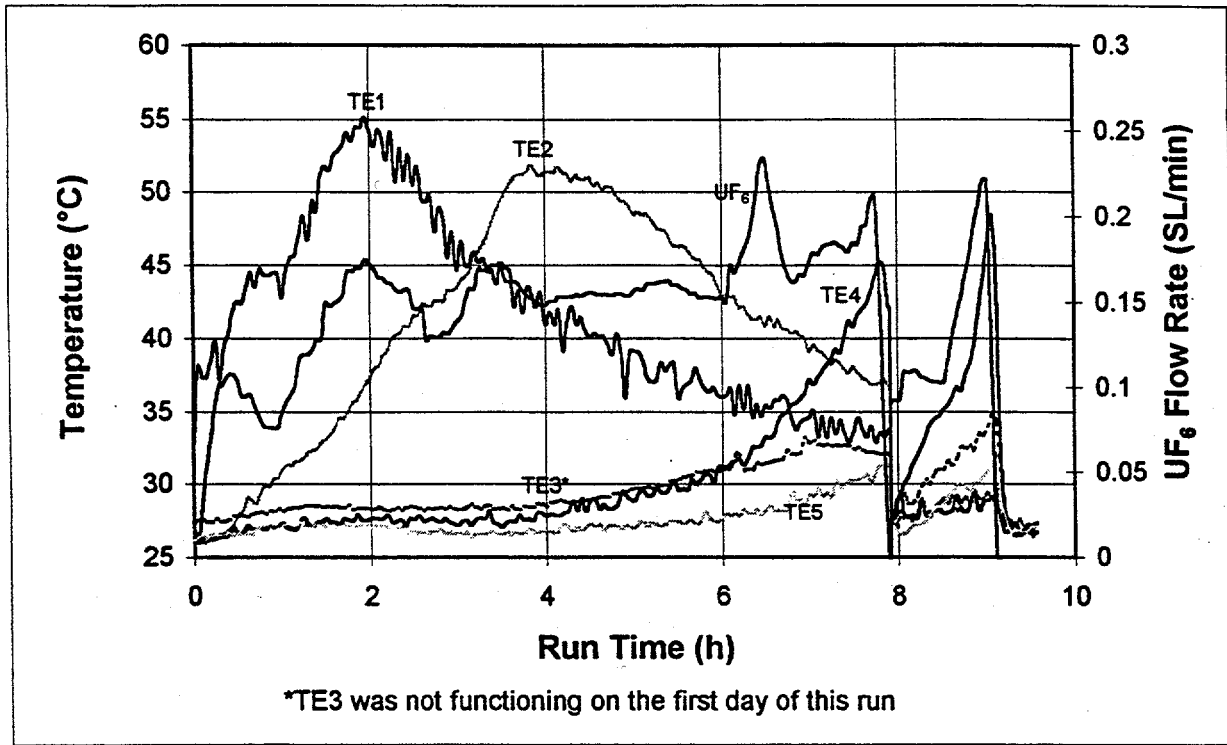


Fig. 11. Sodium fluoride temperatures and UF₆ flow rate, SIT.

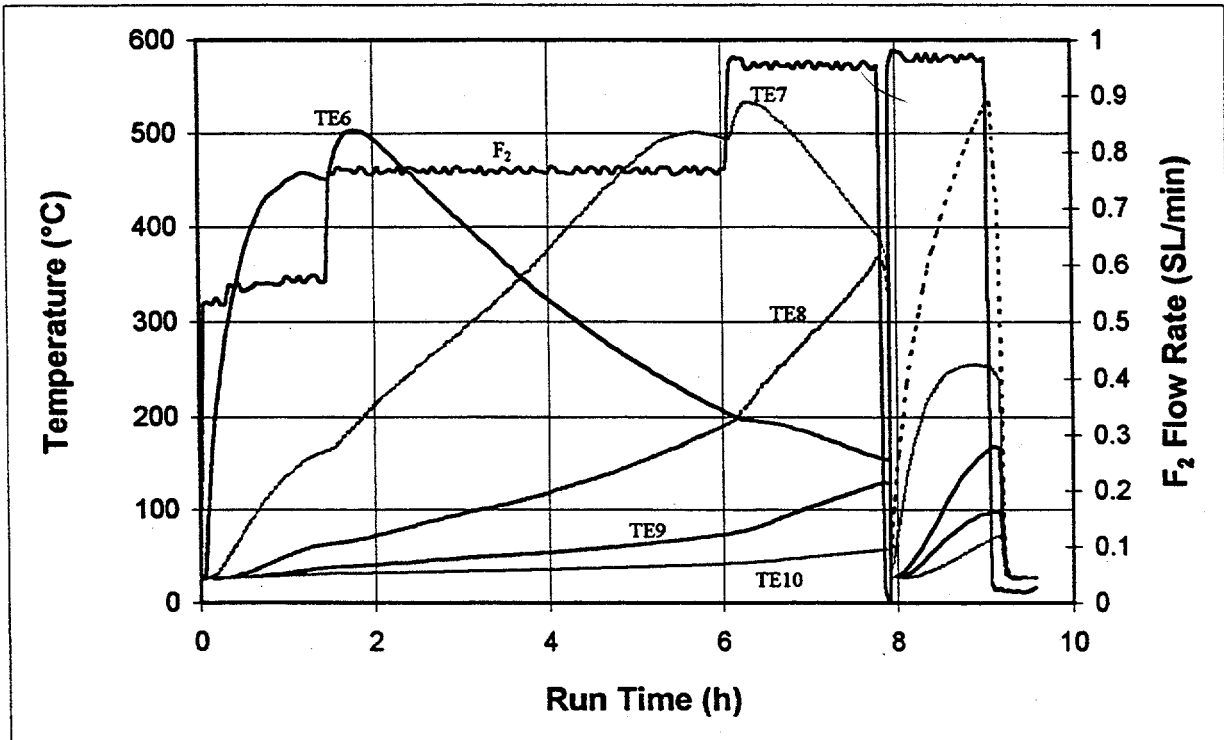


Fig. 12. Alumina internal temperatures and F₂ flow rate, SIT.

Table 14. Parameters and results from direct loading of UF₆ onto alumina

Helium and fluorine flow rate	1.0 SL/min each
Time	46 min
UF ₆ partial pressure	~ 70 torr (average)
Weight change	200 g
Weight of F ₂ added	79.5 g
Weight of O ₂ released	33.5 g
Weight of UF ₆ loaded	154 g

The NaF loaded with UF₆ from this test was tested again for desorption. This desorption cycle was carried out using the actual NaF trap. The process removed 99.3 wt % of the loaded UF₆, leaving only 8.7g on the trap. While the desorption was successful, it was also very slow (approximately 30 h). The desorption was performed by heating the trap up to between 300 and 400°C and flowing helium with 1-4% fluorine through the system at between 0.3 and 0.8 SLM. The exit gas was transferred through a heated line back to the UF₆ saturator, which was cooled with liquid nitrogen to recover the UF₆. The process was monitored using the FTIR cells to ensure that desorption was complete and that little UF₆ bypassed the saturator. Larger flow rates could not be used since high residence time was required to saturate the gas with UF₆; faster rates also tended to cause plugging at the saturator inlet.

8. GLOVE BOX TESTS

These tests used roughly the same configuration as the simple integrated test with the exception that the MSRE traps were located inside the glove box with all of its associated piping⁴ (MSRE drawing no. X3E020794A023). These tests were divided into two categories: positive pressure and vacuum. The first were operated at positive pressure, with the exhaust gases being released to the hood. The vacuum tests operated at subatmospheric pressures, and the exhaust gases were collected in an evacuated tank.

8.1 POSITIVE PRESSURE FLOW TESTS (GBTP)

The positive pressure flow trials were performed first. In addition to the glove box piping, a molecular sieve trap was placed downstream of the alumina trap. All lines between these two traps were

heated to $\sim 120^{\circ}\text{C}$. The purpose of these additions was to keep HF and water generated in the alumina trap in the form of vapors until they reached the molecular sieve, where they would be adsorbed. The copper valves stems on the alumina trap outlet valve and on the molecular sieve inlet valve were gold plated to protect them from corrosion by HF. Included in the glove box setup were three nondestructive analysis (NDA) detectors, located in the bottom, middle, and top of the trap. These detectors measured the increased attenuation of gamma rays, across the trap, from a ^{57}Co source as the reaction front passed its location on the trap.⁶ Table 15 shows the relative positions of the thermocouples and NDA detectors on the alumina trap. Also added was a mass flowmeter at very end of the system. Its purpose was to determine if the oxygen generation in the fluorine trap was actually half of the fluorine input. However, there were difficulties in recording data from the flowmeter, and its output was not used in these tests.

Table 15. Axial positioning of thermocouples and NDA detectors on gas traps^a

Instrument	Bottom	NDA1	TC1	TC2	NDA2	TC3	TC4	NDA3	TC5	Top
Position (in.)	0	.28	.43	4.01	6.376	7.59	11.2	12.48	14.8	15.1

^aMSRE drawings (LMES Central Engineering Services Drawing Nos. X3E020794A013 and X3E020794A09).

When the NaF trap was first attached to the system and the line was fluorinated, HF and water were observed. This indicated that moisture had somehow penetrated the NaF trap. The moisture and HF that came off the NaF trap damaged the 10-cm cell windows. To change the cell windows, the back plate had to be removed from the glove box. The trap was removed and heated to roughly 200°C to remove the moisture. This indicates the importance of confirming and maintaining the dryness of the NaF in the traps, since changing the cell windows is a major task that requires breaking both primary and secondary containment.

Upon reinstalling the cells and the NaF trap, a restriction was identified by a pressure differential across the trap. The trap was again removed, and the inlet and outlet lines on the trap were rodded out. The pressure drop across the trap disappeared, but liquid was observed exiting the outlet line of the trap. Apparently all of the aqueous HF had not been removed in the first treatment. It was then decided to subject the trap to the same conditions used for initial NaF treatment. The trap was reconnected to the system and prepared for the next run. This was done on a weekend so there was a 2-day lag between connecting the trap and starting the test.

When the test was initiated, a restriction was observed and was again traced to the NaF trap. The system was evacuated and then pressurized to 100 psia in an attempt to dislodge the partial plug, but this

process was not successful. The run was then continued at a much slower rate of UF₆ loading. Table 16 shows run parameters and approximate pressure drops across the NaF trap. The second increase in pressure during the first day of testing occurred when the trap was mechanically vibrated in an attempt

Table 16. Parameters for GBTP^a

Date	F ₂ flow (SL/min)	He flow (SL/min)	UF ₆ flow, av (SL/min)	Duration (h)	~ ΔP (torr)
3/25/96	0.56	0.6	0.061	2.5	750
	0.74	0.8	0.065	1.5	1250
	0.74	0.8	0.047	2.5	1750
3/26/96	0.74	0.8	0.041	3	2100
	0.35	1.21	0.052	4.5	1550
3/27/96	0.15	1.45	0.054	9.5	1300
3/28/96	0	1.61	0.058	4 (breakthrough)	1150

^aWeight of NaF = 2003.5 g; weight of alumina = 1387.2 g.

to remove the restriction. When the inlet piping was not heated to increase the vapor pressure of UF₆, the high upstream pressure prevented loading a high UF₆ concentration (Figs. A.36, A.38, A.40, and A.42, see Appendix A). This fact extended the required loading time to 4 days and lowered the peak temperatures observed on the NaF trap. The fluorine trap behaved normally, but reached much lower temperatures than in past tests, as the fluorine concentration was low throughout the run. Table 17 shows the maximum temperatures observed in the two traps (Figs A.36 – A.43 in Appendix A) and UF₆ and F₂ loadings. The UF₆ loading on the trap was quite high during this run (1450 g, or 0.74 g UF₆/g NaF) and can be attributed to the slow loading rate, which produced a very narrow front. As Fig. 13 shows, UF₆ breakthrough was detected at very low concentrations. At the helium flow rate used during this run (1.6 SLM), the UF₆ flow rate of 0.0001 SLM corresponds to 60 ppm. The area under the breakthrough curve represents less than 45 mg of ²³⁸U using the conservative calibration curve developed in Sect. 6 (see Fig. A.35 in Appendix A). This is over a 30-min period from the time breakthrough was detected. The NDA measurements showed a significant decrease in gamma-ray transmission through the bed when the UF₆ front passed the detection zone (Fig. 14). The relative decrease in counts is the important analytical feature. The absolute transmission depends on trap orientation and pellet-packing density in the detection zone, and it will probably be different for each trap.

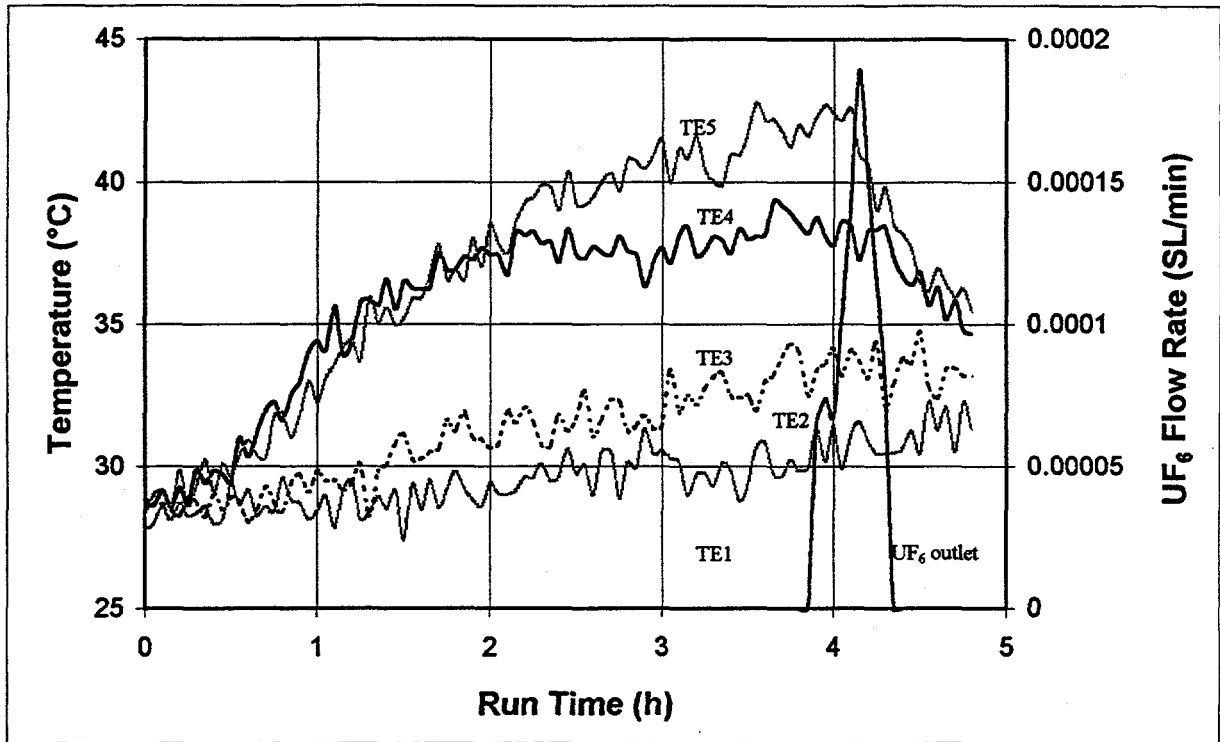


Fig. 13. Sodium fluoride temperatures and UF₆ breakthrough curve, GBTP, March 28, 1996.

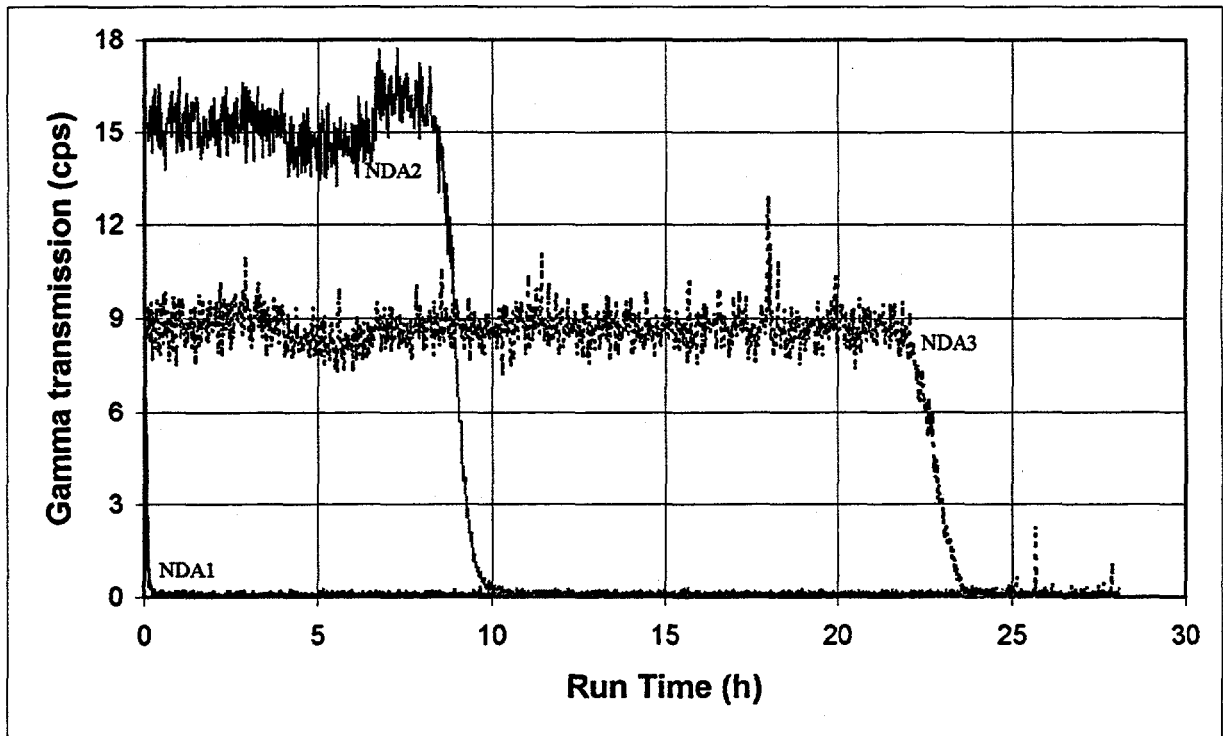


Fig. 14. Gamma transmission for NDA detectors over entire GBTP.

Table 17. Maximum NaF and alumina temperatures and UF₆ and F₂ loading for GBTP

Date	Maximum temperature		UF ₆ loading		F ₂ loading	
	NaF (°C)	Alumina (°C)	By flow (g)	By wt (g)	By flow (SL)	By wt (SL)
3/25/96	53	627	352		266	
3/26/96	40	500	333		232	
3/27/96	42	176	492		86	
3/28/96	43	32	234		0	
Total			1411	1430	584	568

Upon completion of this test, the tubing downstream of the alumina trap was rinsed with 100 mL of deionized water. The resulting solution was analyzed for uranium as well as other metal ions by inductively coupled plasma emission spectrometry (ICP). The results are shown in Table 18. The 1.5 ppm of uranium found accounts for almost all of the uranium present, since UO₂F₂ is very soluble in water. This translates to a total of ~0.15 mg of uranium. The content of other metals is negligible. Values for silver probably represent an error in the report since there is no known source of silver.

8.2 VACUUM TESTS (GBTV)

For the vacuum-draw trials, two modifications were made to the system. A 4-m-long FTIR cell was added downstream of the molecular sieve trap, and an evacuated liquid nitrogen tank (~172 L) was added at the end of the system. These tests were run in batches that brought the evacuated tank up to a specified pressure before they were terminated. Several conditions were tested, including high concentrations of fluorine and UF₆ and low differential pressures, to observe the effects on trap loading and trap temperatures. Four runs were completed. Table 19 gives a summary of the parameters for each run; Table 20 shows the maximum temperatures observed in the two traps and UF₆ and F₂ loadings. Table 21 displays the initial and final system pressures for each batch. By following the location of the maximum trap temperatures, one can track the movement of the reaction front. The first batch was

Table 18. Metals analysis of downstream piping wash (GBTP)^a

Metal	Result (mg/L)
Ag	50.0
Al	0.20
As	<0.05
B	<0.08
Ba	0.028
Be	<0.001
Ca	0.16
Cd	<0.005
Co	<0.004
Cr	<0.004
Cu	1.3
Fe	<0.05
Li	<0.005
Mg	0.063
Mn	0.094
Mo	<0.040
Na	0.47
Ni	0.83
P	<0.30
Pb	<0.050
Sb	0.22
Se	<0.050
Si	<0.20
Sn	<0.05
Sr	<0.005
Ti	<0.02
U	1.5
V	<0.002
Zn	0.037
Zr	<0.020

^aAnalysis Procedure No. EPA 200.7.

Table 19. Parameters for GBTV^a

Date	F ₂ flow (SL/min)	He flow (SL/min)	UF ₆ flow, av (SL/min)	Duration (h)
4/9/96	0.92	1.00	0.136	1.25
	0.76 – 0.72 ^b	0.82 – 0.71 ^b	0.134	0.65
4/10/96	0.47 – 0.57 ^c	0.24 – 0.33 ^c	0.099	2.15
	0.99	0.48	0.104	0.95
	0.99	0	0.085	0.90
4/11/96	0.42	0	0.117	0.63
	0.59	0	0.240	0.87
	0.41	0	0.327	0.23
	0.41	0	0.113	1.47
4/12/96	0.09 – 0.46 ^d	0	0.029	4.43

^aWeight of NaF = 1814 g; weight of alumina = 1407 g.

^bThe fluorine and helium flows were set; the initial value listed indicates this setting. Flows decreased to the second value shown as the pressure drop decreased.

^cFlow rates were controlled with valves on the inlet to the saturator (to keep upstream pressure lower). As pressure drop through the system varied, this valve had to be adjusted, which is the reason for the range of flow rates.

^dThere was a large restriction in the process piping during this batch, and the fluorine flow had to be constantly adjusted to keep the pressure from rising too high.

operated under conditions similar to the ones used in previous tests, with a 50/50 mix of helium and fluorine at relatively high flows.

In the second batch the flowmeter measuring the exiting gases was operational. Its readings were used to calculate the oxygen generation rate, which was expected to be 50% of the fluorine flow rate. This was done by comparing calculated flow rates with actual measured flow rates, as well as comparing calculated pressure rise in the evacuated tank with the actual pressure between two thermocouple positions. The actual “hot spot” in the trap can then be hotter than the temperature at the thermocouple position. Figures 15 and 16 give trap temperature profiles along with UF₆ and F₂ flow rates (refer also to Figs. A.50 and A.51, see Appendix A). The readings were corrected according to the different thermal conductivities of the gases being measured. As Fig. A.50 (Appendix A) depicts, the correlation between “corrected” measured flow rates and the calculated flow rates is very good. If the O₂ generation is assumed to be 50 mol % of the F₂ flow, then the second flowmeter allows for an independent measurement of the F₂ concentration (see Appendix C).

In the third batch the uranium concentration was increased significantly with respect to previous tests. The remainder of the gas was F₂, to simulate what is expected during later runs of the RGRS. This

was the first test in which the inlet line was heated. In the test system a large upstream pressure was necessary to obtain the desired flow rates due to the pressure drop over 30 ft of 0.25-in. tubing on the

Table 20. Maximum temperatures and UF₆ and F₂ loading in GBTV

Date	Duration (h)	Maximum temperature		UF ₆ loading (g)		F ₂ loading (SL)	
		NaF (°C)	Alumina (°C)	By flow	By wt	By flow	By wt
4/9/96	1.25	54	698	160		73	
	0.65	55	700 ^a	81		24	
4/10/96	2.15	43	398	203		71	
	0.95	49	570 ^b	94		56	
	0.90	51	745	73		51	
4/11/96	0.63	39	308	69		17	
	0.87	57	473	197		30	
	0.23	64	420 ^c	71		6	
	1.47	70 ^d - 62 ^c	380 ^c	157		36	
4/12/96	4.43	37	300	120 ^e		64	
Total				1225	1184	428	407

^aThe temperature was initially as shown and then continuously decreased.

^bThe temperature was rapidly rising at the end of the period.

^cThe temperature decreased to this point and then stabilized.

^dThe temperature increased to this point and then stabilized.

^eThis value is believed to be high due to the continuous plugging of the line during the run.

Table 21. Pressure measurements from GBTV

Location	Pressures (torr)							
	Upstream (hood)		10-cm FTIR cell		20-cm FTIR cell		Vacuum tank	
	Initial	Final	Initial	Final	Initial	Final	Initial	Final
4/9/96	1000	980 ^a	264	747	246	739	<0.2	724
4/10/96	540	930 ^b	121	750	110	745	<0.2	734
4/11/96	830	1450 ^c	73	204	62	200	<0.2	176
4/12/96	1900 ^d	3150	53	133	47	130	<0.2	111

^aPressure increased to 1100 torr at end of first parameter setting (Table 19).

^bPressure increased to 1020 torr at end of second parameter setting (Table 19).

^cPressure increased to 2600 torr at end of second parameter setting (Table 19).

^dPressure decreased to 1600 torr during times when flow rate was at the low end of the range (Table 19).

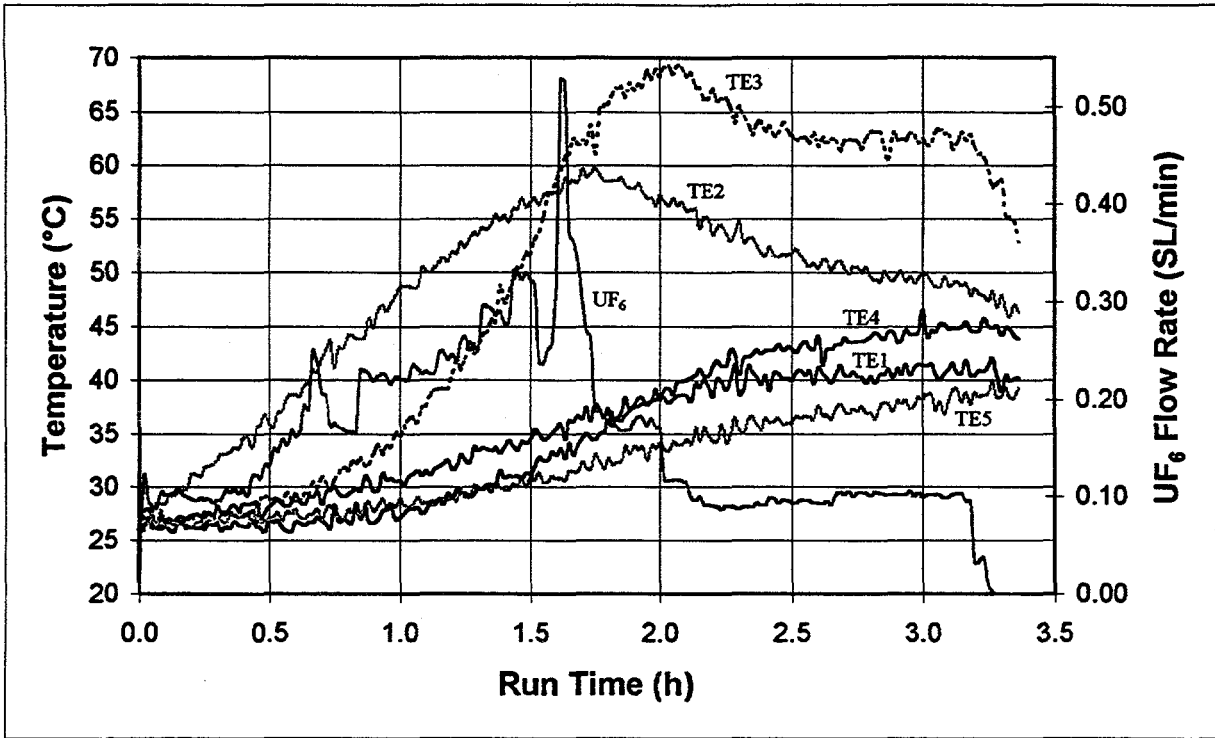


Fig. 15. Sodium fluoride temperatures and UF_6 flow rate, GBTV-3, April 11, 1996.

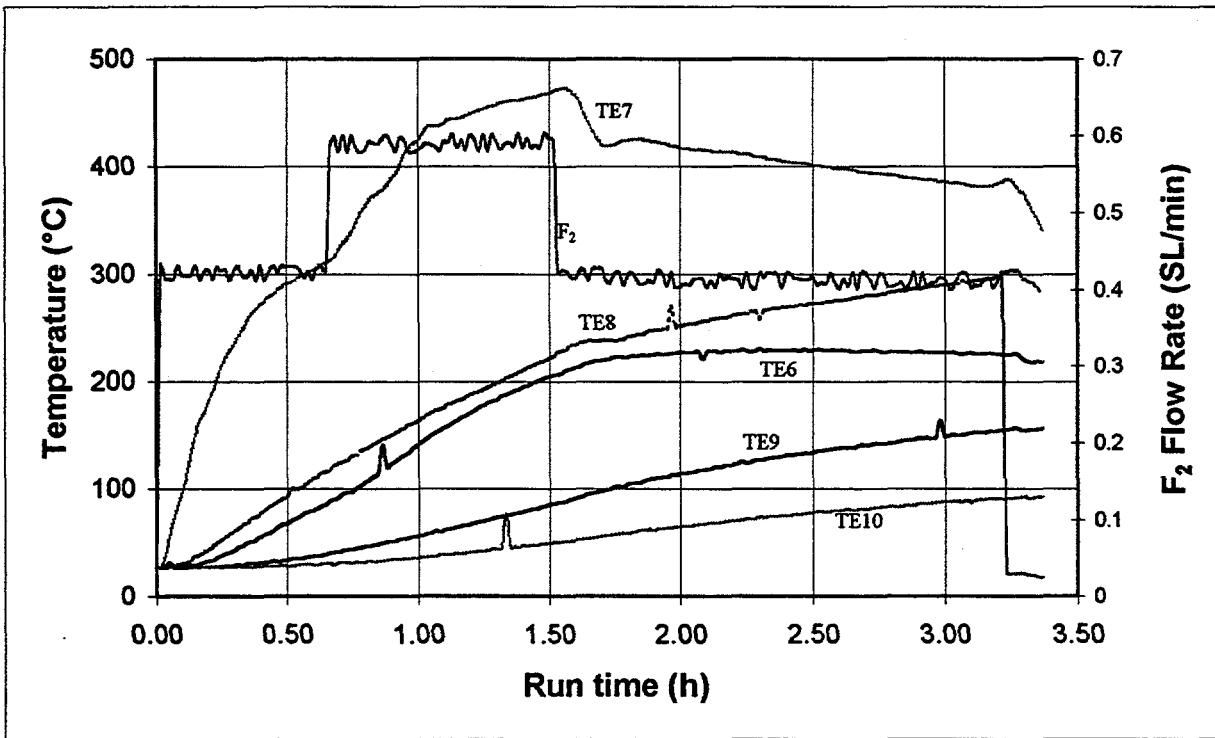


Fig. 16. Alumina temperatures and F_2 flow rate, GBTV-3, April 11, 1996.

inlet line before reaching the trap. These higher pressures required heating the inlet line to 100°C, which is well above the design temperature to be used at MSRE (50°C). Lower flow rates were used in order to increase residence time in the saturator and obtain high UF₆ concentrations. No problems were observed during this run, and high UF₆ concentrations were readily achieved (>50 mol %). These high UF₆ flow rates produced correspondingly high temperatures on the NaF trap during loading (Fig. 15).

In the fourth batch the system was to be run at high gas velocities to determine if greater flow rates than those previously tested could be run safely. From almost the beginning of the run, it appeared that a plug of UF₆ had formed that was greatly restricting, but not stopping, the flow. The run was shut down before breakthrough could occur because the loading rate of UF₆ on the trap was very low. An analysis of the system after the lines were purged showed that no plugging had occurred. The inlet flowmeter/valve had failed and closed because of excessive heating. This failure was caused by the prolonged heating of the piping, as the problem was not evident during the third batch. When allowed to cool, the flowmeter functioned properly, but its calibration was upset. Further testing revealed the failure was mechanical, not electronic. (The electronics were remotely located, and the valve still closed.) The additional testing also showed that the closure occurred at temperatures in excess of 95°C and that it was reversible as the valve reopened after cooling down.

The spectra taken using the 4-m FTIR cell installed downstream of the molecular sieve trap showed only CF₄ (O₂, He, and F₂ cannot be detected by IR analysis). The molecular sieve therefore effectively removed the HF and H₂O as expected. The CF₄ is an impurity present in fluorine supply.

The overall UF₆ loading was 65.3 wt %. The temperature profiles (Figs. 15 and A.47, the latter in Appendix A) indicated that the trap was nearly full. The only reliable NDA measurements were taken by the midposition detector (Fig. A.52, Appendix A). The loading front never reached the NDA detector at the top of the trap.

9. ANALYSIS AND CONCLUSIONS

The major objectives of RGRS laboratory testing were to ensure that all process equipment functioned as intended and to debug the system as much as possible when operated with surrogate UF₆/F₂ mixtures. Several discoveries concerning the process system were made during the laboratory testing

program. The implementations that were made as a result of these discoveries have greatly improved the safety and overall effectiveness of the RGRS. These discoveries included the following:

1. The maximum fluorine flow rate was much lower than initially anticipated. This resulted in the addition of a needle valve to the system to allow control at the lower flow rates.
2. Initially, there were continuous problems with the thermocouples (five thermocouples in one) used to measure interior temperatures in the trap. A problem was discovered with solder joints in the connectors. The solder joints were replaced with a crimped connection, which alleviated the difficulty.
3. Hydrogen fluoride and moisture were observed exiting the alumina trap. A gold-plated valve was placed on the outlet of the alumina trap to prevent corrosion from aqueous HF. A molecular sieve trap was installed downstream of the alumina trap to collect the water and HF produced, and a gold-plated valve was also installed on the trap inlet. The line between the alumina and molecular sieve traps was heated to keep the material in the vapor phase until it reached the molecular sieve trap. Finally, an HF sensor was placed downstream of the molecular sieve trap to detect the HF breakthrough.
4. A restriction in the NaF trap was observed, which was later determined to be caused by pellets trapped in the outlet tube. These pellets were able to bypass the baffle plates because the weld rings that were supposed to prohibit this migration were missing in some of the traps. As a result, all of the traps were cut open and weld rings were installed.

The testing also helped to debug the process monitoring equipment from problems such as stepwise temperature rising and a maximum temperature reading of 560°C. The instrumentation for the system was checked out, and analysis equipment such as the FTIR cells and NDA detectors was proven to be effective. Temperature profiles were shown to predict the trap loading accurately.

The second objective of RGRS testing was to determine safe operating conditions for the overall process. The conditions can be summarized as follows. The overall flow rate was limited only by the fluorine concentration. (Rates up to 2.0 SL/min were tested.) The fluorine flow rate was <1.0 SLM. The operating temperature for Al₂O₃ was <700°C; no known limit existed for NaF. (Temperatures up to 71°C were tested.) No known maximum concentration was determined for UF₆; up to 54 mol % was

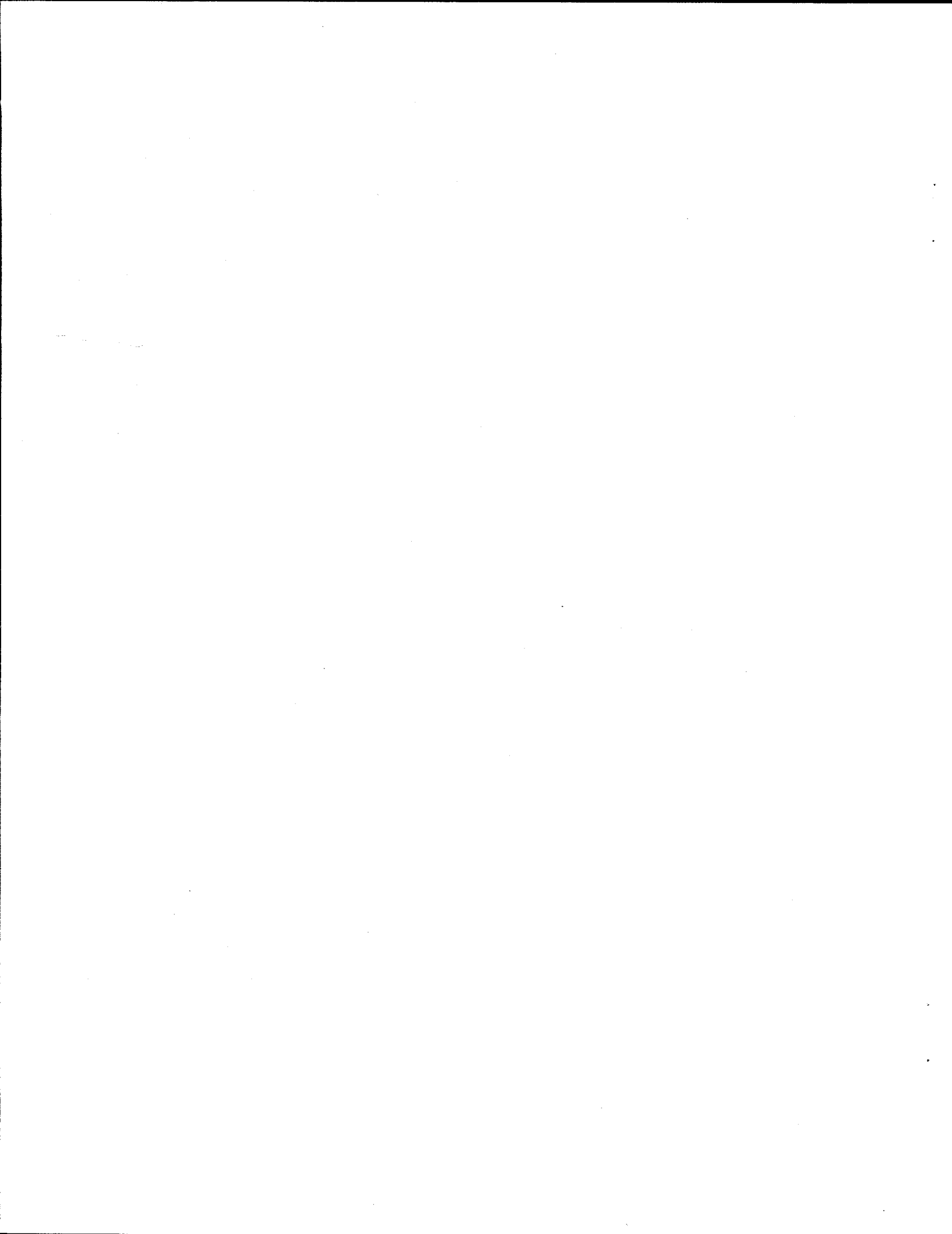
tested with complete success. In terms of trap loading, tests indicated that the NaF trap may be safely loaded (no detectable breakthrough) until either the top NDA detector goes to <5% of the number of initial counts or the fourth (80% full) thermocouple reaches a maximum. The alumina trap can be safely loaded until the temperature of the top thermocouple surpasses that of the fourth thermocouple. This still provides protection in the event of UF₆ breakthrough of the NaF trap.

10. REFERENCES

- ¹*Nuclear Applications and Technology* 8(2), 105–208 (February 1970).
- ²G. D. Del Cul, L. M. Toth, D. F. Williams, and S. Dai, *Some Investigations on the Chemistry of Activated Charcoal with Uranium Hexafluoride and Fluorine*, to be published as ORNL/TM-13052.
- ³L. D. Trowbridge et al., *Technical Bases of Selection of Trapping Technology for the MSRE Interim Vent and Trapping Project*, K/TCD-1142, August 1995.
- ⁴“MSRE Temporary Ventilation and Trap System General Arrangement Assembly,” LMES Central Engineering Services Drawing No. X3E020794A023.
- ⁵R. S. McDowell, L. B. Asprey, and R. T. Paus, *Journal of Chemical Physics* 61, 3571–80 (1974).
- ⁶“MSRE UF₆ In Process Carrier Assembly,” LMES Central Engineering Services Drawing No. X3E020794A008.

Appendix A

ADDITIONAL FIGURES



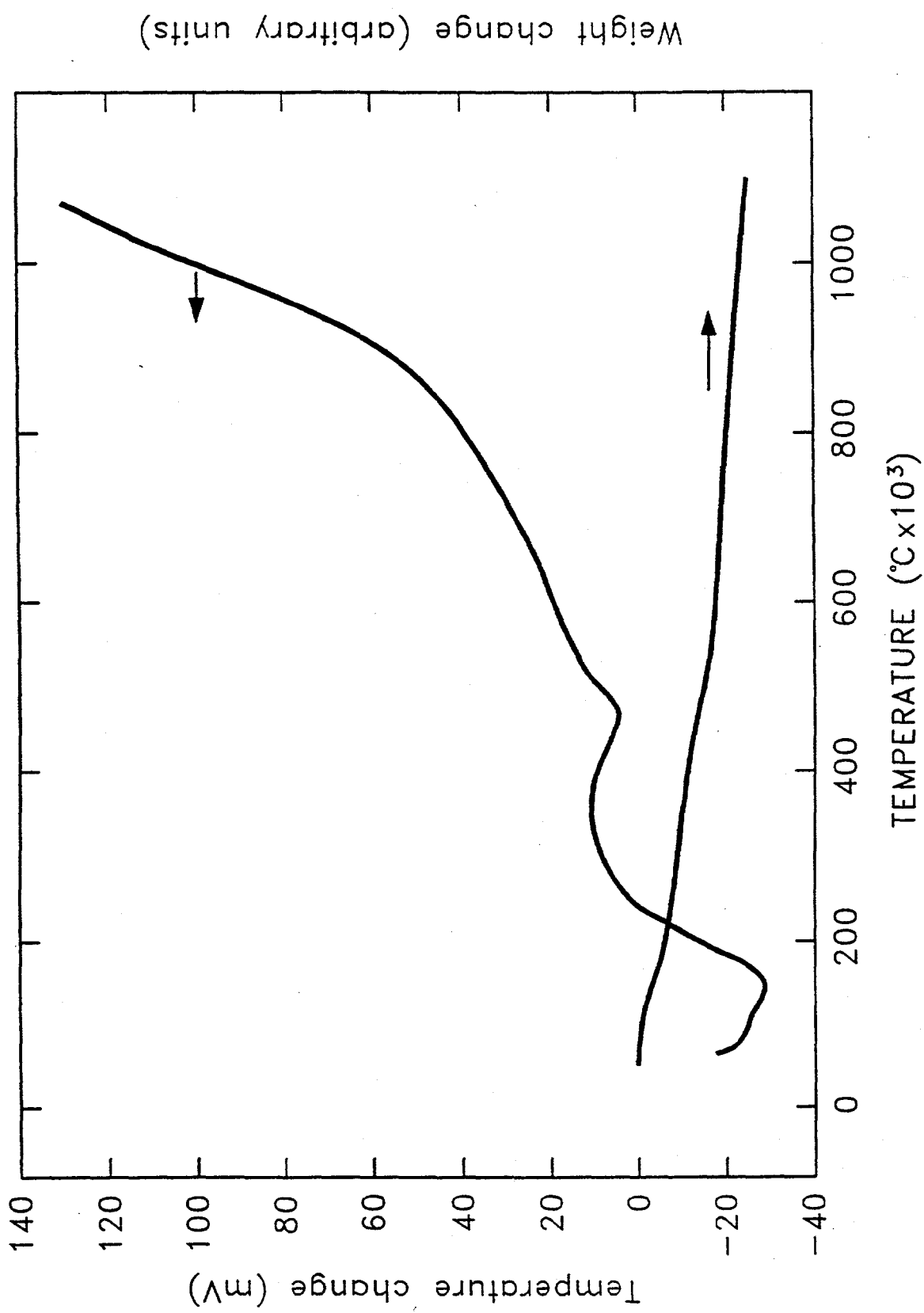


Fig. A-1. TGA of uniform alumina prior to drying.

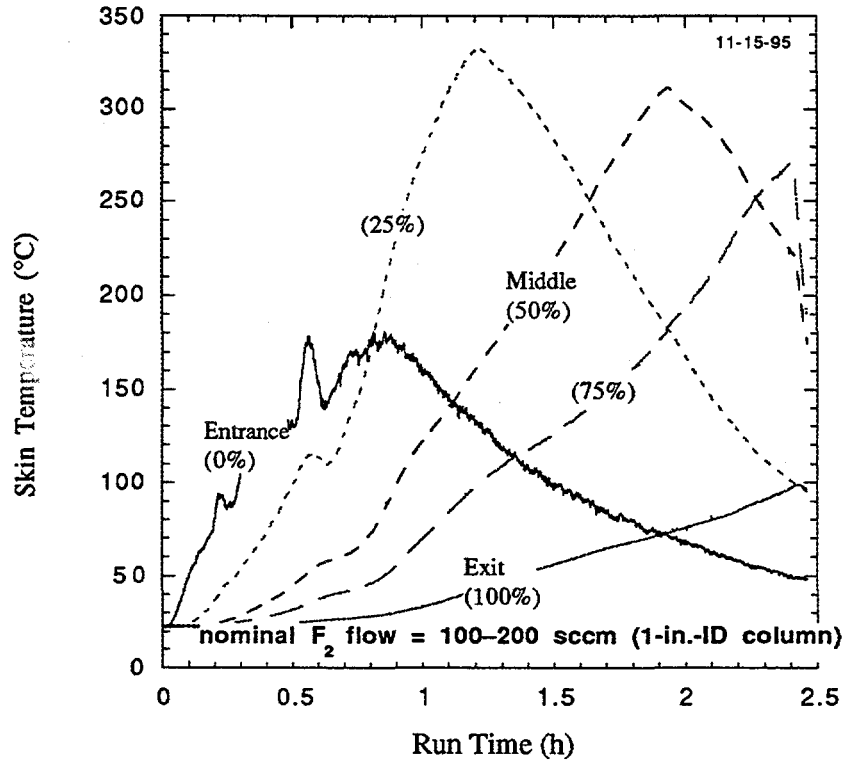


Fig. A-2. Skin temperatures for FTT-1A, 100-200 sccm fluorine, 1-in.-ID trap.

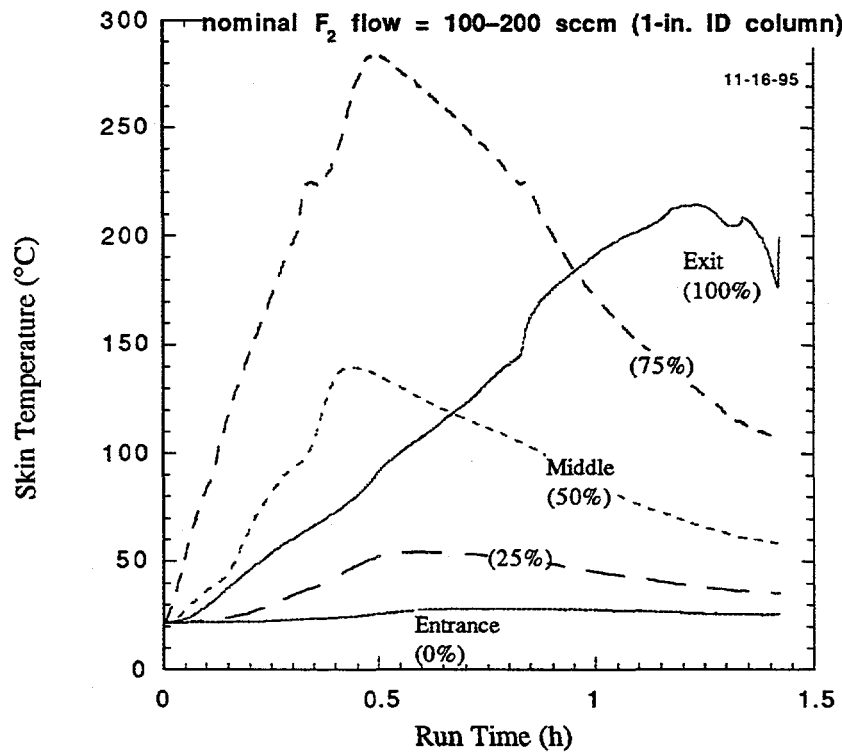


Fig. A-3. Skin temperatures for FTT-1B, 100-200 sccm fluorine, 1-in.-ID trap.

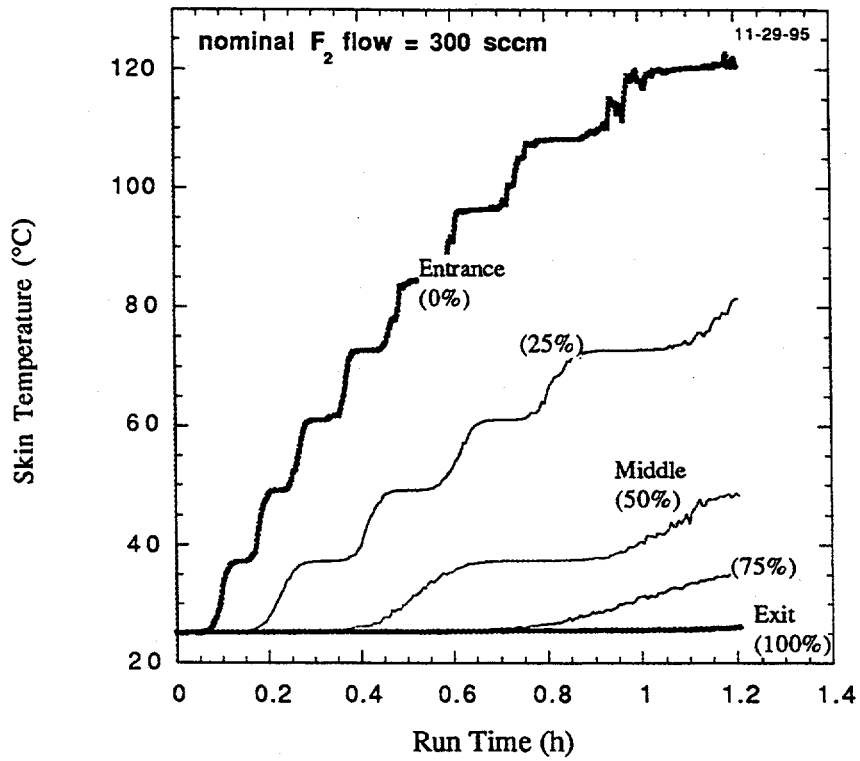


Fig. A-4. Skin temperatures for FTT-3A, 300 sccm fluorine.

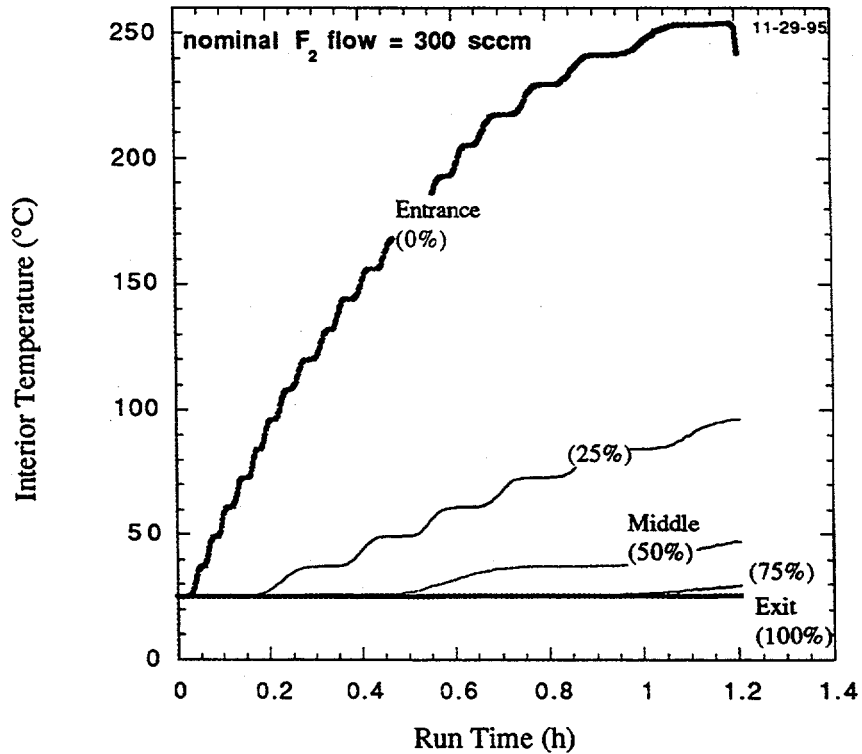


Fig. A-5. Internal temperatures for FTT-3A, 300 sccm fluorine.

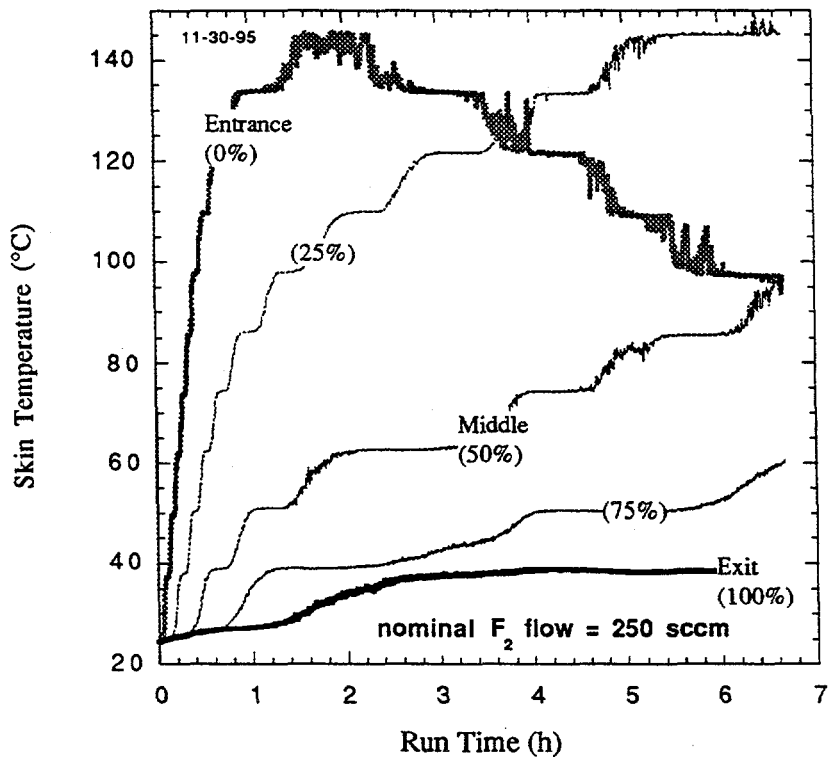


Fig. A-6. Skin temperatures for FTT-3B, 250 sccm fluorine.

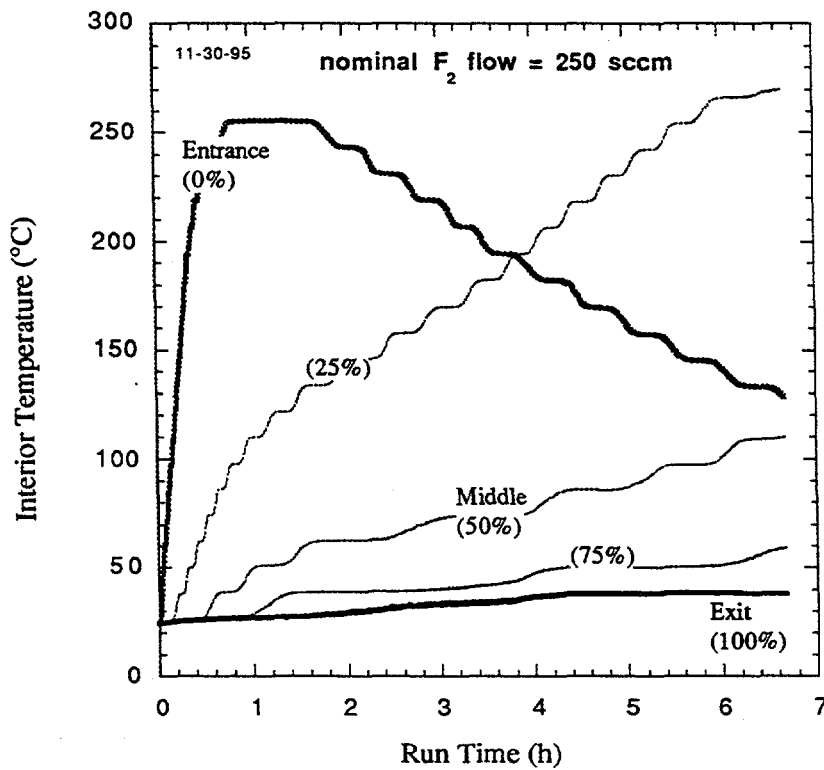


Fig. A-7. Internal temperatures for FTT-3B, 250 sccm fluorine.

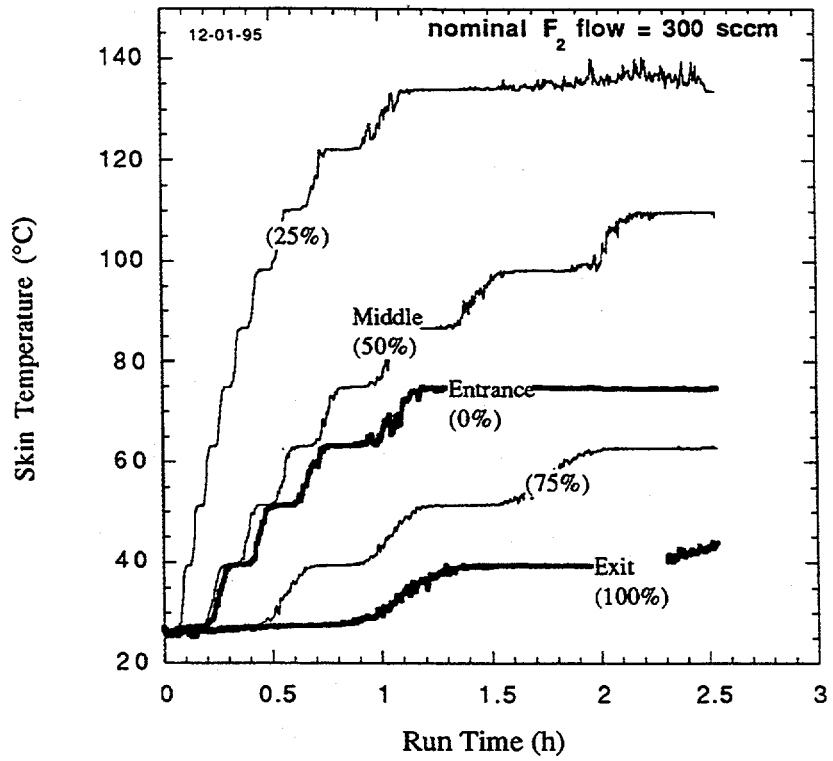


Fig. A-8. Skin temperatures for FTT-3C, 300 sccm fluorine.

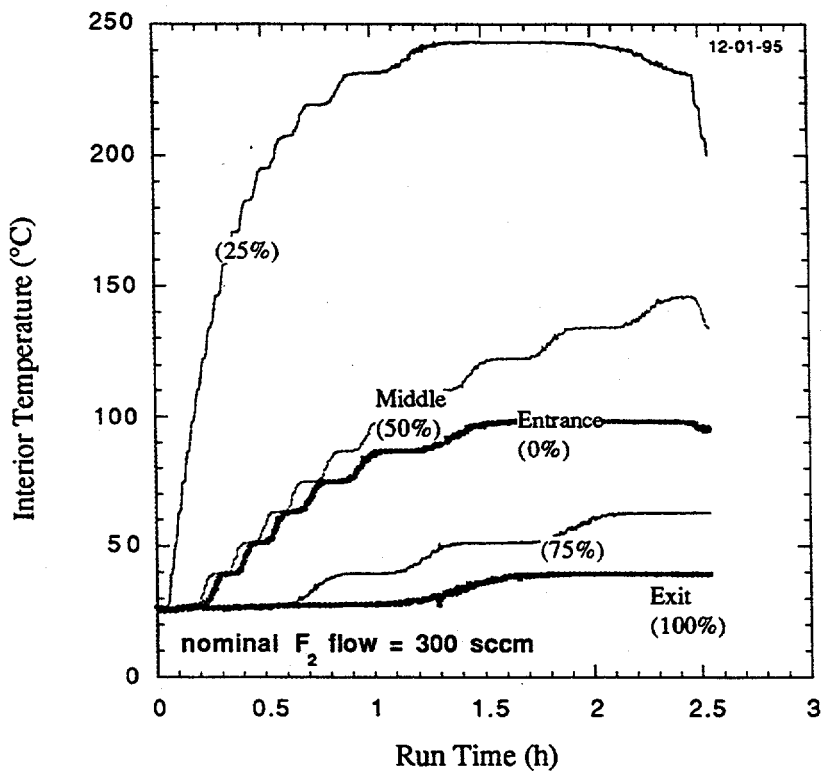


Fig. A-9. Internal temperatures for FTT-3C, 300 sccm fluorine.

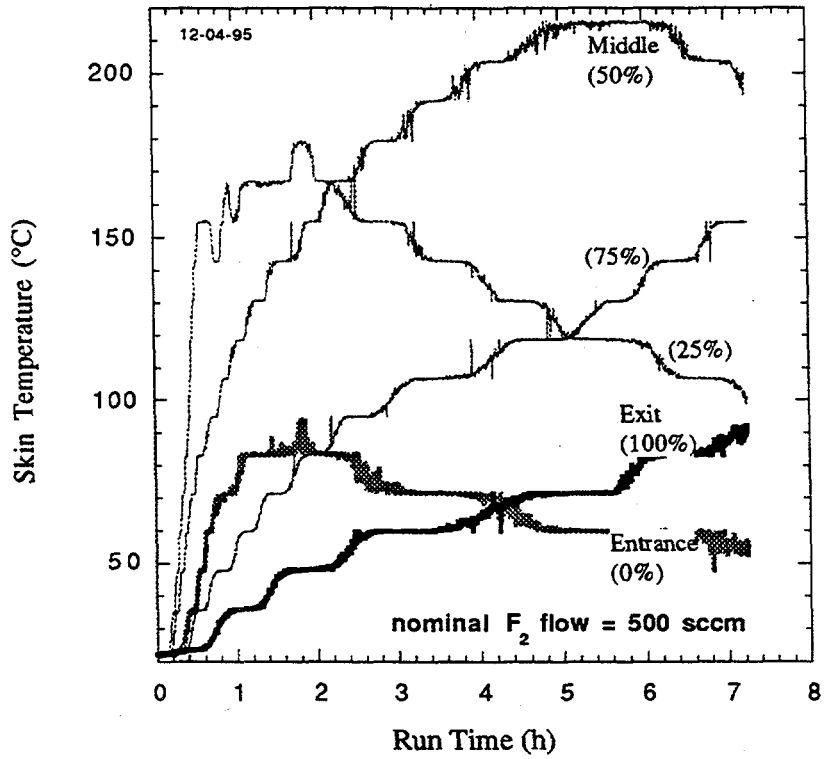


Fig. A-10. Skin temperatures for FTT-3D, 500 sccm fluorine.

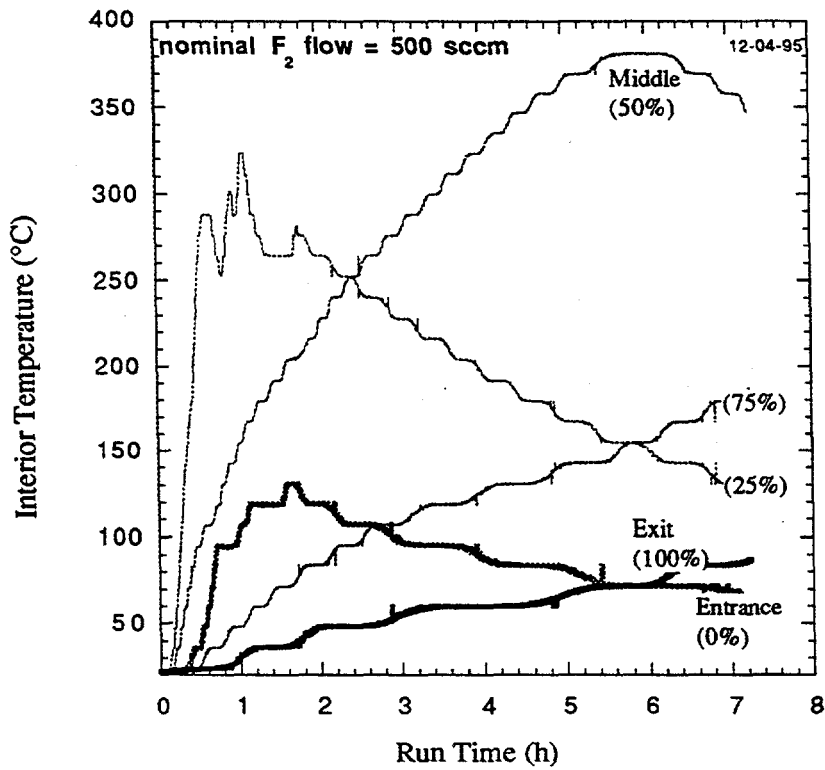


Fig. A-11. Internal temperatures for FTT-3D, 500 sccm fluorine.

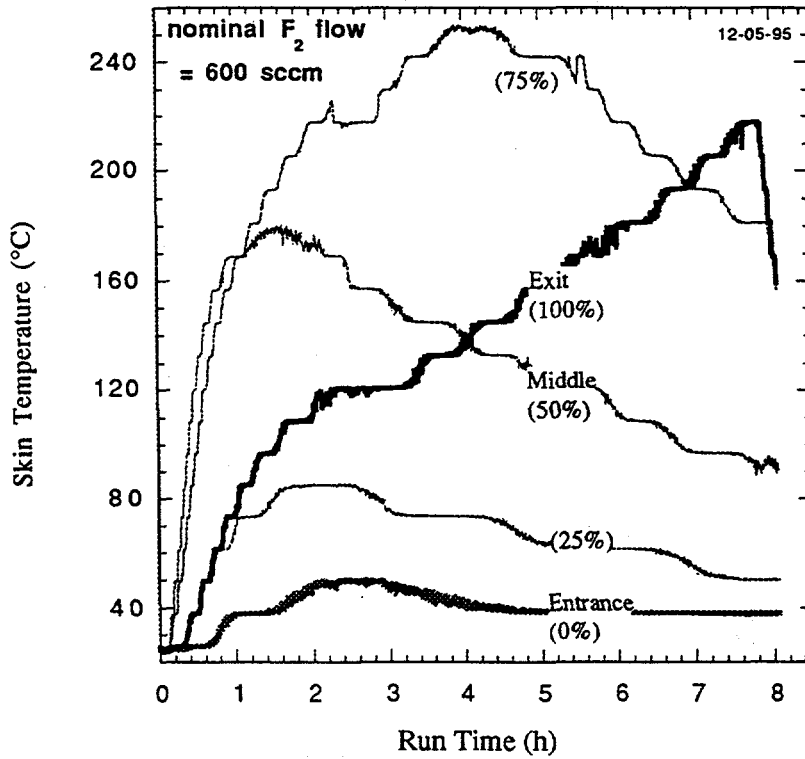


Fig. A-12. Skin temperatures for FTT-3E, 600 sccm fluorine.

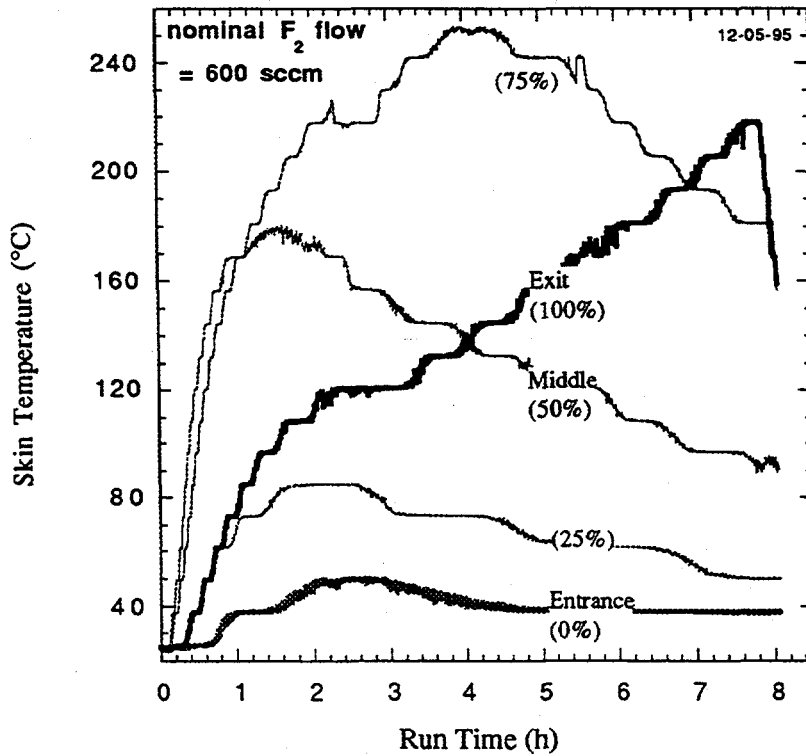


Fig. A-13. Internal temperatures for FTT-3E, 600 sccm fluorine.

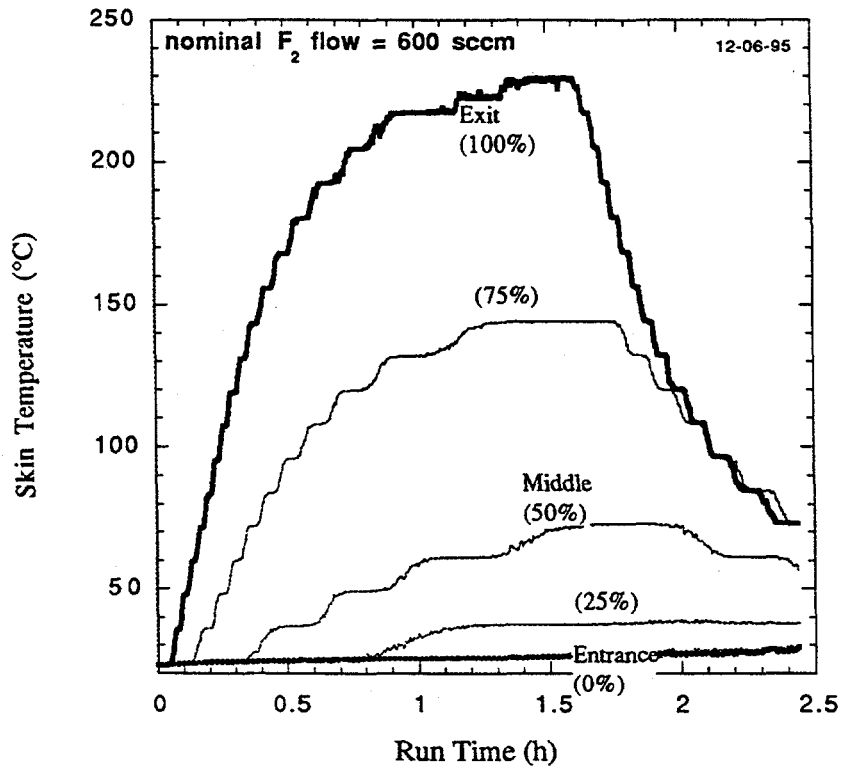


Fig. A-14. Skin temperatures for FTT-3F, 600 sccm fluorine.

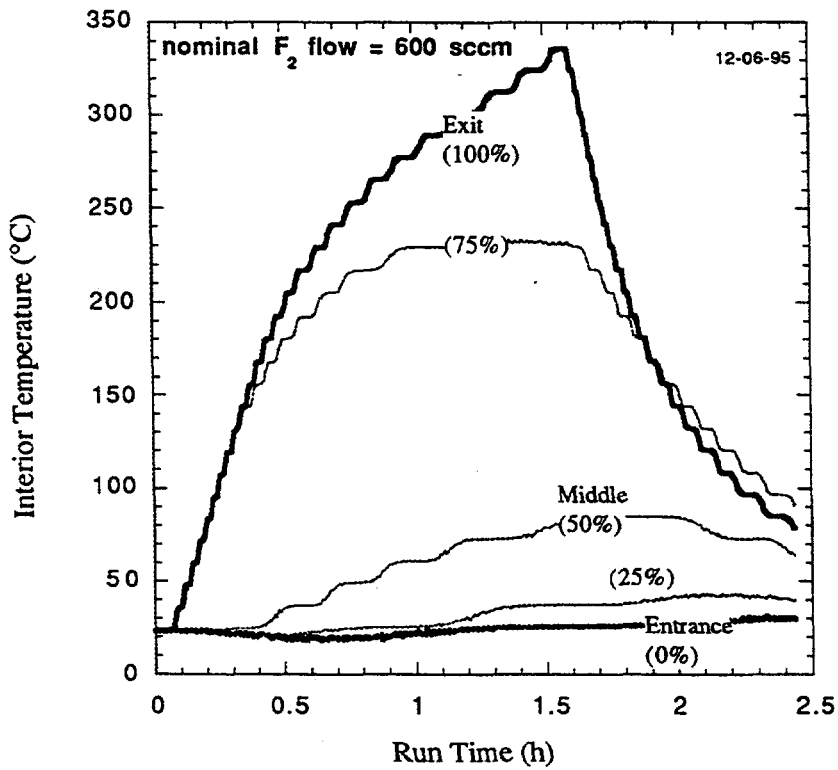


Fig. A-15. Internal temperatures for FTT-3F, 600 sccm fluorine.

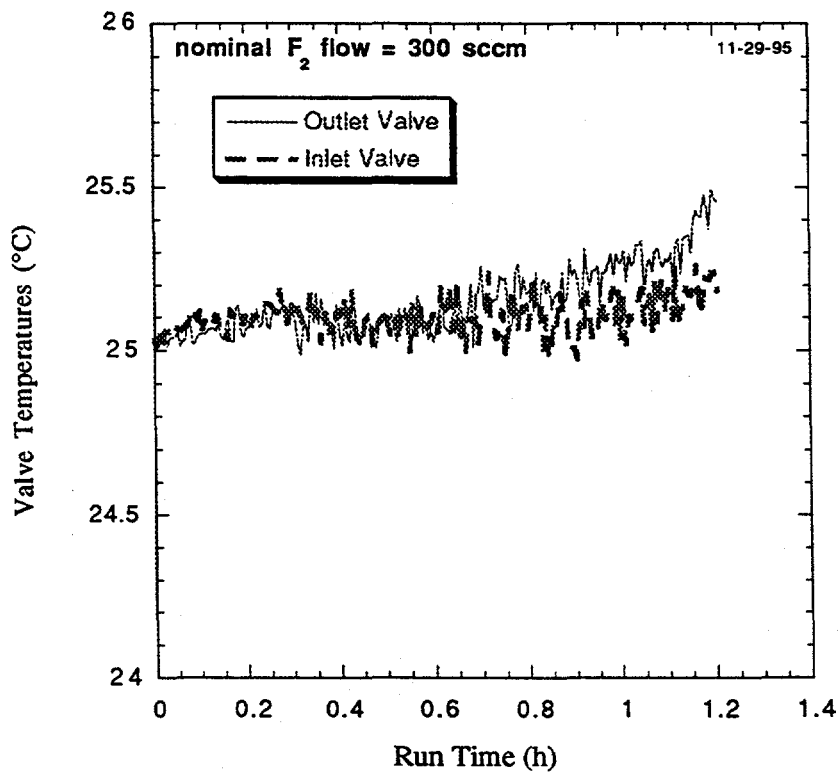


Fig. A-16. Valve temperatures for FTT-3A, 300 sccm fluorine.

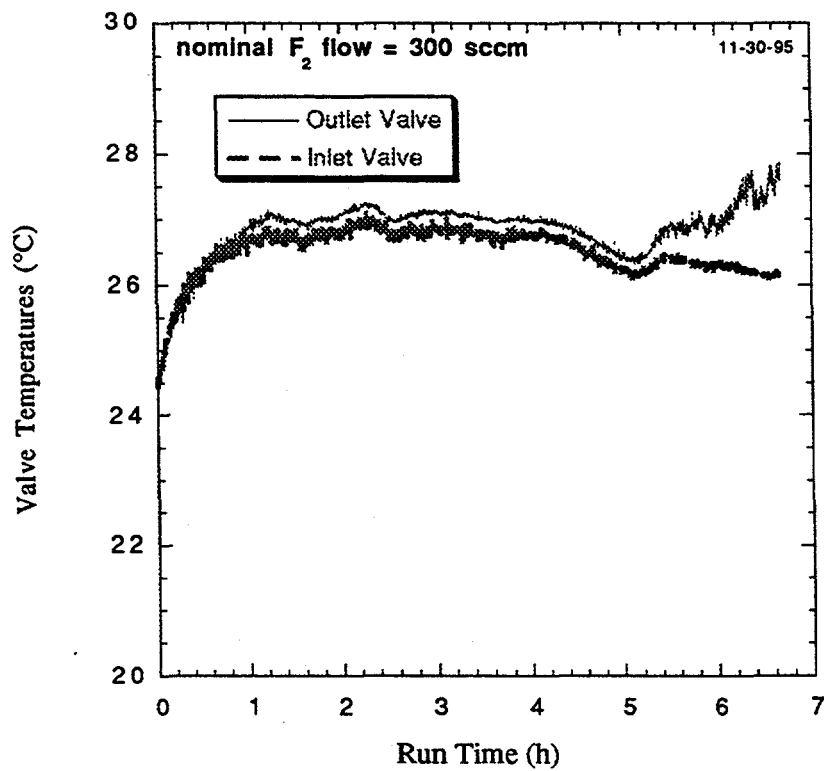


Fig. A-17. Valve temperatures for FTT-3B, 250 sccm fluorine.

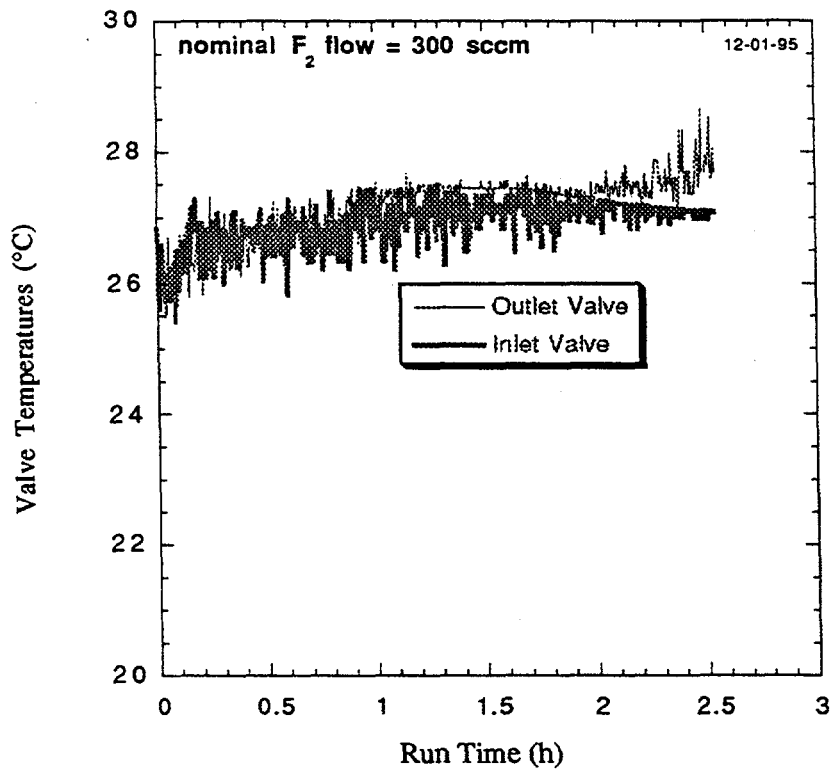


Fig. A-18. Valve temperatures for FTT-3C, 300 sccm fluorine.

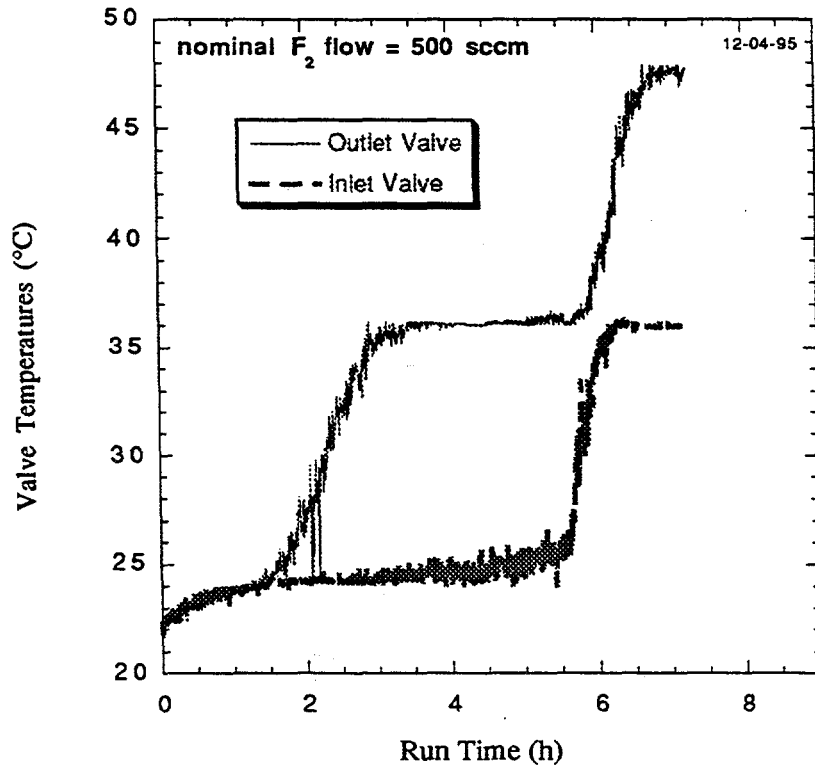


Fig. A-19. Valve temperatures for FTT-3D, 500 sccm fluorine.

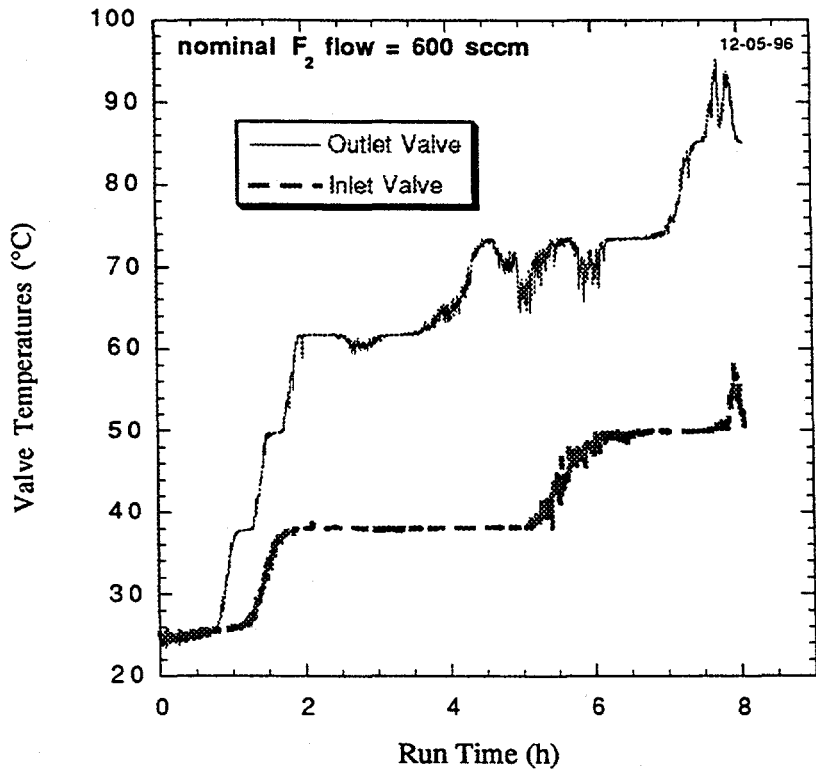


Fig. A-20. Valve temperatures for FTT-3E, 600 sccm fluorine.

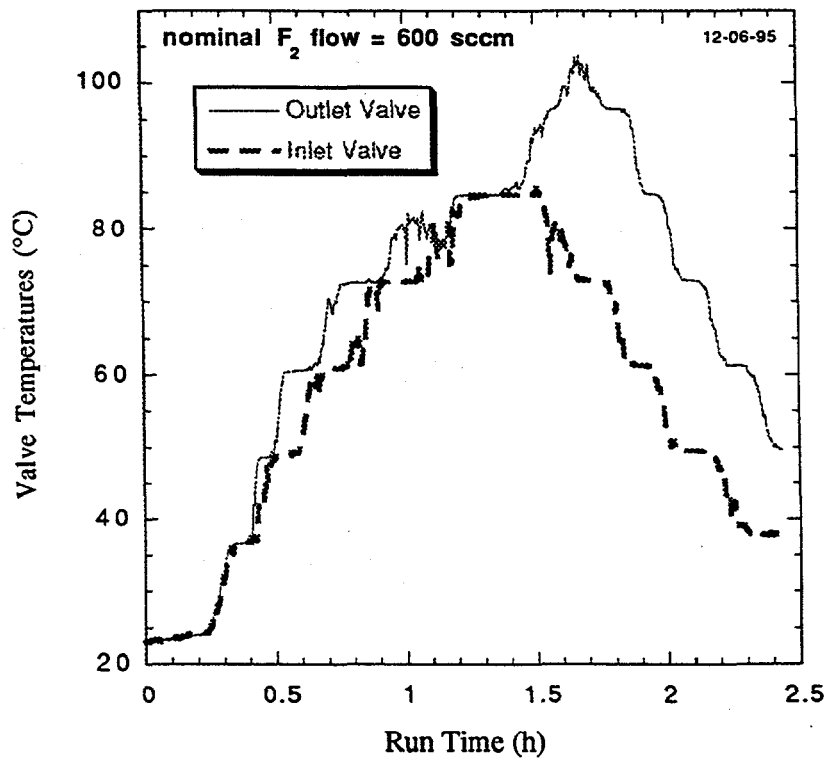


Fig. A-21. Valve temperatures for FTT-3F, 600 sccm fluorine.

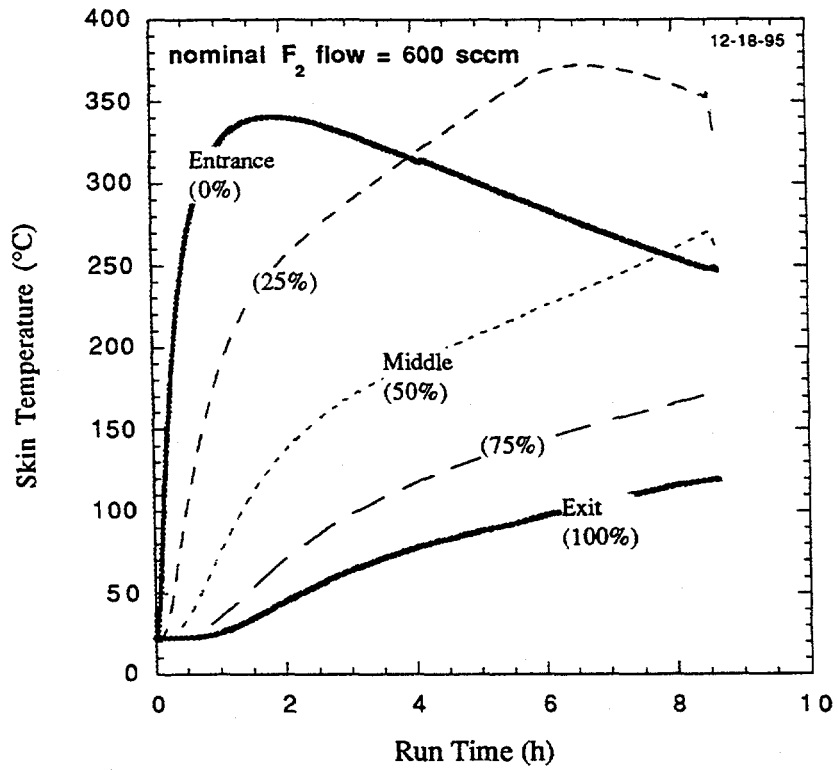


Fig. A-22. Skin temperatures for FTT-4A, 600 sccm fluorine.

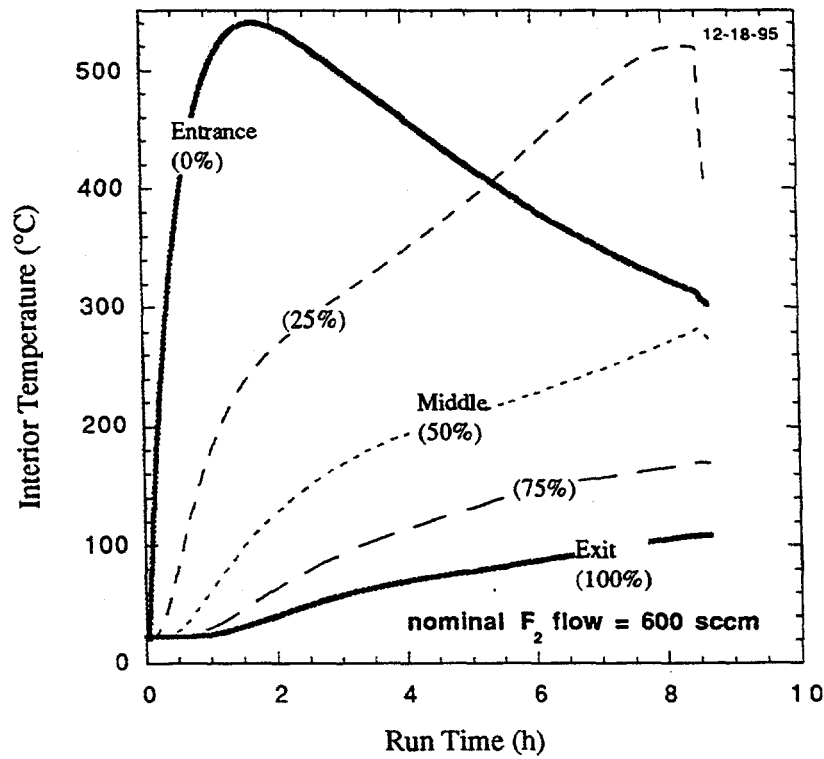


Fig. A-23. Internal temperatures for FTT-4A, 600 sccm fluorine.

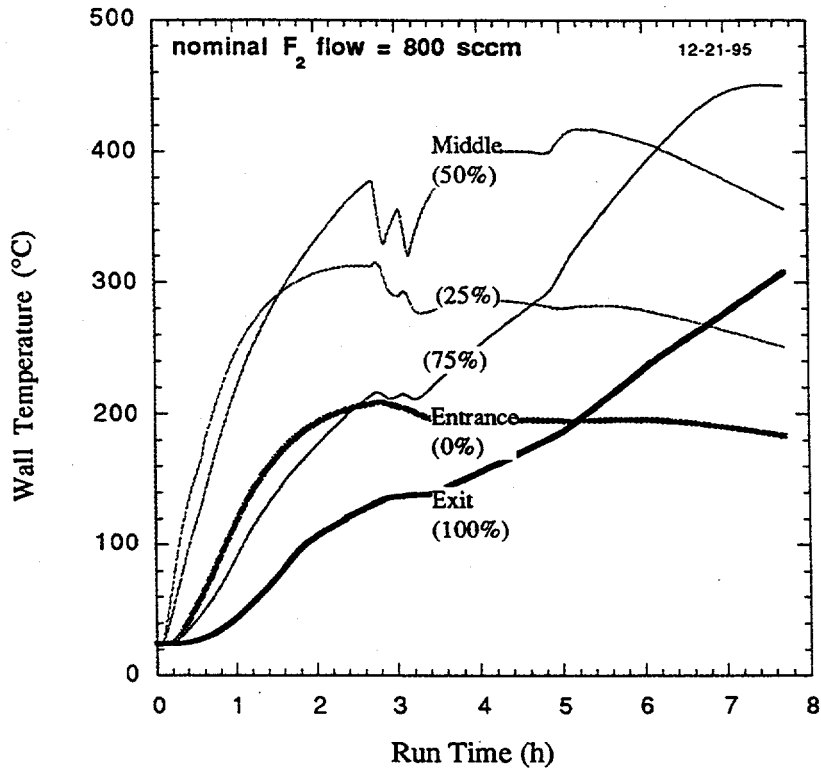


Fig. A-24. Skin temperatures for FTT-4B, 800 sccm fluorine.

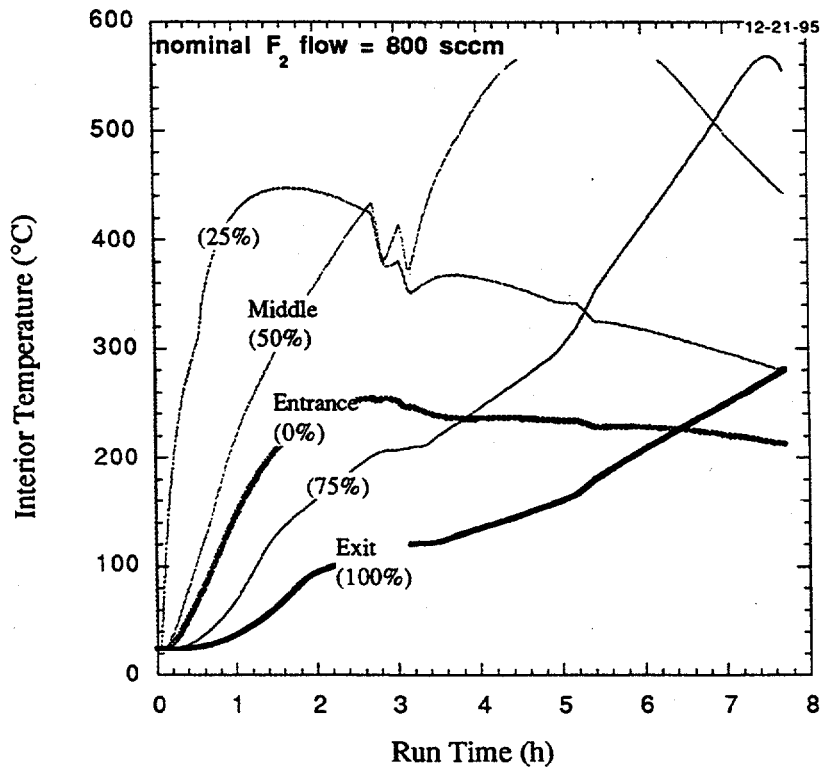


Fig. A-25. Internal temperatures for FTT-4B, 800 sccm fluorine.

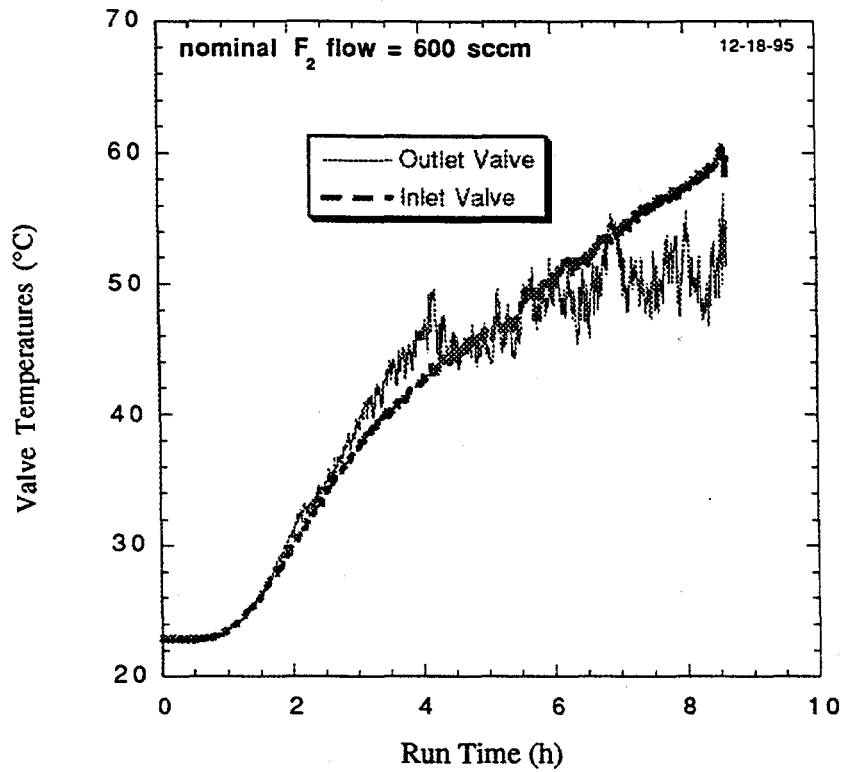


Fig. 26. Valve temperatures for FTT-4A, 600 sccm fluorine.

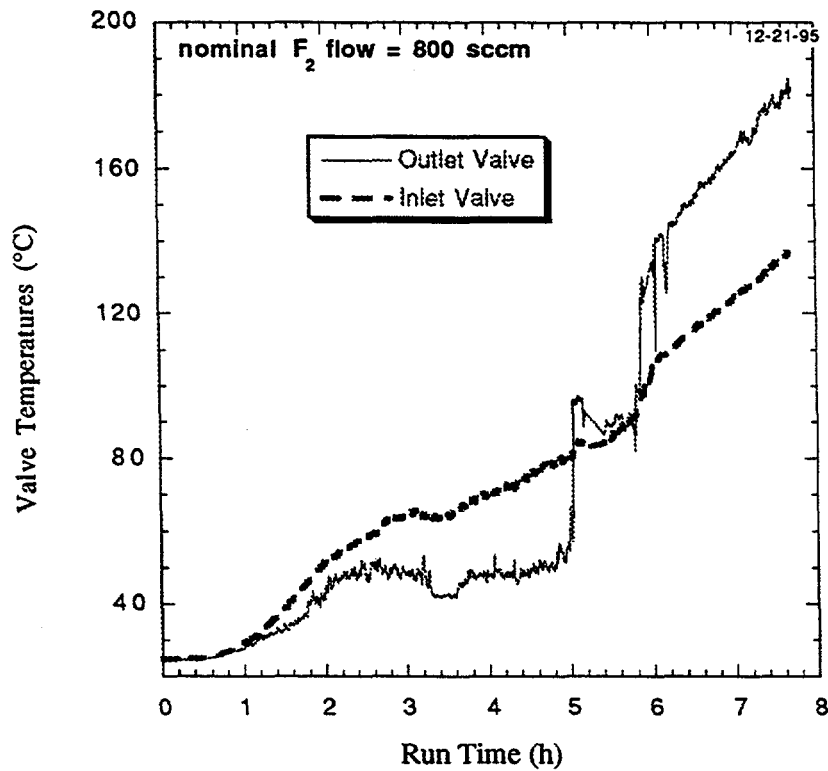


Fig. A-27. Valve temperatures for FTT-4B, 800 sccm fluorine.

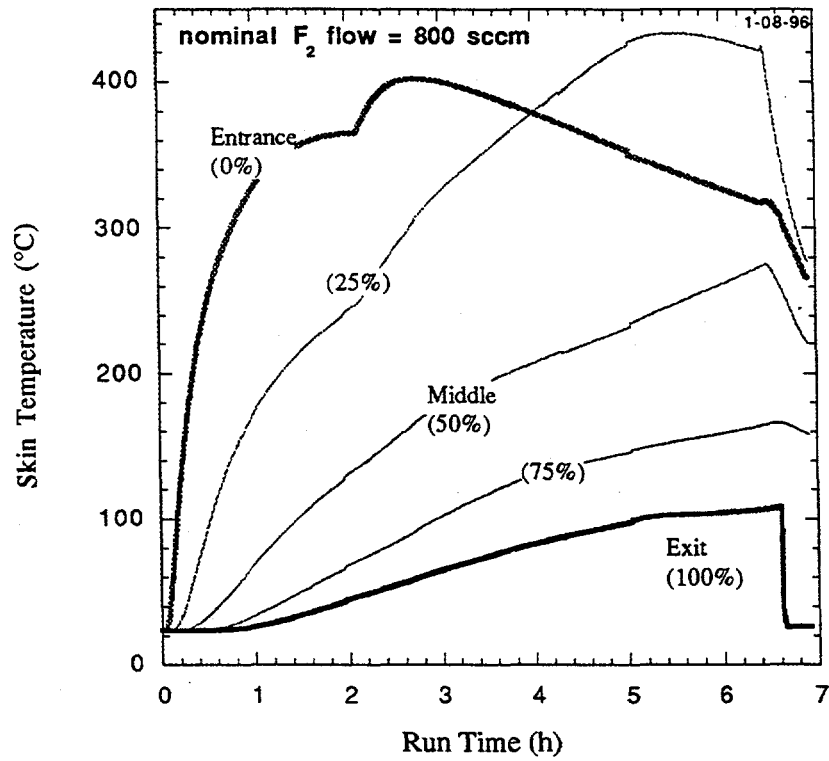


Fig. A-28. Skin temperatures for FTT-5A, 800 sccm fluorine.

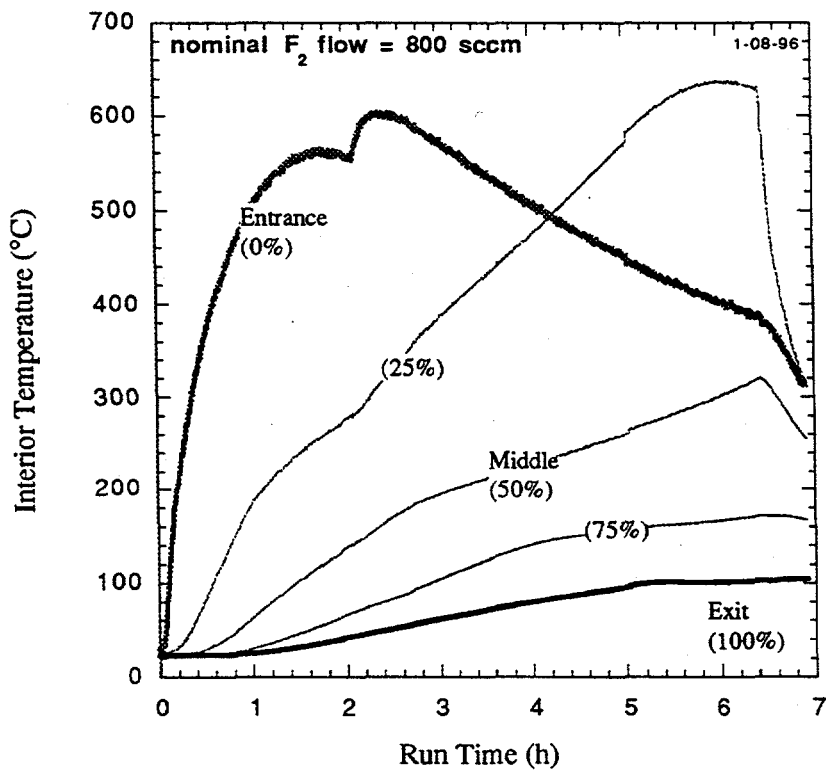


Fig. A-29. Internal temperatures for FTT-5A, 800 sccm fluorine.

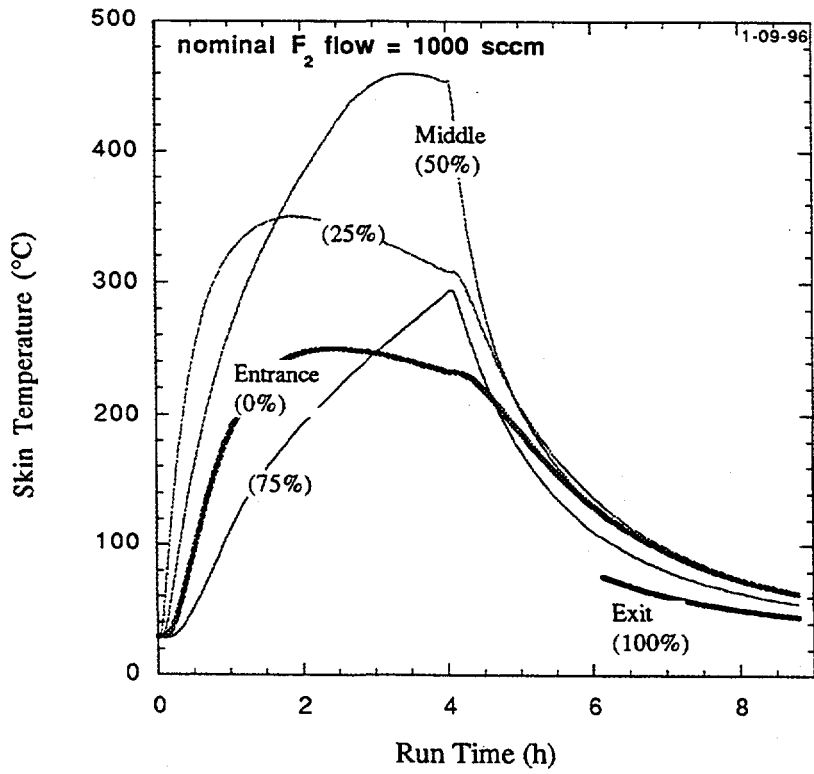


Fig. A-30. Skin temperatures for FTT-5B, 1000 sccm fluorine.

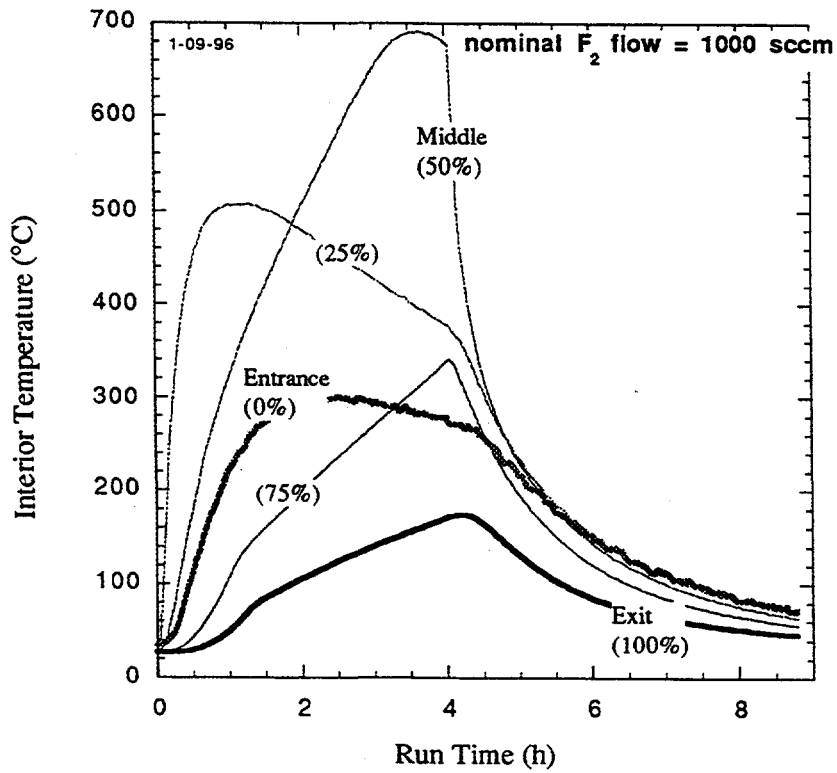


Fig. A-31. Internal temperatures for FTT-5B, 1000 sccm fluorine.

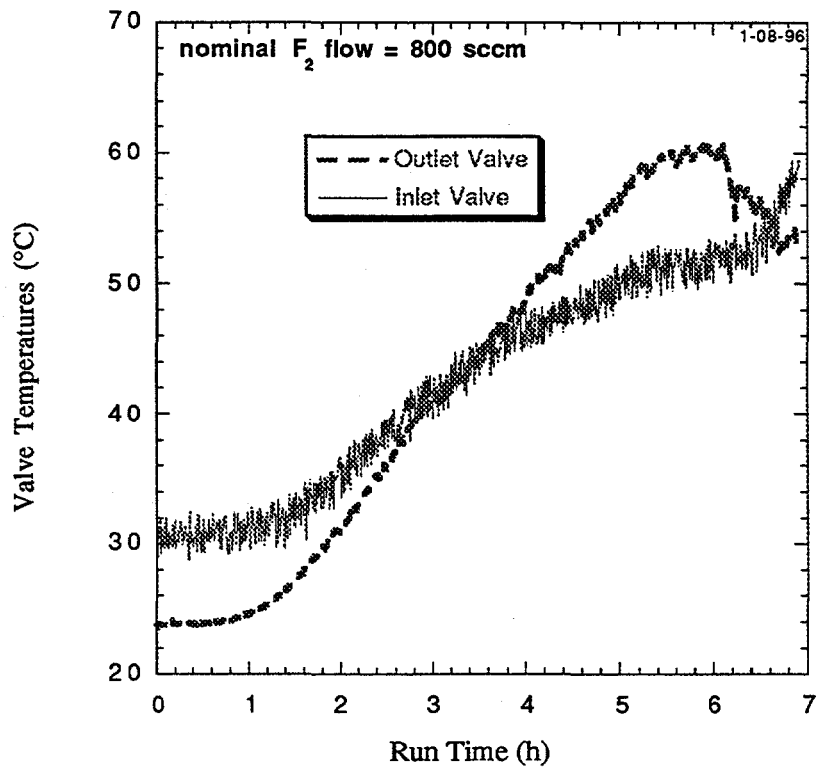


Fig. A-32. Valve temperatures for FTT-5A, 800 sccm fluorine.

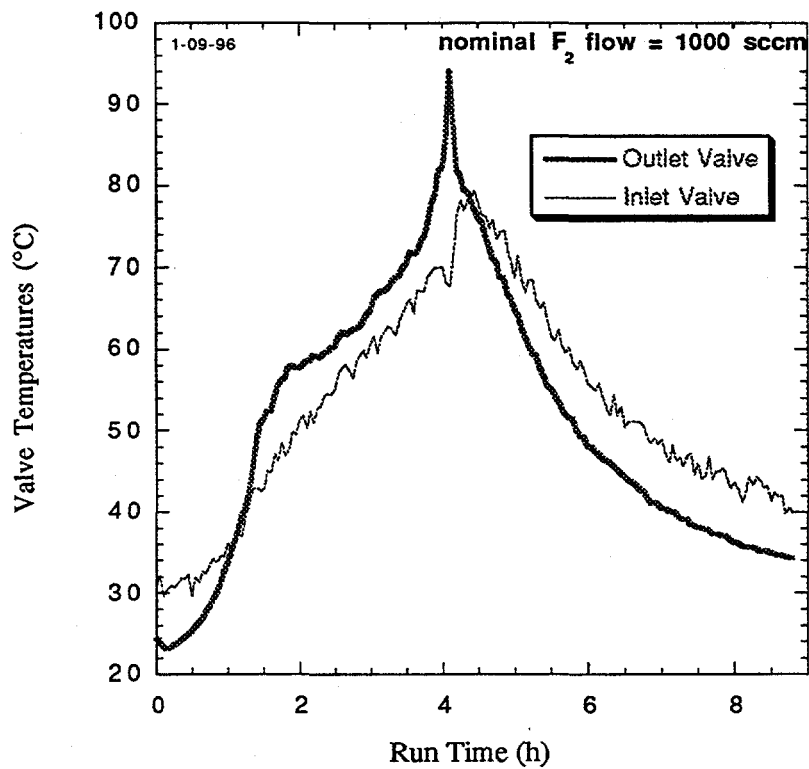


Fig. A-33. Valve temperatures for FTT-5A, 1000 sccm fluorine.

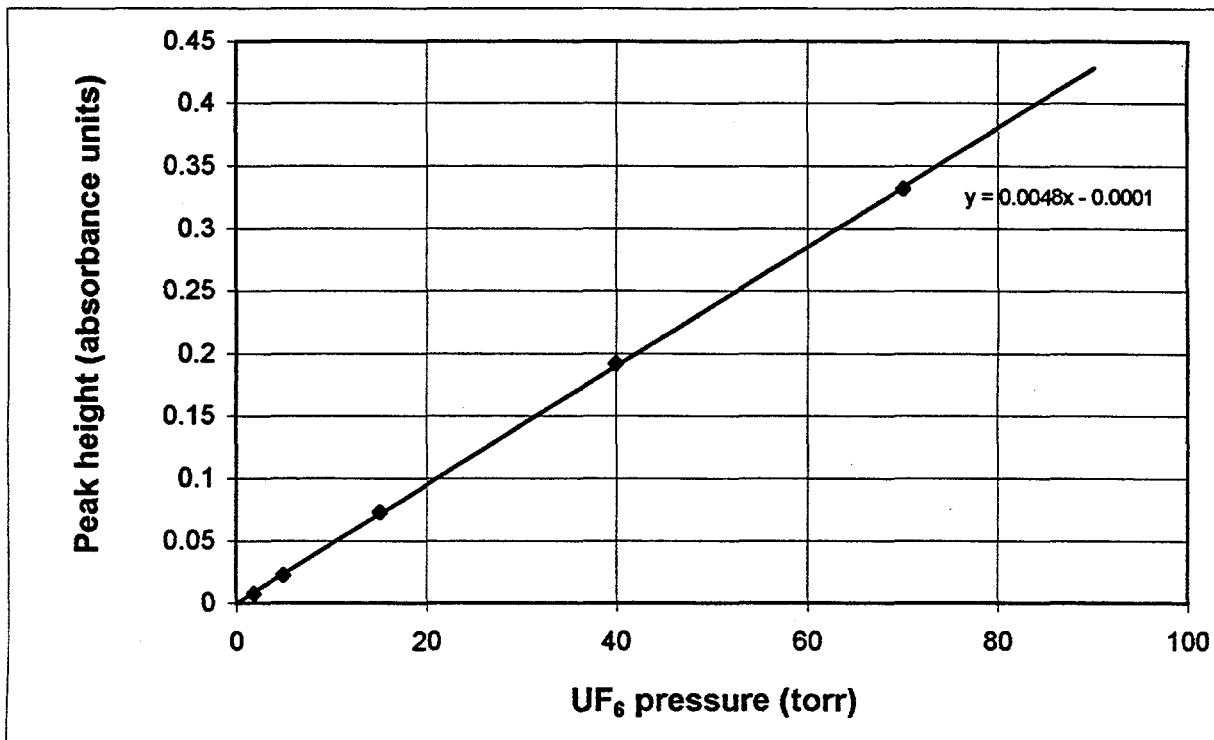


Fig. A-34. Peak height (1157 cm^{-1}) vs UF_6 partial pressure in the 10-cm IR cell.

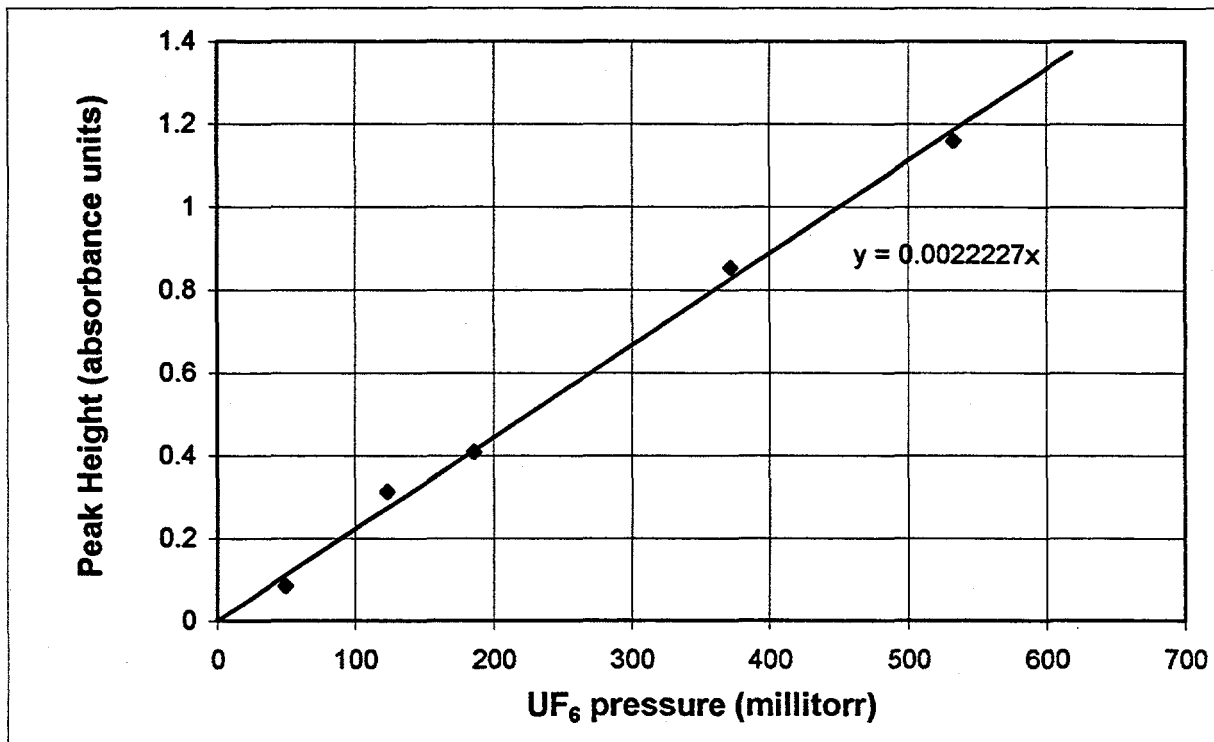


Fig. A-35. Peak height (625 cm^{-1}) vs UF_6 partial pressure in the 20-cm IR cell.

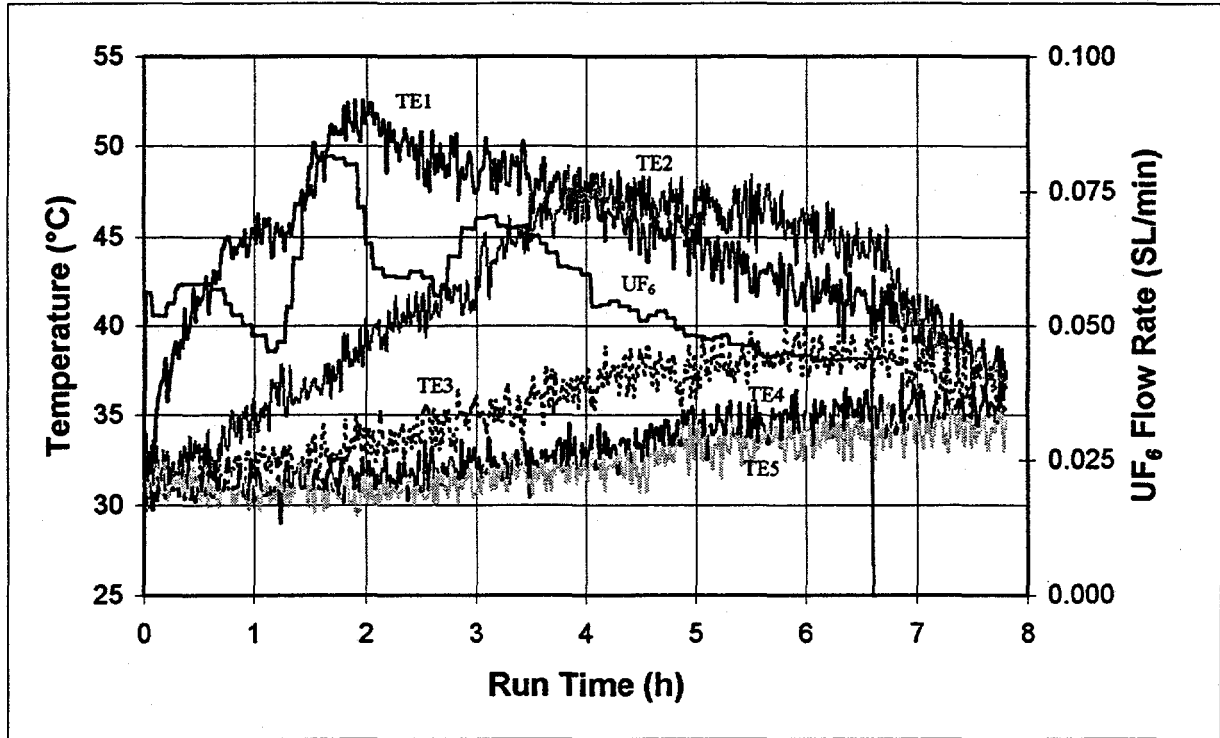


Fig. A-36. Sodium fluoride temperatures and UF₆ flow rate, GBTP, March 25, 1996.

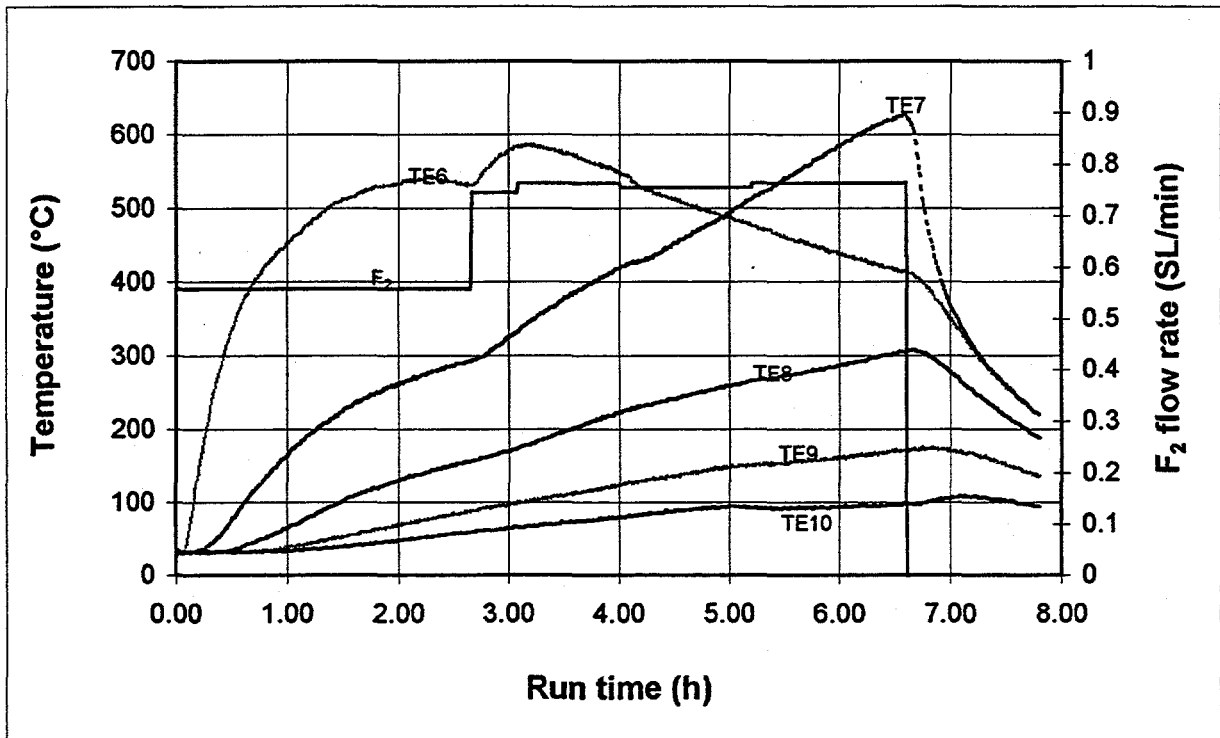


Fig. A-37. Alumina temperatures and F₂ flow rate, GBTP, March 25, 1996.

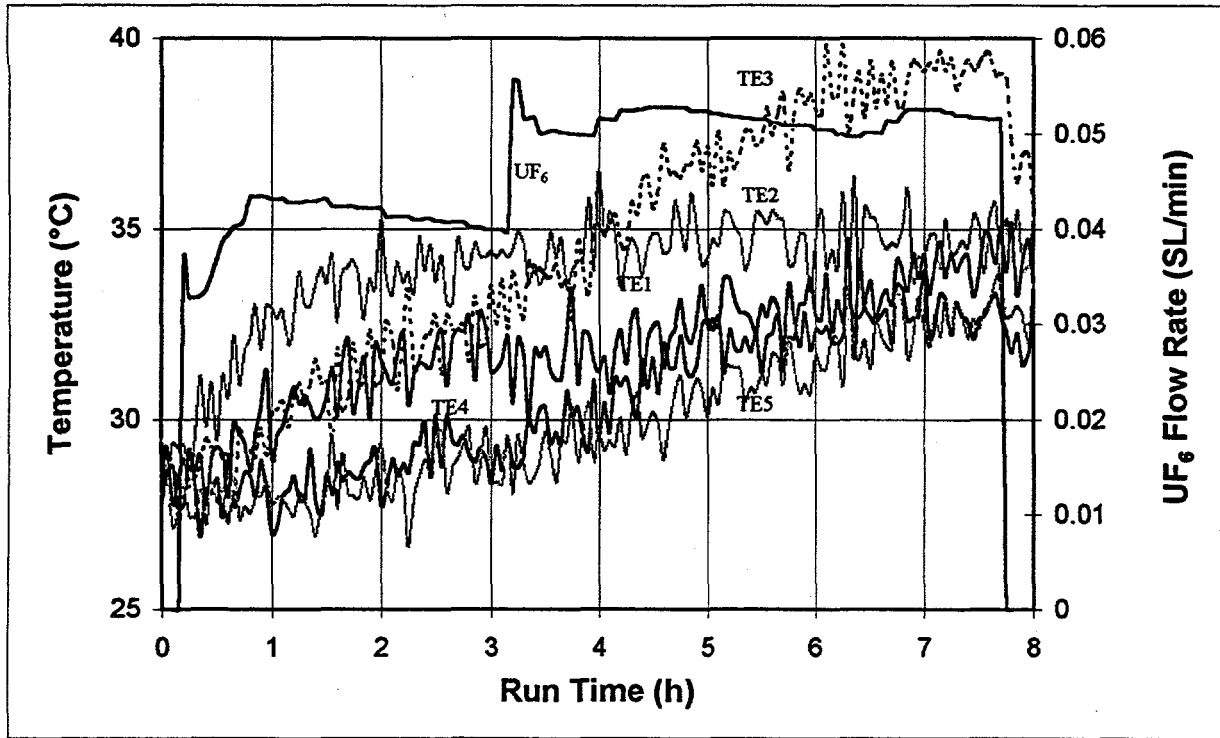


Fig. A-38. Sodium fluoride temperatures and UF_6 flow rate, GBTP, March 26, 1996.

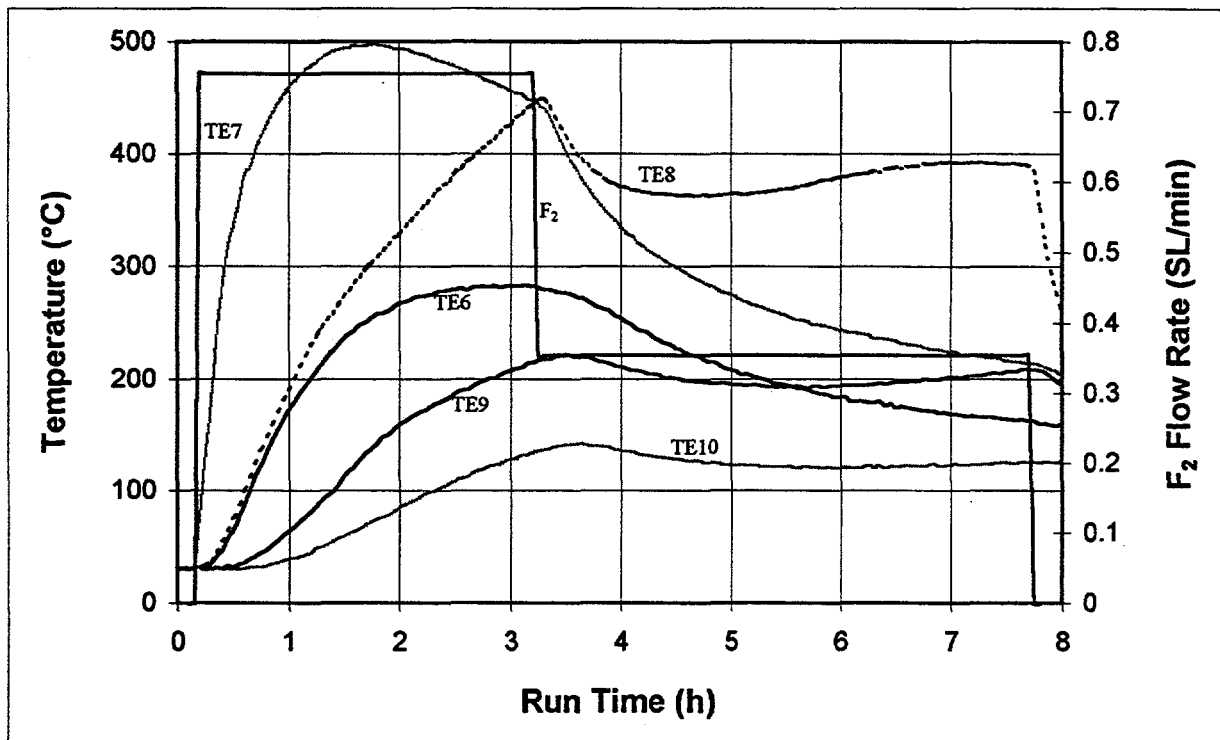


Fig. A-39. Alumina temperatures and F_2 flow rate, GBTP, March 26, 1996.

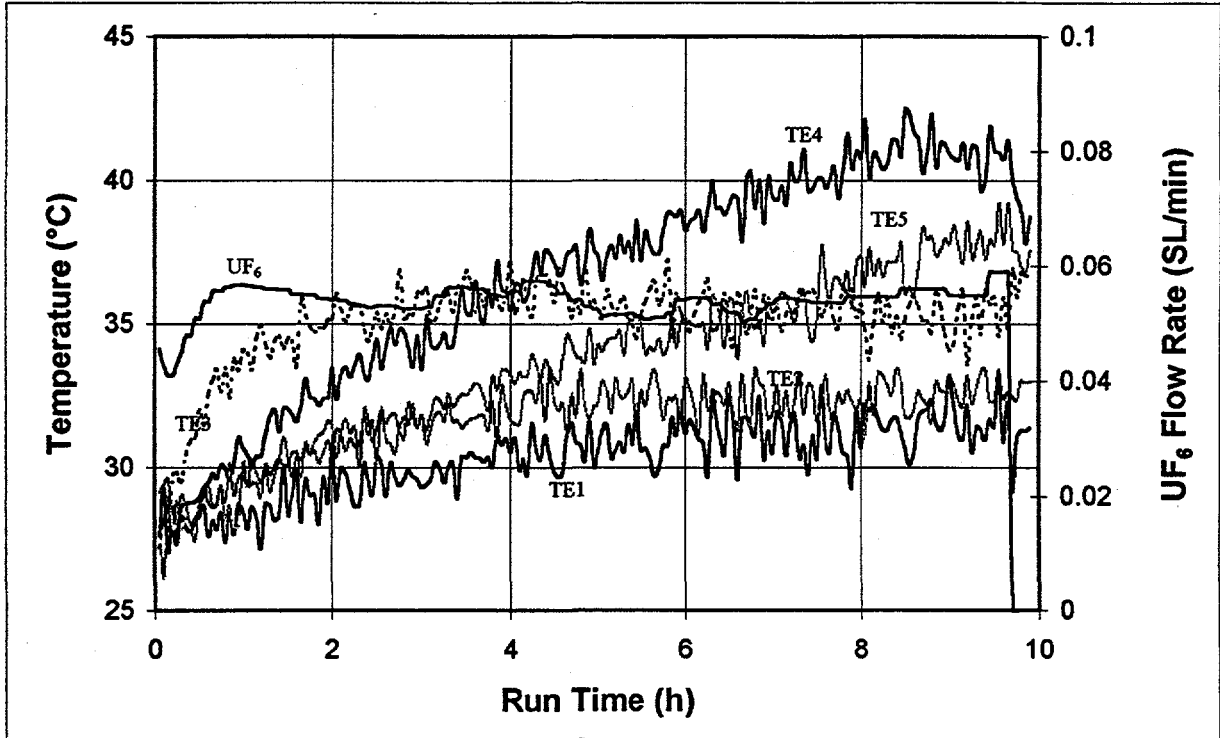


Fig. A-40. Sodium fluoride temperatures and UF_6 flow rate, GBTP, March 27, 1996.

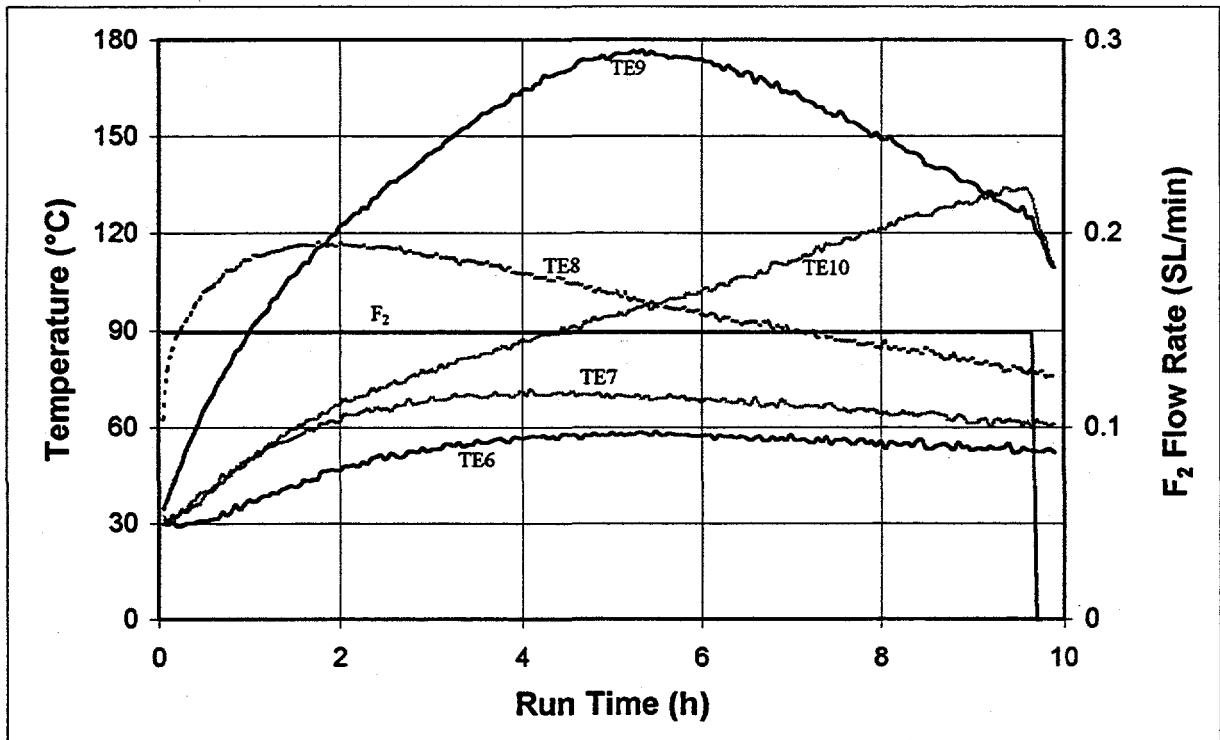


Fig. A-41. Alumina temperatures and F_2 flow rate, GBTP, March 27, 1996.

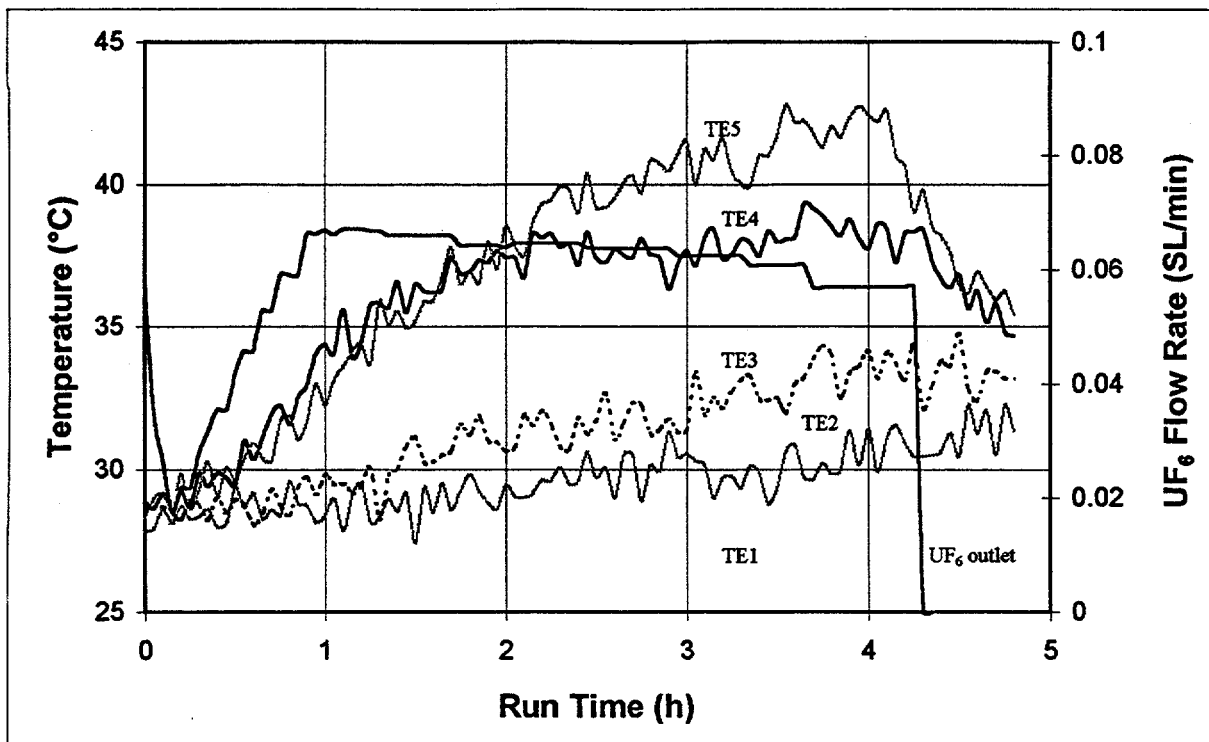


Fig. A-42. Sodium fluoride temperatures and UF₆ flow rate, GBTP, March 28, 1996.

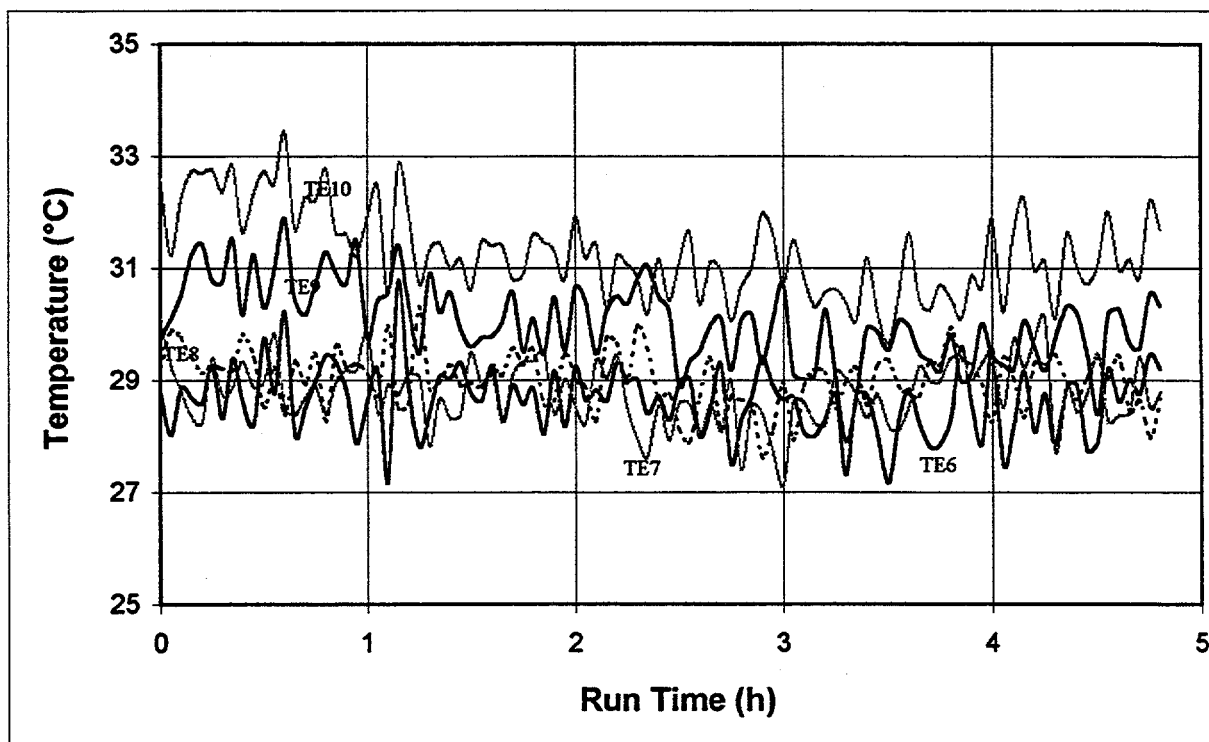


Fig. A-43. Alumina temperatures, no F₂ flow, GBTP, March 28, 1996.

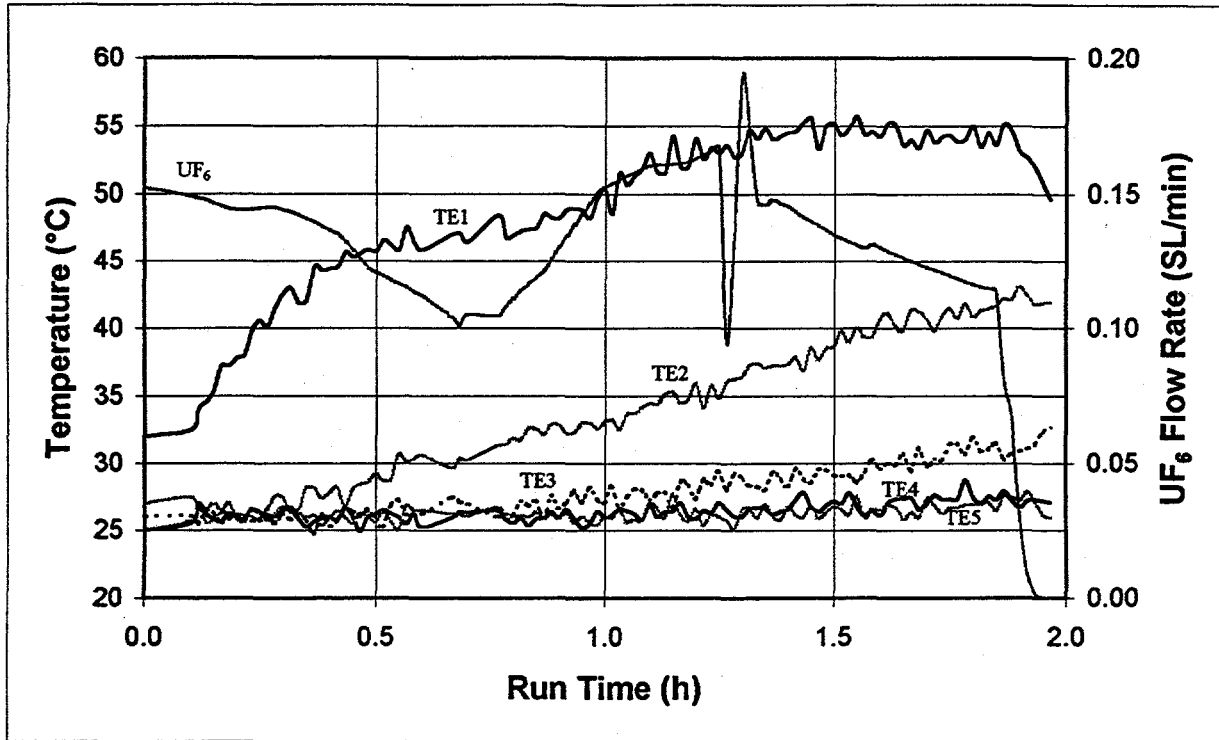


Fig. A-44. Sodium fluoride temperatures and UF_6 flow rate, GBTV-1, April 9, 1996.

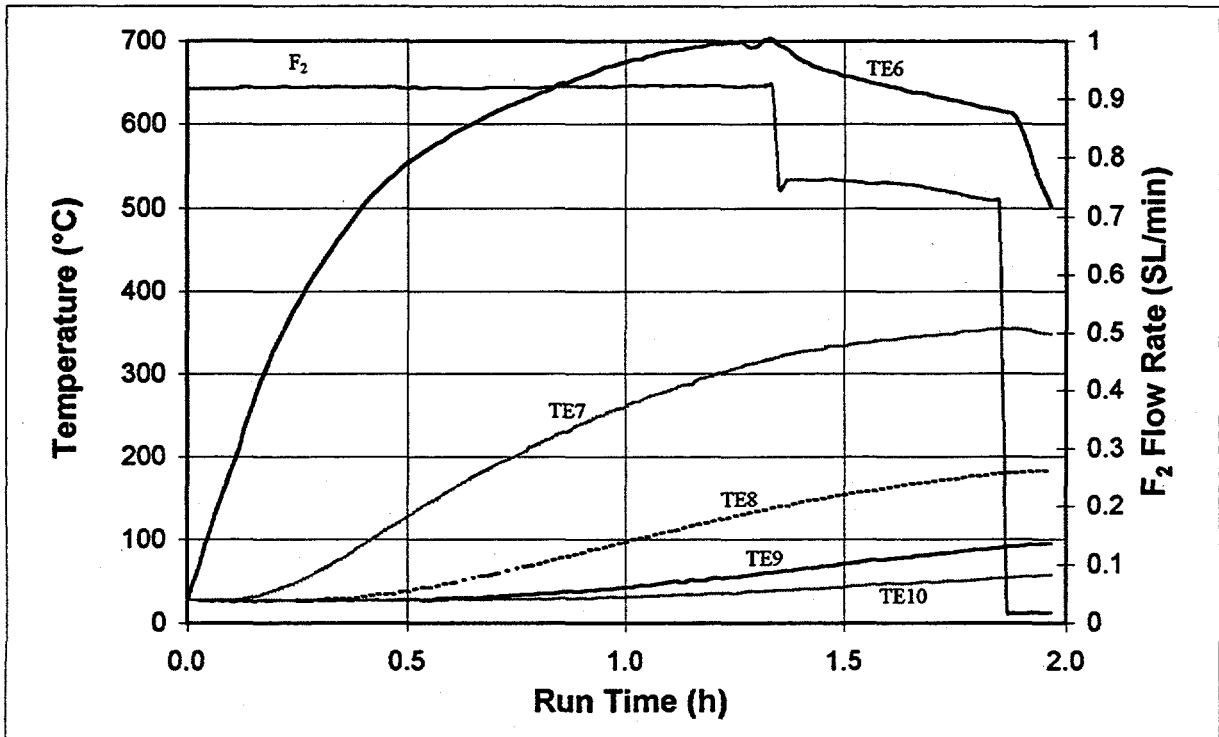


Fig. A-45. Alumina temperatures and F_2 flow rate, GBTV-1, April 9, 1996.

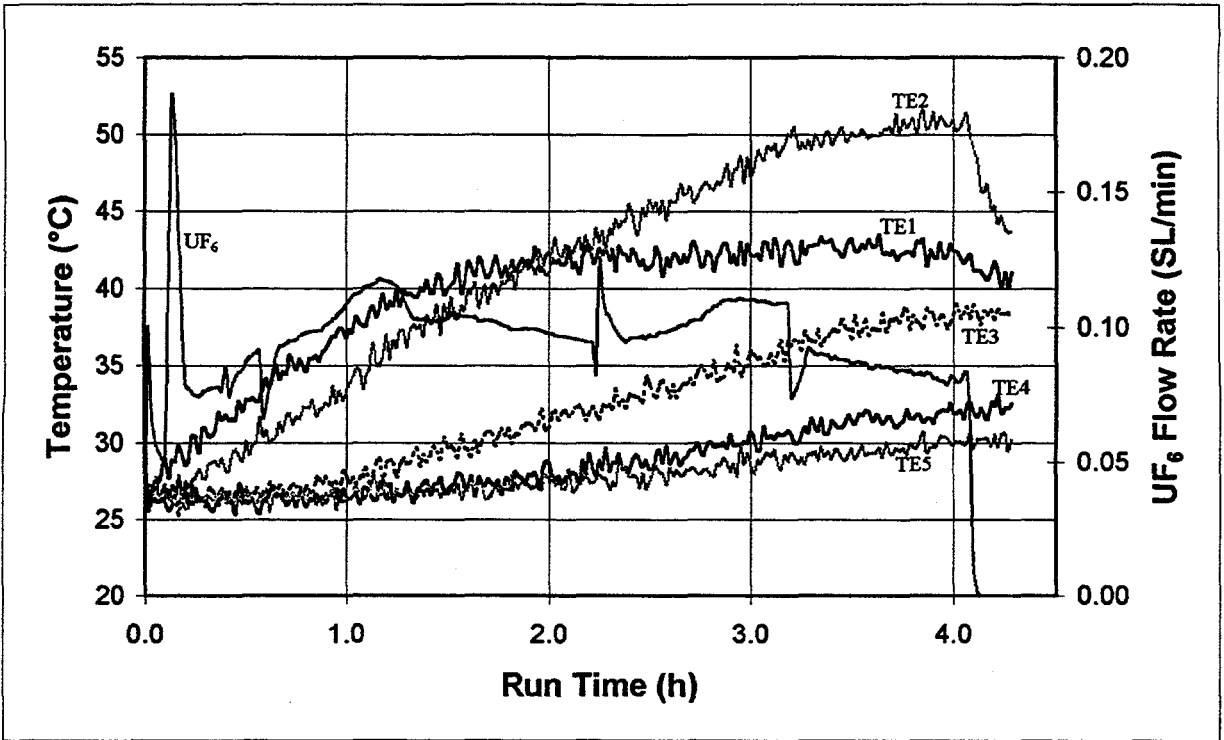


Fig. A-46. Sodium fluoride temperatures and UF_6 flow rate, GBTV-2, April 10, 1996.

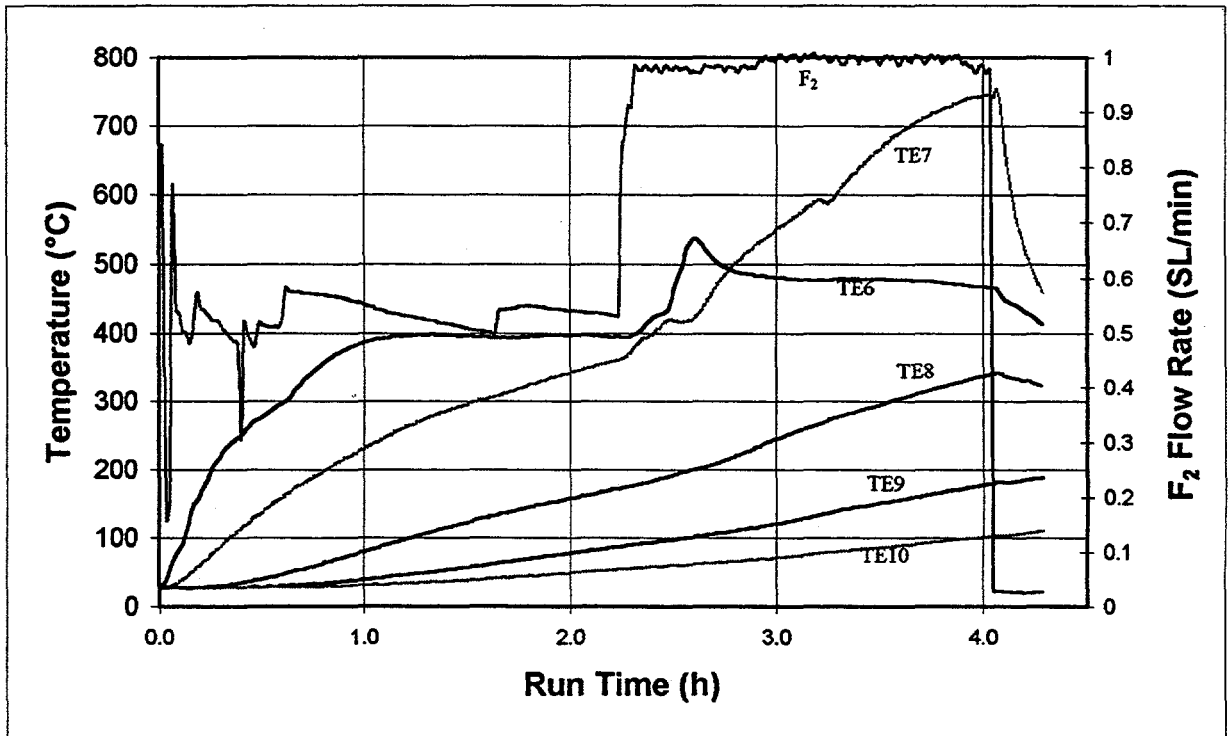


Fig. A-47. Alumina temperatures and F_2 flow rate, GBTV-2, April 10, 1996.

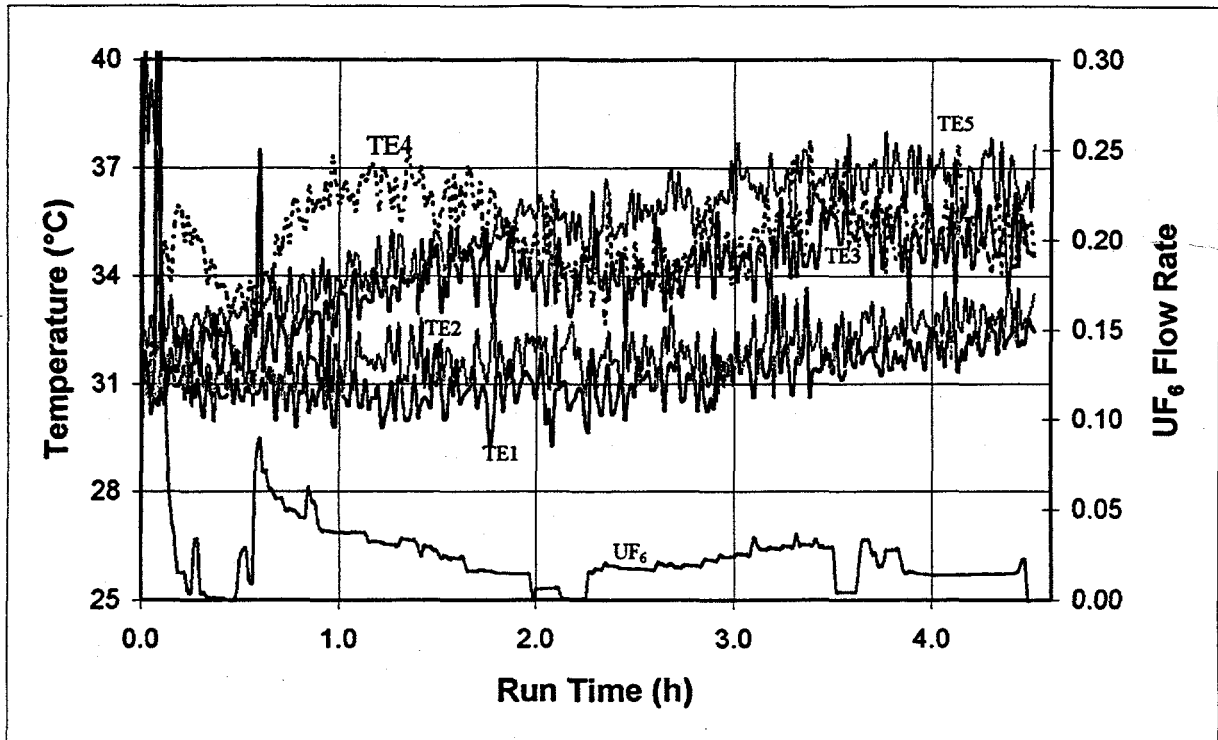


Fig. A-48. Sodium fluoride temperatures and UF₆ flow rate, GBTV-4, April 12, 1996.

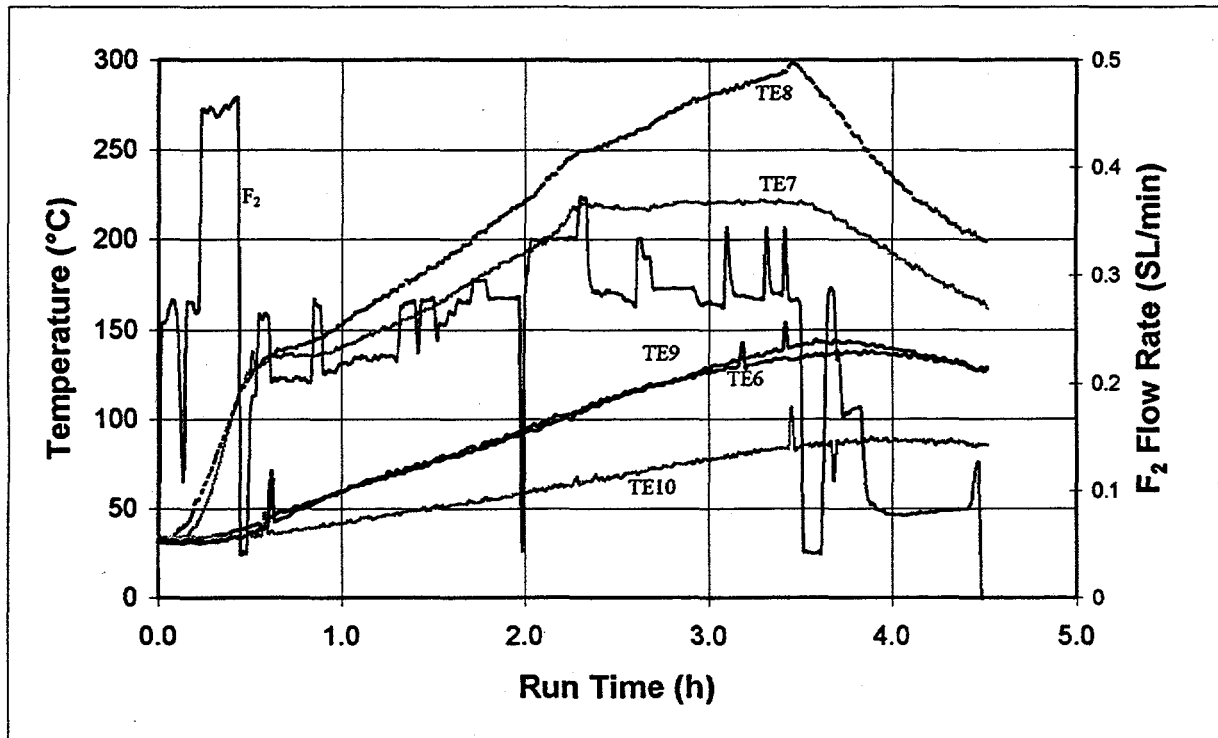


Fig. A-49. Alumina temperatures and F₂ flow rate, GBTV-4, April 12, 1996.

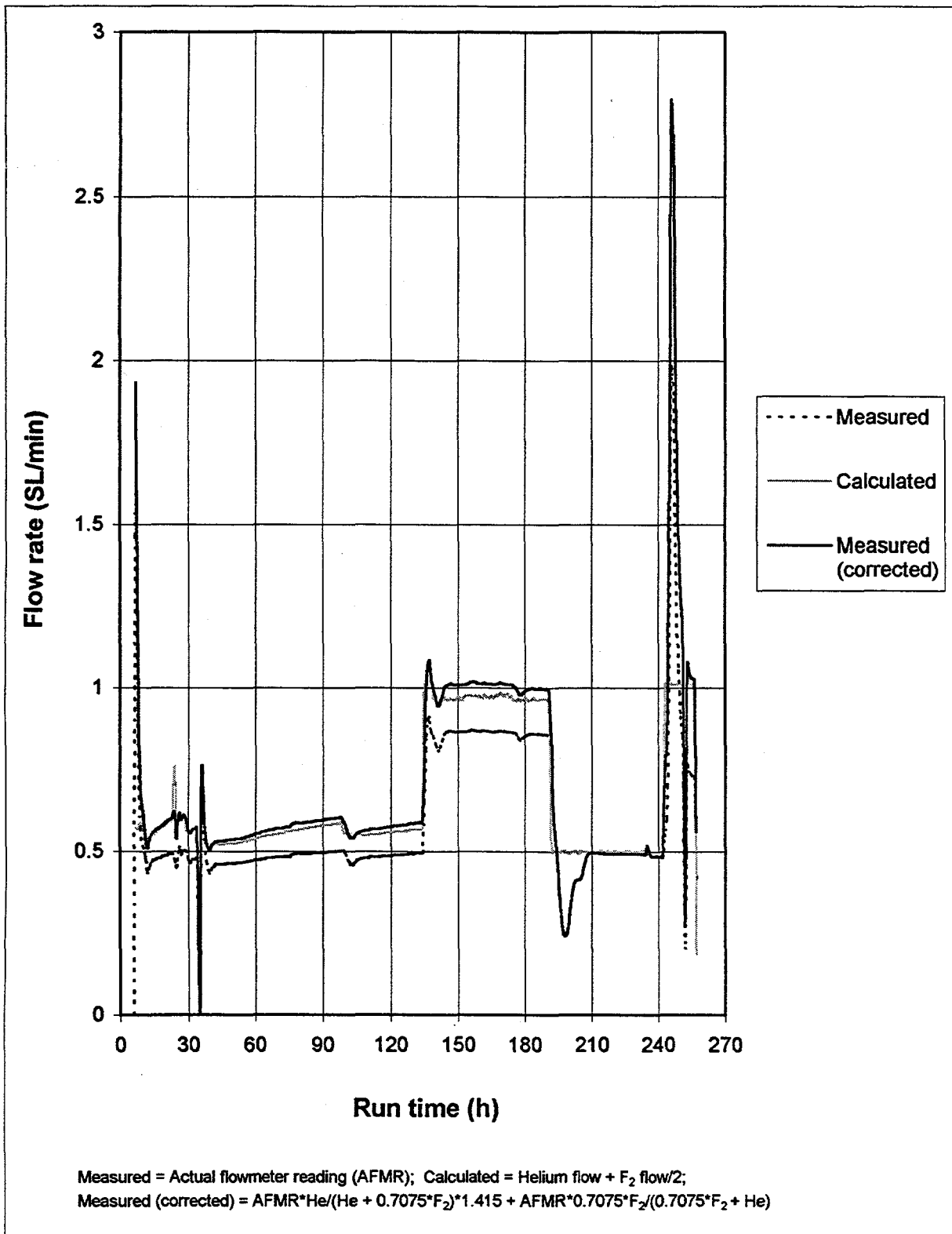


Fig. A-50. Exit flow measurements, GBTV-2, April 10, 1996.

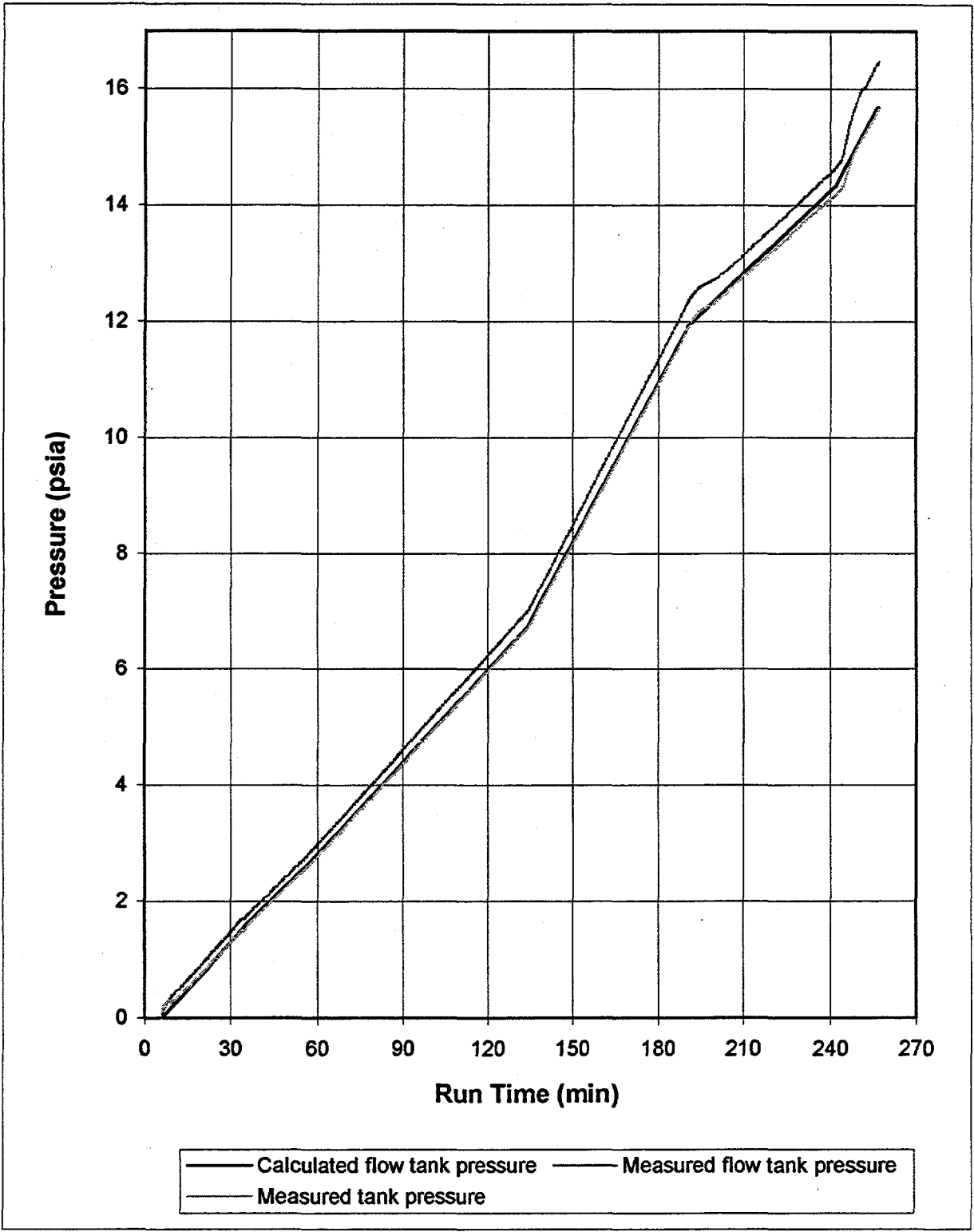


Fig. A-51. Tank pressure rise, GBTV-2, April 10, 1996.

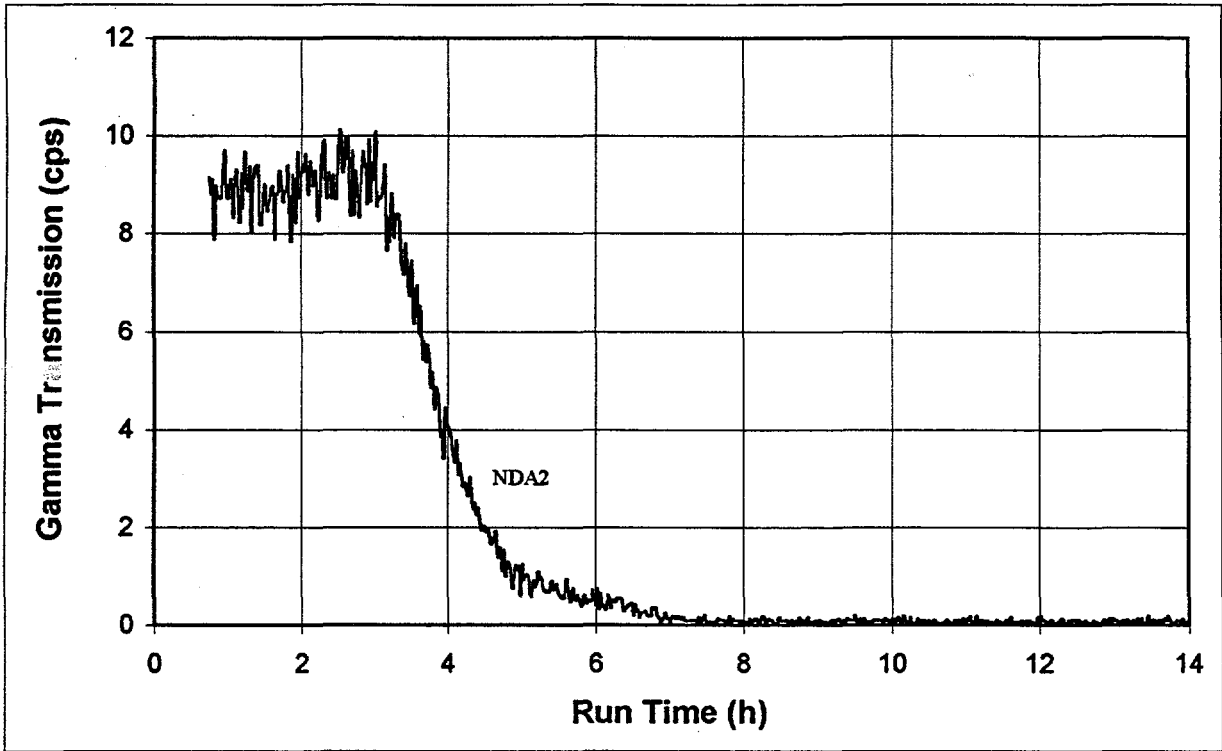
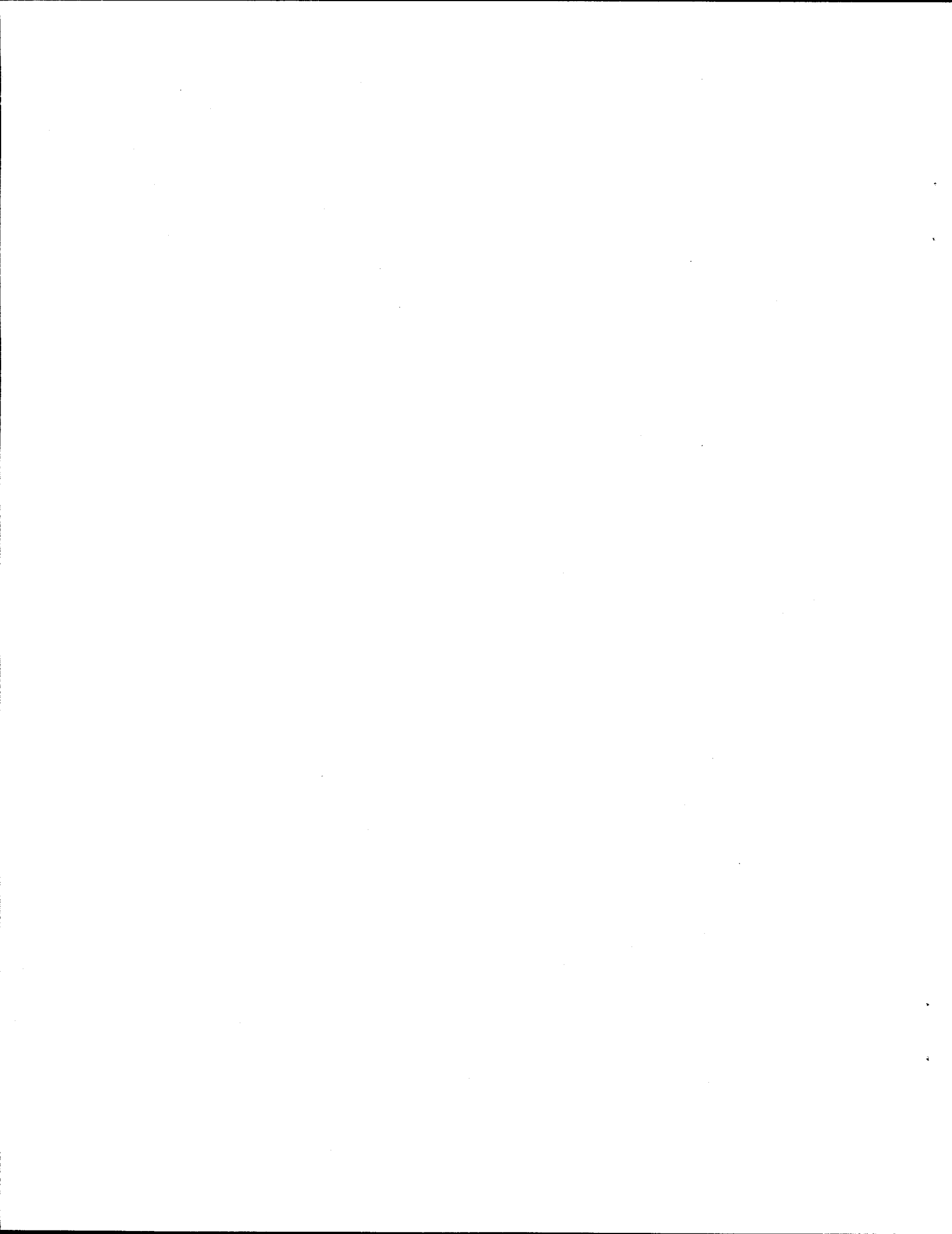


Fig. A-52. Gamma transmission received by second NDA detector throughout GBTV.

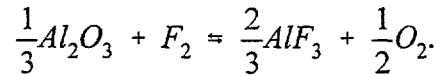
Appendix B

DETERMINATION OF FLUORINE LOADING PER GRAM INCREASE OF TRAP WEIGHT



**Appendix B. DETERMINATION OF FLUORINE LOADING
PER GRAM INCREASE OF TRAP WEIGHT**

The stoichiometric reaction for F₂ and Al₂O₃ is



The molecular weights for the compounds are

AlF₃, 83.977 g/mol;

Al₂O₃, 101.661 g/mol;

F₂, 39.997 g/mol; and

O₂, 31.999 g/mol.

Therefore, the weight change per mole of fluorine added is

$$2/3 * 83.977 - 1/3 * 101.661 = 22.098 \text{ g/mol } F_2.$$

Assuming an ideal gas:

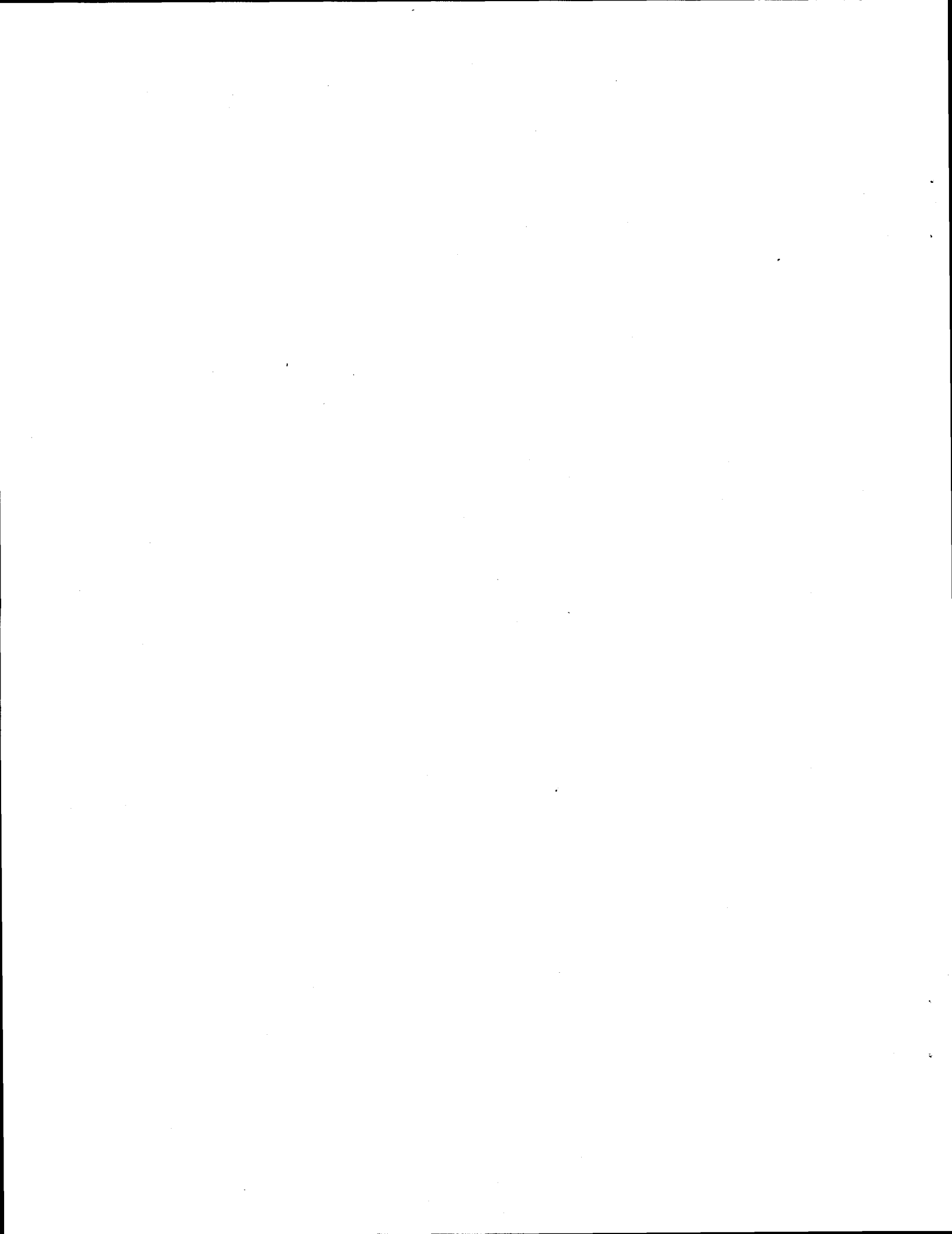
$$22.4147 \text{ L } F_2 / \text{mol } F_2$$

Therefore:

$$22.4147 \text{ L } F_2 / \text{mol } F_2 / 22.098 \text{ g/mol } F_2 = 1.014 \text{ L } F_2 \text{ trapped per gram of weight increase.}$$

Appendix C

**CALCULATION OF FLUORINE FLOW RATE BASED ON EXIT FLOWMETER READING
AND HOLDING TANK PRESSURE RISE**



Appendix C. CALCULATION OF FLUORINE FLOW RATE BASED ON EXIT FLOWMETER READING AND HOLDING TANK PRESSURE RISE

The exit flowmeter can be used to determine the fluorine flow rate because the variation in thermal conductivities of different gases causes different correction factors to be applied for these gases. This means that if there are only two main constituent gases with significantly different correction factors, the molar composition of the gas can be determined from one indicated flow rate. This is the case with gas (usually helium and oxygen) entering the holding tank.

The fluorine flow rate can be determined from the following equation:

$$n = \frac{P1 * VI}{R * T1}$$

where $P1$ = holding tank pressure, $T1$ = tank pressure, VI = tank volume, R = gas constant, and n = moles of gas.

The value of VI is known, and $P1$ and $T1$ are continuously measured. By taking pressure and temperature measurements over time, a molar flow rate n' can be determined. From n' ,

$$VI' = \frac{n' * R * T2}{P2},$$

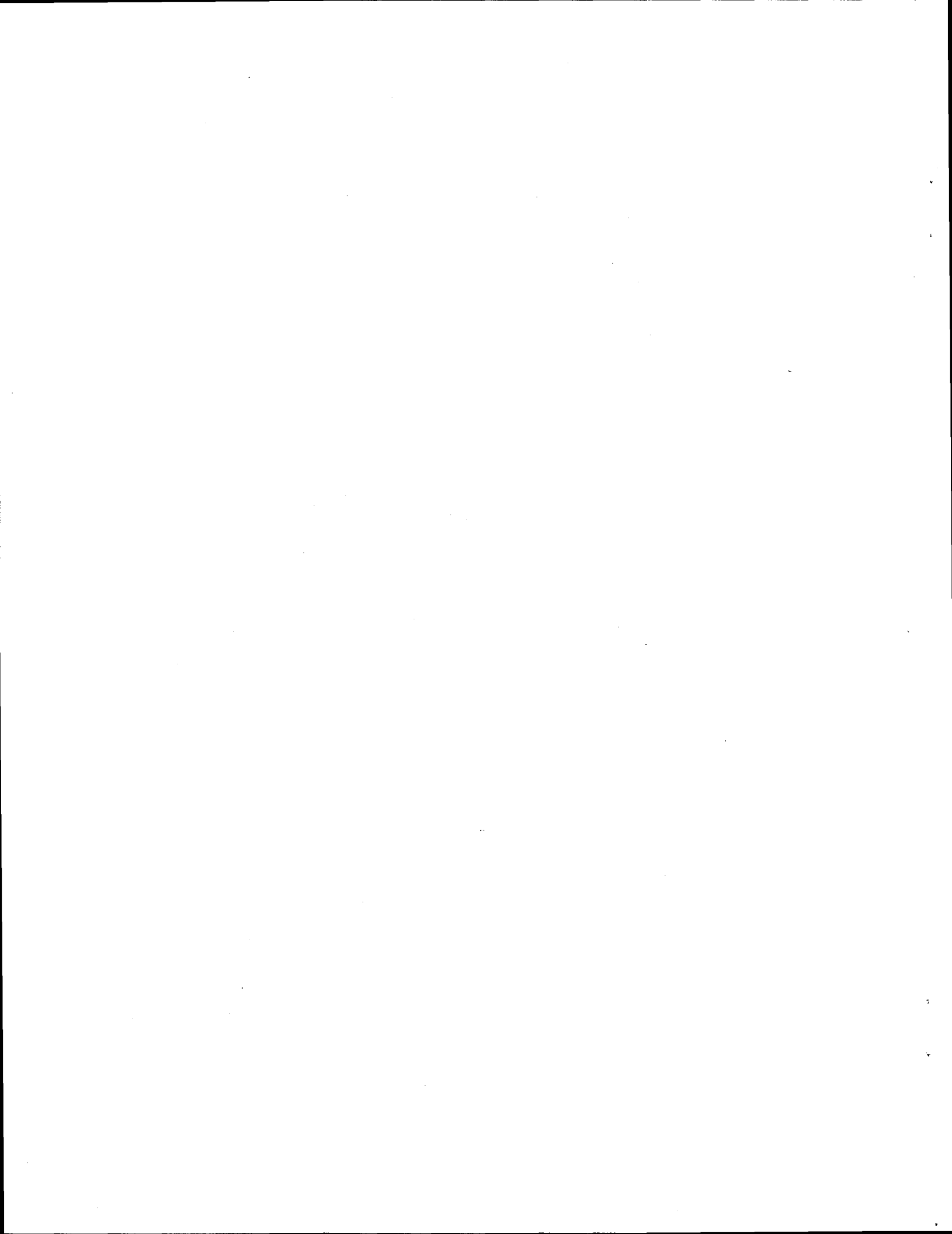
where $T2$ = standard temperature (273.15 K); $P2$ = standard pressure (1 atm); and VI' = gas flow rate. Using the manufacturer-specified conversions for helium and oxygen as compared with those for fluorine (1.520 He/F₂, 1.074 O₂/F₂) and the total flow volume calculated above, the problem reduces to two equations and two unknowns:

$$\frac{He'}{1.52} + \frac{O_2'}{1.074} = V2'$$

$$He' + O_2' = VI',$$

where He' = helium flow rate, O_2' = oxygen flow rate, and $V2'$ = indicated flow rate on exit flowmeter.

Solving these equations gives the oxygen and helium flow rates. The fluorine flow rate is equal to twice the oxygen flow rate (see Appendix B).



INTERNAL DISTRIBUTION

- | | |
|----------------------|--|
| 1. R. R. Aigner | 29. R. A. Kite |
| 2. J. F. Alexander | 30. S. L. Loghry |
| 3. D. P. Armstrong | 31. L. E. McNeese |
| 4. C. E. Bamberger | 32. T. C. Morelock |
| 5. W. D. Brickeen | 33. S. H. Park |
| 6. M. E. Buchanan | 34. B. D. Patton |
| 7. S. N. Burman | 35. S. J. Pawel |
| 8. W. A. Camp | 36. F. J. Peretz |
| 9. R. A. Campbell | 37. D. W. Ramey |
| 10. O. E. Clark | 38-42. J. C. Rudolph |
| 11. S. G. Coffey | 43-46. J. E. Rushton |
| 12. A. G. Croff | 47. D. W. Simmons |
| 13. S. Dai | 48. N. R. Smyrl |
| 14-17. G. D. Del Cul | 49. R. M. Szoza |
| 18. J. R. DeVore | 50-54. L. M. Toth |
| 19. J. R. DiStefano | 55. L. D. Trowbridge |
| 20. R. L. Faulkner | 56. K. L. Walker |
| 21. U. Gat | 57. D. F. Williams |
| 22. L. L. Gilpin | 58. ER Document Management
Center |
| 23. Q. G. Grindstaff | 59. Central Research Library |
| 24. E. C. Hickman | 60. ORNL Laboratory Records-RC |
| 25. J. S. Ivey | 61-62. ORNL Laboratory Records
for OSTI |
| 26. P. S. Johnson | |
| 27. R. T. Jubin | |
| 28. J. R. Keiser | |

EXTERNAL DISTRIBUTION

63. J. Caja, 9052 Highbridge Drive, Knoxville, TN 37922
64. J. H. DeVan, 107 Orange Lane, Oak Ridge, TN 37830
65. J. R. Engel, 118 E. Morningside Drive, Oak Ridge, TN 37830
66. P. A. Haas, 1205 Chickering Way, Knoxville, TN 37923
67. G. R. Hudson, Project Management Division, Department of Energy, Oak Ridge Operations, P. O. Box 2001, Oak Ridge, TN 37831
68. R. L. Jones, Paducah Gaseous Diffusion Plant, Bldg. C300, P. O. Box 1410, Paducah, KY 42002-1410
69. M. R. Jugan, Environmental Restoration, Department of Energy, Oak Ridge Operations, P. O. Box 2001, Oak Ridge, TN 37831
70. J. J. Laidler, Director, Chemical Technology Division, Argonne National Laboratory, 9700 S. Cass Avenue - Bldg. 205, Argonne, IL 60439

71. N. W. Lingle, Environmental Restoration, Department of Energy, Oak Ridge Operations, P. O. Box 2001, Oak Ridge, TN 37831
72. D. W. Neiswander, 9317 Norlake Circle, Knoxville, TN 37922
73. K. J. Notz, Henley Point-River Road, Kingston, TN 37763
74. A. L. Olson, Idaho National Engineering Laboratory, P. O. Box 1625, MS-5219, Idaho Falls, ID 83415-5219
75. L. P. Pugh, 2024 Cedar Lane, Kingston, TN 37763
76. R. G. Russell, Paducah Gaseous Diffusion Plant, Bldg. C710, P. O. Box 1410, Paducah, KY 42002-1410
77. A. J. Saraceno, Portsmouth Gaseous Diffusion Plant, Bldg. X710, P. O. Box 628, MS-2212, Portsmouth, OH 45661-2212
78. J. E. Shoemaker, Jr., Portsmouth Gaseous Diffusion Plant, Bldg. X100, P. O. Box 628, MS-1223, Portsmouth, OH 45661-1223
79. R. E. Thoma, 119 Underwood Road, Oak Ridge, TN 37830
80. P. G. Wooldridge, Paducah Gaseous Diffusion Plant, Bldg. C710, P. O. Box 1410, Paducah, KY 42002-1410
81. R. G. Wymer, 188-A Outer Drive, Oak Ridge, TN 37830
82. E. L. Youngblood, 198 N. Purdue Avenue, Oak Ridge, TN 37830